INFORMATION TO USERS

This manuscript has been reproduced from the microfilm master. UMI films the text directly from the original or copy submitted. Thus, some thesis and dissertation copies are in typewriter face, while others may be from any type of computer printer.

The quality of this reproduction is dependent upon the quality of the copy submitted. Broken or indistinct print, colored or poor quality illustrations and photographs, print bleedthrough, substandard margins, and improper alignment can adversely affect reproduction.

In the unlikely event that the author did not send UMI a complete manuscript and there are missing pages, these will be noted. Also, if unauthorized copyright material had to be removed, a note will indicate the deletion.

Oversize materials (e.g., maps, drawings, charts) are reproduced by sectioning the original, beginning at the upper left-hand corner and continuing from left to right in equal sections with small overlaps.

ProQuest Information and Learning
300 North Zeeb Road, Ann Arbor, MI 48106-1346 USA
800-521-0600

UMI®

Reproduced with permission of the copyright owner. Further reproduction prohibited without permission.

Reproduced with permission of the copyright owner. Further reproduction prohibited without permission.

NOTE TO USERS

This reproduction is the best copy available.

UMI®

Reproduced with permission of the copyright owner. Further reproduction prohibited without permission.

Reproduced with permission of the copyright owner. Further reproduction prohibited without permission.

University of Alberta

The Effect of CO_2 Content for Oil Recovery Optimization with Sequestration

by

Serhat CANBOLAT

A thesis submitted to the Faculty of Graduate Studies and Research in partial fulfillment of the
requirements for the degree of Master of Science

in

Petroleum Engineering

Department of Civil & Environmental Engineering

Edmonton, Alberta

Fall 2005

Reproduced with permission of the copyright owner. Further reproduction prohibited without permission.

Library and Archives Canada
Bibliothèque et Archives Canada

Published Heritage Branch
Direction du Patrimoine de l'édition

395 Wellington Street
Ottawa ON K1A 0N4
Canada

395, rue Wellington
Ottawa ON K1A 0N4
Canada

0-494-09134-7

Your file *Votre référence*
ISBN:
Our file *Notre référence*
ISBN:

NOTICE:
The author has granted a non-exclusive license allowing Library and Archives Canada to reproduce, publish, archive, preserve, conserve, communicate to the public by telecommunication or on the Internet, loan, distribute and sell theses worldwide, for commercial or non-commercial purposes, in microform, paper, electronic and/or any other formats.

The author retains copyright ownership and moral rights in this thesis. Neither the thesis nor substantial extracts from it may be printed or otherwise reproduced without the author's permission.

AVIS:
L'auteur a accordé une licence non exclusive permettant à la Bibliothèque et Archives Canada de reproduire, publier, archiver, sauvegarder, conserver, transmettre au public par télécommunication ou par l'Internet, prêter, distribuer et vendre des thèses partout dans le monde, à des fins commerciales ou autres, sur support microforme, papier, électronique et/ou autres formats.

L'auteur conserve la propriété du droit d'auteur et des droits moraux qui protège cette thèse. Ni la thèse ni des extraits substantiels de celle-ci ne doivent être imprimés ou autrement reproduits sans son autorisation.

In compliance with the Canadian Privacy Act some supporting forms may have been removed from this thesis.

While these forms may be included in the document page count, their removal does not represent any loss of content from the thesis.

Conformément à la loi canadienne sur la protection de la vie privée, quelques formulaires secondaires ont été enlevés de cette thèse.

Bien que ces formulaires aient inclus dans la pagination, il n'y aura aucun contenu manquant.

Canada

Reproduced with permission of the copyright owner. Further reproduction prohibited without permission.

DEDICATION

To my daughter Irem and my wife Özlem, for their support, patience, sacrifice and eternal love.

Reproduced with permission of the copyright owner. Further reproduction prohibited without permission.

ABSTRACT

Carbon dioxide (CO_2) emissions are of importance due to continuously increasing hydrocarbon consumption around the world. This is in opposition to the protocol signed in 1997 in Kyoto, which states that the signators have agreed to reduce such emissions. This study looks at one such scenario to reduce the CO_2 emissions using the existing heavy oil reservoirs as sink. CO_2 injection into the reservoir prior steam flooding was first considered and the influence of CO_2 gas storage on the oil recovery investigated. Consequently, CO_2 sequestration in depleted (steam flooded) heavy oil reservoirs was studied.

For understanding and analyzing the effect of CO_2 gas storage, a series of flow simulations were carried out with a heavy oil field model. The model used in this study considers both dead and live oils in order to study the effect of methane (CH_4) gas on the storage and sequestration.

The sequestration results show that, after producing to the economic limit, Lloydminster type of heavy oil reservoirs can provide a huge sink for CO_2 sequestration, and an opportunity to not only tap into a huge energy source for the future, but also reduce on-site generated greenhouse gas emissions significantly.

Reproduced with permission of the copyright owner. Further reproduction prohibited without permission.

ACKNOWLEDGEMENTS

First of all, the author wishes to express his appreciation to Dr. Marcel POLIKAR for his supervision, wise guidance, understanding and encouragement through the preparation of this work.

Moreover, I would like to thank to the Natural Sciences and Engineering Research Council of Canada (NSERC) for financial support.

Besides, the author extends his thanks to Dr. I.Yücel AKKUTLU for his valuable comments and advice during the study.

In addition, special thanks are extended to committee member Dr. Octavian Catuneanu for his valuable suggestions and comments.

Finally, this thesis could not have been possible without some people who were involved from the start of the admission application at the Middle East Technical University, until the completion of this study at the University of Alberta.

Reproduced with permission of the copyright owner. Further reproduction prohibited without permission.

TABLE OF CONTENTS

CHAPTER 1 ..... **1**

INTRODUCTION 1

CHAPTER 2 ..... **3**

LITERATURE REVIEW 3

2.1 Carbon Sources and Capture Processes 3

2.1.1 Flue Gas Separation 3

2.1.2. Oxy-Fuel Combustion 4

2.1.3. Pre-Combustion Capture 4

2.2 Economics of Capture Process 4

2.2.1 Cost of Capture 5

2.2.2 Cost of Transportion 6

2.2.3 Cost of Injection and Storage 6

2.2.4 Overall Costs 7

2.3 CO_2 Disposal Options of Steam Flooded Reservoirs 7

2.3.1 Major CO_2 Disposal Options 8

2.3.1.1 Disposal in Exhausted Steam Flooded Reservoirs 8

2.4 Carbon Dioxide Flooding 10

2.4.1 Enhanced Oil Recovery with Carbon Dioxide 11

2.5 Steam Flooding 13

2.5.1 Steam-Assisted Gravity Drainage 14

2.6 Carbon Dioxide with Steam Injection 15

CHAPTER 3 ..... **17**

STATEMENT OF THE PROBLEM 17

CHAPTER 4 ..... **18**

4.1 NUMERICAL SIMULATIONS 18

4.1.1 Numerical Model 18

4.2 Simulations Performed 21

4.2.1 Reservoir with Dead Oil 21

Reproduced with permission of the copyright owner. Further reproduction prohibited without permission.

4.2.2 Reservoir with Live Oil 21
4.3 Sequestration Calculations with Solubility Effects 22

CHAPTER 5 ..... **24**
RESULTS AND DISCUSSIONS 24
5.1 Carbon Dioxide Injection Prior to Steam Injection 24
5.1.1 Reservoir with Dead Oil 24
5.1.2 Reservoir with Live Oil 31
5.1.3 Comparison of the Dead and Live Oil Cases 35
5.1.4 Economic Analysis of the Dead and Live Oil Cases 40
5.2 Carbon Dioxide Sequestration After Steam Injection 41
5.2.1 Reservoir with Dead Oil 41
5.2.2 Reservoir with Live Oil 44

CHAPTER 6 ..... **48**
CONCLUSIONS AND RECOMMENDATIONS FOR FUTURE WORK 48
6.1 CONCLUSIONS 48
6.2 RECOMMENDATIONS FOR FUTURE WORK 49

REFERENCES **50**

APPENDICES **55**
Appendix A Data File for the Simulator 56
Appendix B Oil Recovery Curves with CO_2 Injection 62
Appendix C CO_2 Storage percent at Different Well Pair Distances 64
Appendix D Comparison of Temperature Profiles with and without CO_2 Injection 66
Appendix E Comparison of Dead and Live Oil Reservoirs 73

Reproduced with permission of the copyright owner. Further reproduction prohibited without permission.

LIST OF TABLES

Table 1 Reservoir and Fluid Characteristics for Wilmington, Weyburn and Bati Raman Fields 12

Table 2 Lloydminster Reservoir and Fluid Characteristics for Dead Oil Case 18

Table 3 Simple Economics Calculation of a Project with and without CO_2 Injection 40

Table 4 Simulation Results at 100 sm^3/day/well CO_2 Injection Prior to 100 sm^3/day/well Steam Flooding 42

Table 5 CO_2 Sequestration Results of a Dead Oil Reservoir at Different Well Pair Distance after Steam Flooding by Analytical Calculations 42

Table 6 Comparison of CO_2 Sequestration Results after Steam Flooding in a Dead Oil Reservoir 44

Table 7 Simulation Results to the Economic Producing Life of a Live Oil Reservoir 45

Table 8 CO_2 Sequestration Results of a Live Oil Reservoir at Different Pressures of Steam Flooding by Analytical Calculations 45

Table 9 Comparison of CO_2 Sequestration Results after Steam Flooding in a Live Oil Reservoir 46

Reproduced with permission of the copyright owner. Further reproduction prohibited without permission.

LIST OF FIGURES

Figure 1 Cost of Electricity with Capture for Various Types of Power Plants 5
Figure 2 Cost for CO_2 Transport via Pipeline as a Function of CO_2 Mass Flow Rate 6
Figure 3 Range of Costs for Various Carbon Storage Methods (after Herzog and Golomb [8]) 7
Figure 4 CO2 Phase Diagram (after Bachu [4]) 19
Figure 5 Crude Oil Viscosity versus Temperature (after Butler [3]) 19
Figure 6 Front View of the Numerical Model 20
Figure 7 Side View of the Numerical Model 20
Figure 8 CO_2 Solubility Curves in Fresh Water [36, 37, 38] 22
Figure 9 CO_2 Solubility in Crude Oil at 21°C [40] 23
Figure 10 Cumulative Oil Recovery as a Function of Steam Injection Rate 24
Figure 11 Cumulative Steam-Oil Ratio as a Function of Steam Injection Rates 25
Figure 12 Cumulative Water-Oil Ratio as a Function of Steam Injection Rates 26
Figure 13 Soaking Time Optimization as a Function of CO_2 Injection Rates and Storage % 26
Figure 14 Comparison of Storage percent of CO_2 Soaking and No Soaking at Different CO_2 Injection Rates 27
Figure 15 Comparison of CSOR of CO_2 Soaking and No Soaking at Different CO_2 Injection Rates 28
Figure 16 Comparison of CWOR of CO_2 Soaking and No Soaking at Different CO_2 Injection Rates 28
Figure 17 Comparison of Oil Recoveries of CO_2 Soaking and No Soaking at Different CO_2 Injection Rates 29
Figure 18 Effect of CO_2 Injection Rates on Oil Recovery as a Function of Steam Injection Rate 30
Figure 19 Effect of CO_2 Injection Rates on Storage as a Function of Steam Injection Rate 30
Figure 20 Cumulative Oil Recovery as a Function of CO_2 Injection Rate and Pressure 32
Figure 21 Cumulative CH_4 Recovery as a Function of CO_2 Injection Rate and Pressure 32
Figure 22 Effect of CO_2 Injection Rates on Storage as a Function of Reservoir Pressure 33
Figure 23 Effect of CO_2 Injection Rates on CSOR as a Function of Reservoir Pressure 34
Figure 24 Effect of CO_2 Injection Rates on CWOR as a Function of Reservoir Pressure 34

Reproduced with permission of the copyright owner. Further reproduction prohibited without permission.

Figure 25 Comparison of Cumulative Oil Recoveries of Reservoirs with Dead and Live Oil at 3500 kPa Pressure 35
Figure 26 Comparison of Temperature Profiles in Dead Oil and Live Oil Reservoirs after 6 Months of Steam Flooding 36
Figure 27 Comparison of Temperature Profiles in Dead Oil and Live Oil Reservoirs after 1 Year of Steam Flooding 37
Figure 28 Comparison of Cumulative Steam-Oil Ratios of Reservoirs with Dead and Live Oil at 3500 kPa Pressure 39
Figure 29 Comparison of Cumulative Water-Oil Ratios of Reservoirs with Dead and Live Oil at 3500 kPa Pressure 39
Figure 30 Cumulative Oil Recovery to Economic Producing Life of Reservoir at Optimum Conditions for CO_2 and Steam Injection Rates 41
Figure 31 CO_2 Sequestration in Dead Oil Reservoir at 3500 kPa Reservoir Pressure 43
Figure 32 Comparison of Numerical and Analytical CO_2 Sequestration Calculations in Dead Oil 44
Figure 33 CO_2 Sequestration in Live Oil Reservoir at 3500 kPa Pressure 46
Figure 34 Comparison of Numerical and Analytical CO_2 Sequestration Calculations in Live Oil 47
Figure B.1 Effect of CO_2 Injection Rates on Oil Recovery as a Function of Steam Injection Rate for Well Pair Spacing of 80 m 62
Figure B.2 Effect of CO_2 Injection Rates on Oil Recovery as a Function of Steam Injection Rate for Well Pair Spacing of 90 m 62
Figure B.3 Effect of CO_2 Injection Rates on Oil Recovery as a Function of Steam Injection Rate for Well Pair Spacing of 110 m 63
Figure B.4 Effect of CO_2 Injection Rates on Oil Recovery as a Function of Steam Injection Rate for Well Pair Spacing of 120 m 63
Figure C.1 Effect of CO_2 Injection Rates on Storage as a Function of Steam Injection Rate for Well Pair Spacing of 80 m 64
Figure C.2 Effect of CO_2 Injection Rates on Storage as a Function of Steam Injection Rate for Well Pair Spacing of 90 m 64
Figure C.3 Effect of CO_2 Injection Rates on Storage as a Function of Steam Injection Rate for Well Pair Spacing of 110 m 65
Figure C.4 Effect of CO_2 Injection Rates on Storage as a Function of Steam Injection Rate for Well Pair Spacing of 120 m 65

Reproduced with permission of the copyright owner. Further reproduction prohibited without permission.

Figure D.1 Comparison of Temperature Profiles in Dead Oil with and without CO_2 Injection after 6 Months of Steam Flooding 66
Figure D.2 Comparison of Temperature Profiles in Dead Oil with and without CO_2 Injection after 1 Year of Steam Flooding 67
Figure D.3 Comparison of Temperature Profiles in Live Oil with and without CO_2 Injection after 2 Years of Steam Flooding 68
Figure D.4 Comparison of Temperature Profiles in Live Oil with and without CO_2 Injection after 3 Years of Steam Flooding 69
Figure D.5 Comparison of Temperature Profiles in Live Oil with and without CO_2 Injection after 6 Months of Steam Flooding 70
Figure D.6 Comparison of Temperature Profiles in Live Oil with and without CO_2 Injection after 1 Year of Steam Flooding 71
Figure D.7 Comparison of Temperature Profiles in Live Oil with and without CO_2 Injection after 2 Years of Steam Flooding 72
Figure E.1 Comparison of Cumulative Oil Recoveries of Reservoirs with Dead and Live Oil at 3000 kPa Pressure 73
Figure E.2 Comparison of Cumulative Steam-Oil Ratios of Reservoirs with Dead and Live Oil at 3000 kPa Pressure 73
Figure E.3 Comparison of Cumulative Water-Oil Ratios of Reservoirs with Dead and Live Oil at 3000 kPa Pressure 74
Figure E.4 Comparison of Cumulative Oil Recoveries of Reservoirs with Dead and Live Oil at 2500 kPa Pressure 74
Figure E.5 Comparison of Cumulative Steam-Oil Ratios of Reservoirs with Dead and Live Oil at 2500 kPa Pressure 75
Figure E.6 Comparison of Cumulative Water-Oil Ratios of Reservoirs with Dead and Live Oil at 2500 kPa Pressure 75
Figure E.7 Comparison of Cumulative Oil Recoveries of Reservoirs with Dead and Live Oil at 2000 kPa Pressure 76
Figure E.8 Comparison of Cumulative Steam-Oil Ratios of Reservoirs with Dead and Live Oil at 2000 kPa Pressure 76
Figure E.9 Comparison of Cumulative Water-Oil Ratios of Reservoirs with Dead and Live Oil at 2000 kPa Pressure 77

Reproduced with permission of the copyright owner. Further reproduction prohibited without permission.

ABBREVIATIONS

CWE	Cold Water Equivalent
COR	Cumulative Oil Recovery
CCS	Carbon Capture and Storage
CG	Cumulative Gas
CSOR	Cumulative Steam-Oil Ratio
CWOR	Cumulative Water-Oil Ratio
EOR	Enhanced Oil Recovery
FG	Flue Gas
GHG	Green House Gas
MEA	Monoethanolamine
MMP	Minimum Miscibility Pressure
OOIP	Original Oil In Place
PV	Pore Volume
PVT	Pressure Volume Temperature
SAGD	Steam-Assisted Gravity Drainage
SAGP	Steam And Gas Push
WAG	Water Alternating Gas

Reproduced with permission of the copyright owner. Further reproduction prohibited without permission.

CHAPTER 1

INTRODUCTION

Heavy oil and bitumen represent a huge amount of natural resources; the world's total estimated original oil in place (OIP) in these forms is approximately 6 trillion barrels, which corresponds to six times the conventional world oil reserves. Under anticipated economic conditions, and using current technology, the province of Alberta has about 175.6 billion barrels of remaining heavy oil reserves, the ultimate recovery of which is estimated to be over 315 billion barrels [1].

Moreover, carbon dioxide (CO_2) emissions are increasing due to the hydrocarbons produced increasingly around the world. Simply, in the Natural Resource Canada production scenario, it was reported that Alberta's green house gas (GHG) emissions from in-situ bitumen production would increase from 6.1 Mega-tonnes (Mt) in 1997 to 18.8 Mt in 2015, a three fold increase[2].

There is potential for reducing CO_2 emissions by capturing and disposing them into the oil reservoirs. This research has several aims, one of which is to show that it is feasible to store CO_2 and let it soak some time in a heavy oil reservoir prior to producing it by steam flooding. The second is to analyze the effects of previously injected CO_2 on this process using some of the simpler mitigative solutions recommended by the Kyoto protocol. The third is to present an overview of CO_2 sequestration, once the economic producing life of steam-flooded reservoirs has been achieved. This is done by using the experimental work from the literature for CO_2 solubility and verification with the commercial numerical simulator CMG STARS™.

The presence of gas in a heavy oil reservoir is known to decrease not only the cumulative steam-oil ratio (CSOR), which accounts for 30% of the total cost of a project [3], but also to result in the emission of generated GHGs to atmosphere, which is associated with energy requirements. For the purpose of sequestrating CO_2, it should be captured first and transported to the field. Considering the cost associated with the capture process, the storage of CO_2 was evaluated prior to and after steam flooding a heavy oil reservoir, such as those located in the vicinity of Lloydminster in Alberta.

In this study, simulations are carried out for various scenarios based on the well known characteristics of heavy oil reservoirs of the Lloydminster area. In the numerical simulations, both dead oil and live oil cases are analyzed.

Reproduced with permission of the copyright owner. Further reproduction prohibited without permission.

The numerical procedure consists of two parts. In the first part, CO_2 is injected into the reservoir at a constant rate and is left soaking for some time. Then, steam flooding is started and carried out until the economic producing limit of the reservoir, which is assumed as CSOR equal to six. The residual saturations of the reservoir fluids are determined at that stage. Then, the sequestration of CO_2 after steam flooding is determined using the solubility curves for oil and water generated experimentally for CO_2.

In the second part of the simulations, using the saturation values obtained from the first part, CO_2 is sequestrated into the steam flooded reservoir neglecting the cooling time until the injection pressure reached the fracture pressure. Finally, the analytical results of CO_2 sequestration are compared with the numerical simulator results. Such simulations were performed in order to use the reservoir as a sink for the sequestration [4] of CO_2, once the economic producing life of the reservoir has been achieved.

Reproduced with permission of the copyright owner. Further reproduction prohibited without permission.

CHAPTER 2

LITERATURE REVIEW

2.1 Carbon Sources and Capture Processes

Fossil fuelled power plants emit more than one-third of the CO_2 emissions worldwide. Power plants are usually built in large centralized units, typically delivering 500-1000 mega-watts (MW) of electrical power. A 1000 MW pulverized coal fired power plant emits between 6-8 Mt/y of CO_2, an oil fired single cycle power plant about two thirds of that, and a natural gas combined cycle power plant about one half of that [5].

For a steam injection operation, a simple steam boiler, using the 100 MW of power gas-fired configuration, emits approximately 2500 tonnes/day (1.4 Mm^3/day) CO_2 gas, generating 78020 m^3/day of 80% quality steam [6]. However, the prospective amounts of CO_2 that can be utilized are but a very small fraction of the CO_2 emissions from anthropogenic sources.

CO_2 capture processes during power production fall into three general categories: (1) flue gas separation; (2) oxy-fuel combustion in power plants; and (3) pre-combustion separation. Each of these technologies carries both an energy and economic penalty.

2.1.1 Flue Gas Separation

This capture process is based on chemical absorption. Chemical absorption refers to the process where CO_2 is chemically absorbed in a liquid solvent [5, 7]. The most commonly used absorbent for CO_2 absorption is monoethanolamine (MEA). The fundamental reaction for this process is:

$$C_2H_4OHNH_2 + H_2O + CO_2 \leftrightarrow C_2H_4OHNH_3 + HCO_3^-$$

During the absorption process, the reaction proceeds from left to right; cooling and heating of the solvent, pumping and compression require power input from the power plant thermal cycle, derating the thermal efficiency (heat rate) of the power plant.

Reproduced with permission of the copyright owner. Further reproduction prohibited without permission.

2.1.2. Oxy-Fuel Combustion

When a fossil fuel (coal, oil or natural gas) is combusted in air, the fraction of CO_2 in the flue gas ranges from 3-15% depending on the carbon content of the fuel and the amount of excess air necessary for the combustion process. The separation of CO_2 from the rest of the flue gases (mostly N_2) by chemical or physical means is energy and capital intensive. An alternative is to burn the fossil fuel in pure or enriched oxygen. When this approach is taken, the flue gas will contain mostly CO_2 and H_2O. A part of the flue gas needs to be recycled into the combustion chamber in order to control the flame temperature. From the non-recycled flue gas, water vapor can be readily condensed, and the CO_2 can be compressed and piped directly to a storage site [8].

2.1.3. Pre-Combustion Capture

Pre-combustion capture is usually applied in coal gasification combined cycle power plants. This process includes gasifying the coal to produce a synthesis gas composed of CO and H_2; reaction of the CO with water (water-gas shift reaction) to produce CO_2 and H_2; capturing the CO_2; and sending the H_2 to a turbine to produce electricity. Since the primary fuel sent to the gas turbine is now hydrogen, some can be bled off as a fuel for separate use, such as in hydrogen fuel cells to be used in transportation vehicles. Worldwide, gasification facilities exist today that do not generate electricity, but rather synthesis gas and various other by-products of coal gasification. In these facilities, CO_2 is separated after the gasification stage from the other gases, such as methane, hydrogen or a mix of carbon monoxide and hydrogen. For example, the Great Plains Synfuel Plant, near Beulah, North Dakota, gasifies 16,326 metric tonnes per day of lignite coal into 3.5 million standard cubic meters per day of combustible syngas and close to 7 million standard cubic meters of CO_2. A part of the CO_2 is captured by a physical solvent based on methanol. The captured CO_2 is compressed and 2.7 million standard cubic meters per day are piped over a 325 km distance to the Weyburn, Saskatchewan, oil field, where the CO_2 is used for enhanced oil recovery [7].

2.2 Economics of Capture Process

The largest potential market for CO_2 is in EOR. The most economical sources of CO_2 are CO_2 wells and natural gas sweetening or synthesis gas purification by-products. Flue gases have long been an important source of CO_2 for the merchant CO_2 market, especially in remote locations where by-product CO_2 sources are unavailable. In the simplest case, fuel is combusted to produce flue gas. CO_2 is then extracted from the flue gas using a dilute MEA solution, as sufficient heat is available from the combustion process to support the heat required for the CO_2

Reproduced with permission of the copyright owner. Further reproduction prohibited without permission.

capture. This process is widely used but is wasteful of energy. Where a source of flue gas is available and lower energy consumption is desired, skid-mounted units employing the Econamine Flue Gas (FG) technology can be utilized [7].

Carbon Capture and Storage (CCS) costs can be considered in terms of four components: separation, compression, transport, and injection [8]. These costs depend on many factors, including the source of the CO_2, transportation distance, and the type and characteristics of the storage reservoir. In this section, the costs associated with capture from fossil fuel-fired power plants with subsequent transport and storage are considered. In this case, the cost of capture includes both separation and compression costs because both of these processes almost always occur at the power plant.

2.2.1 Cost of Capture

Figure 1 shows the present cost of electricity (COE) from three types of CO_2 capture power plants: Integrated Gasification Combined Cycles (IGCC), Pulverized Coal Fired Single Cycle (PC), and Natural Gas Combined Cycles (NGCC). This results in an increase in the cost of electricity of 1-2¢/kWh (50%) for an NGCC plant, 1-3¢/kWh (47%) for an IGCC plant, and 2-4¢/kWh (87%) for a PC plant [8].

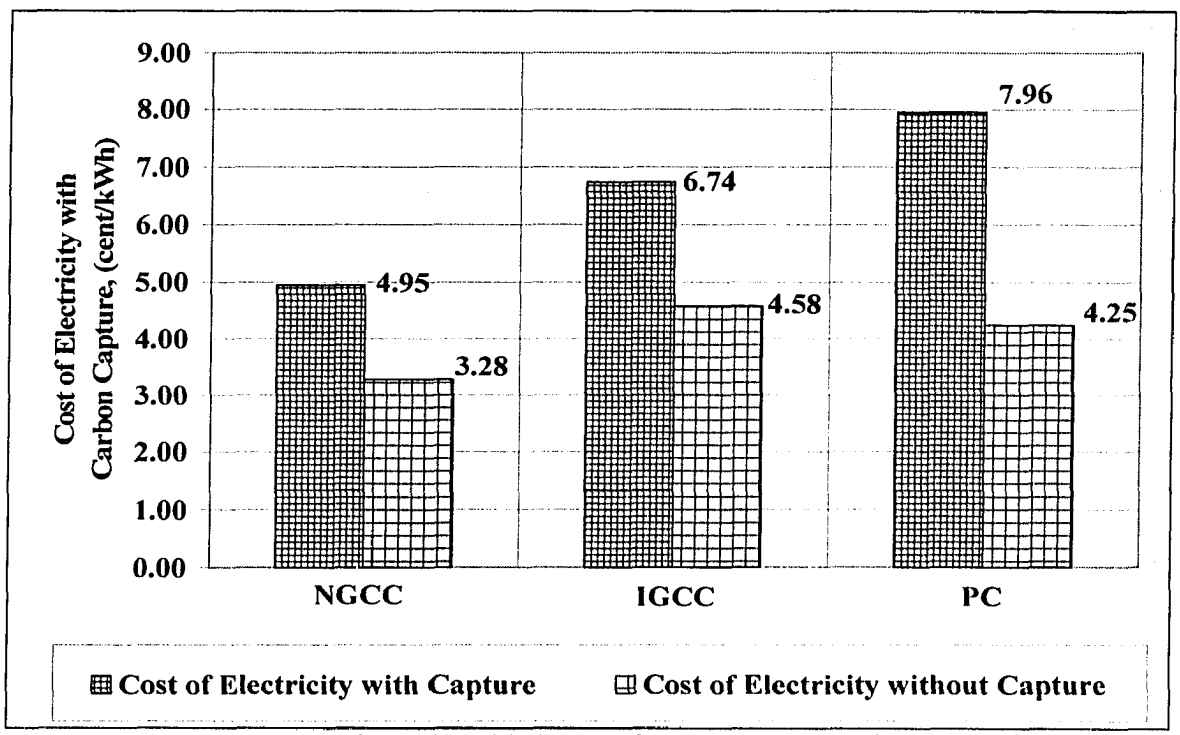

Figure 1 Cost of Electricity with Capture for Various Types of Power Plants (after Herzog and Golomb [8])

Reproduced with permission of the copyright owner. Further reproduction prohibited without permission.

2.2.2 Cost of Transportation

In Figure 2 the cost of transporting CO_2 in large quantities by pipeline is given. Costs can vary greatly because pipeline costs depend on terrain, population density, etc. Economies of scale are realized when dealing with over 10 million metric tons per year (equivalent to about 1500 MW of coal-fired power). This cost is about \$0.50/metric tonne/100 km, compared to truck transport of \$6/metric tonne/100 km [8].

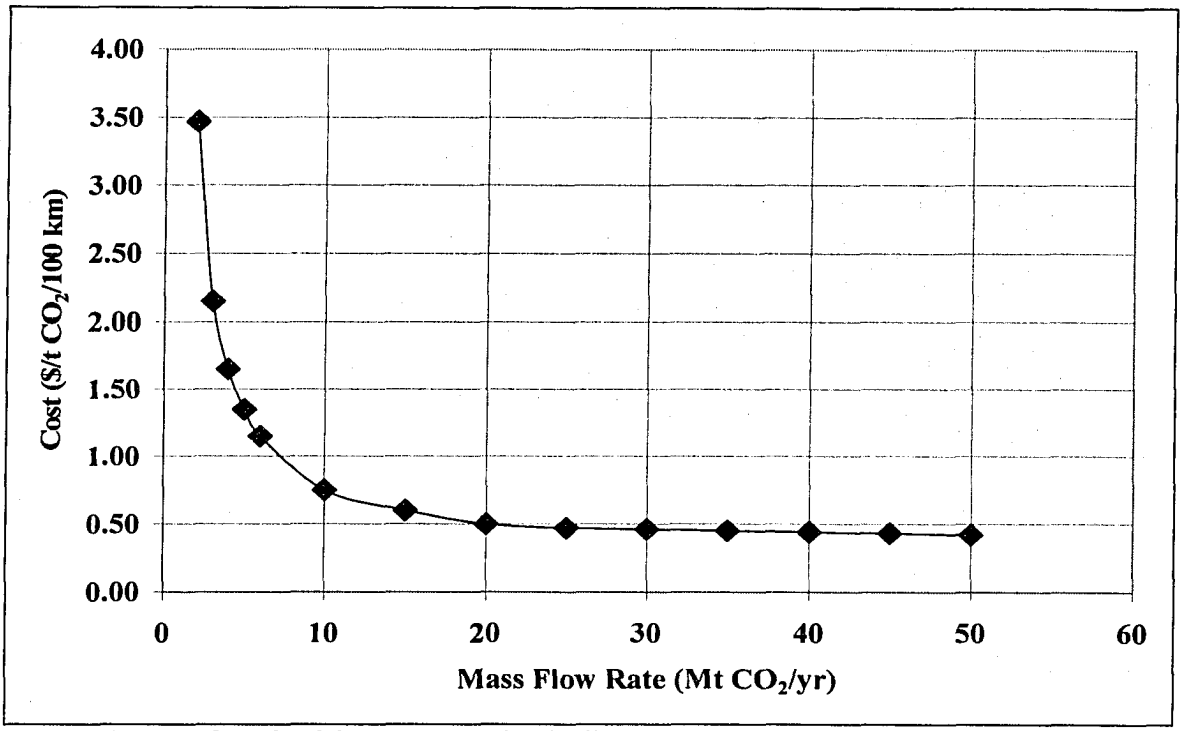

Figure 2 Cost for CO_2 Transport via Pipeline as a Function of CO_2 Mass Flow Rate (after Herzog and Golomb [8])

2.2.3 Cost of Injection and Storage

Figure 3 summarizes the cost of the various carbon storage technologies. The points on the graphs are the average values for a typical base case storage. The results include the range of conditions found in the various reservoirs (depth, permeability, etc.), distance between source and sink (a range of 0-300 km here), and by-product prices (i.e., oil and gas). Excluding the more expensive ocean tanker option, the typical base case costs for CO_2 storage (transport + injection) without oil or gas by-product credit is in the range of \$3-5.50 per tonne CO_2 [8]. The overall cost range can be characterized as \$2-15 per tonne CO_2. With a by-product credit for the gas or oil, the

Reproduced with permission of the copyright owner. Further reproduction prohibited without permission.

credit will offset the storage costs in many instances. For example, in the base EOR case, the cost of CO_2 storage is $-12.21 per tonne.

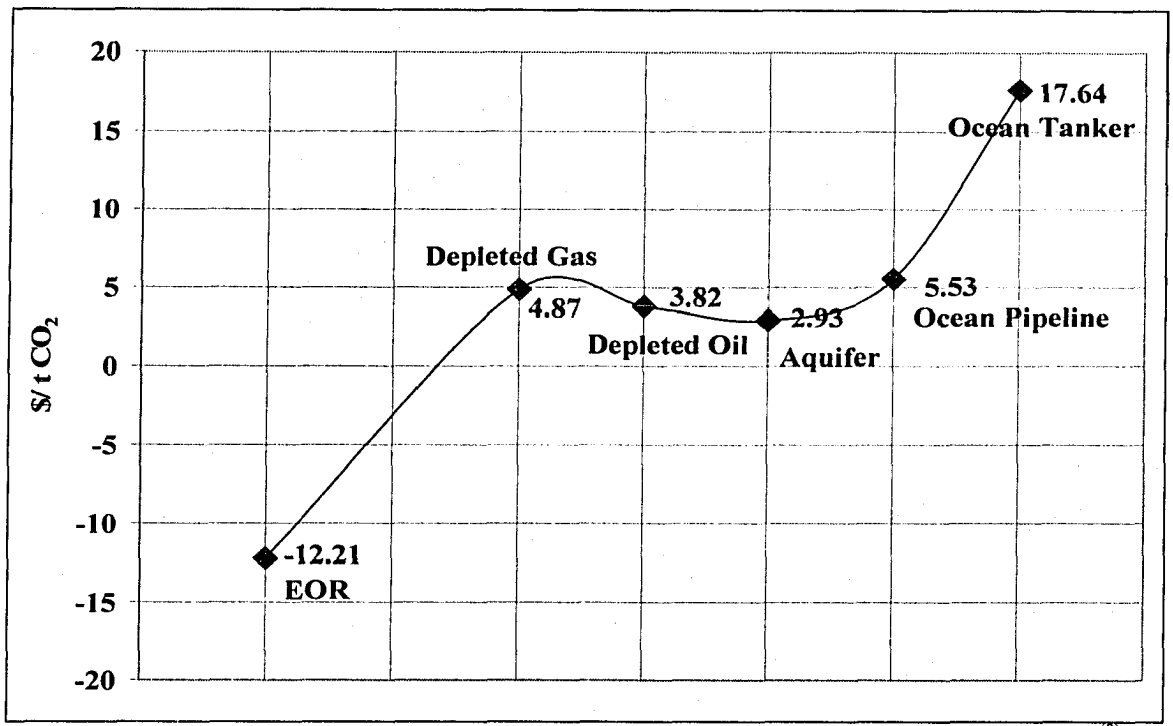

Figure 3 Range of Costs for Various Carbon Storage Methods (after Herzog and Golomb [8])

2.2.4 Overall Costs

The market price of CO_2 varies widely, for instance from $13/tonne delivered at pressure in Canada in 1997 to $55/tonne in the U.S. in 1986. In 1985, the North American EOR market was commercially successful with a US $190/sm^3 ($30/bbl) oil price and a CO_2 price of approximately $0.35to $0.70/sm^3, which is equivalent to $19 to $38/tonne CO_2 [8].

Finally, the results of CO_2 recovery from flue gas add $37.80/sm^3 ($6/bbl) [7] to the oil production cost. All the commercial scale CO_2 storage projects either in operation (Sleipner, Weyburn) or planned (Snovit by Statoil in North Sea and In Salah by BP in Algeria) can be classified as targets of opportunity. Finally, new technologies can reduce the costs associated with CCS.

2.3 CO_2 Disposal Options of Steam Flooded Reservoirs

To meet targets for greenhouse gas emission reductions set by the Kyoto Protocol [5], developed countries are considering a range of near-term options to reduce their greenhouse gas

Reproduced with permission of the copyright owner. Further reproduction prohibited without permission.

emissions, such as fuel switching, energy efficiency improvements and use of renewable sources of energy. However, to meet the goal of the UN Framework Convention on Climate Change, namely the stabilization of greenhouse gas concentrations in the atmosphere, it is likely that deeper reductions in emissions will be needed. To achieve deep reduction in emissions, additional measures will be needed such as geological storage of CO_2. Geological storage of CO_2 would be used to sequester CO_2 captured from anthropogenic sources, such as power and large industrial plants. There are a number of reservoirs suitable for geological storage of CO_2 including depleted oil and gas fields.

2.3.1 Major CO_2 Disposal Options

Several key criteria must be applied to the storage method [9]: (a) the storage period should be prolonged, preferably hundreds of thousands of years; (b) the cost of storage, including the cost of transportation from the source to the storage site, should be minimized; (c) the risk of accidents should be eliminated; (d) the environmental impact should be minimal; (e) the storage method should not violate any national or international laws and regulations.

The major options available for large scale disposal of CO_2 are: 1-Disposal in the deep ocean, 2-Disposal in deep aquifers, 3-Disposal in exhausted gas and oil reservoirs.

Storage media include geologic sinks and the deep ocean. Geologic storage includes deep saline formations (sub-terranean and sub-seabed), depleted oil and gas reservoirs, and unminable coal seams. Deep ocean storage includes direct injection of liquid carbon dioxide into the water column at intermediate depths (1000-3000 m). At depths greater than 3000 m, liquid CO_2 becomes heavier than sea water, and if released there, would descend to greater depths. When liquid CO_2 is in contact with water at temperatures less than 10 °C and pressures greater than 4.5 MPa, a solid hydrate is formed in which the CO_2 molecule occupies the center of a cage surrounded by water molecules. Therefore, it would drop to the ocean bottom and form a so-called "CO_2 lake" [8].

In addition, it is also theoretically possible to store CO_2 as a solid in thermally insulated repositories, although there is a significant energy penalty associated with producing solid CO_2 and the practicality of constructing such a repository is questionable.

2.3.1.1 Disposal in Exhausted Steam Flooded Reservoirs

The general concept of CO_2 disposal in depleted oil reservoirs is that the underground volume of the ultimately recoverable hydrocarbons is replaced by CO_2. In order to make full use of the storage capacity, the CO_2 should be stored as a dense phase fluid that is above the critical

Reproduced with permission of the copyright owner. Further reproduction prohibited without permission.

pressure of 7.4 MPa (Figure 4). This condition is met at depths below 800 m. At this depth the temperature is also above the critical temperature (31°C). About 80% of the world's oilfields are at depths greater than 800 m [9].

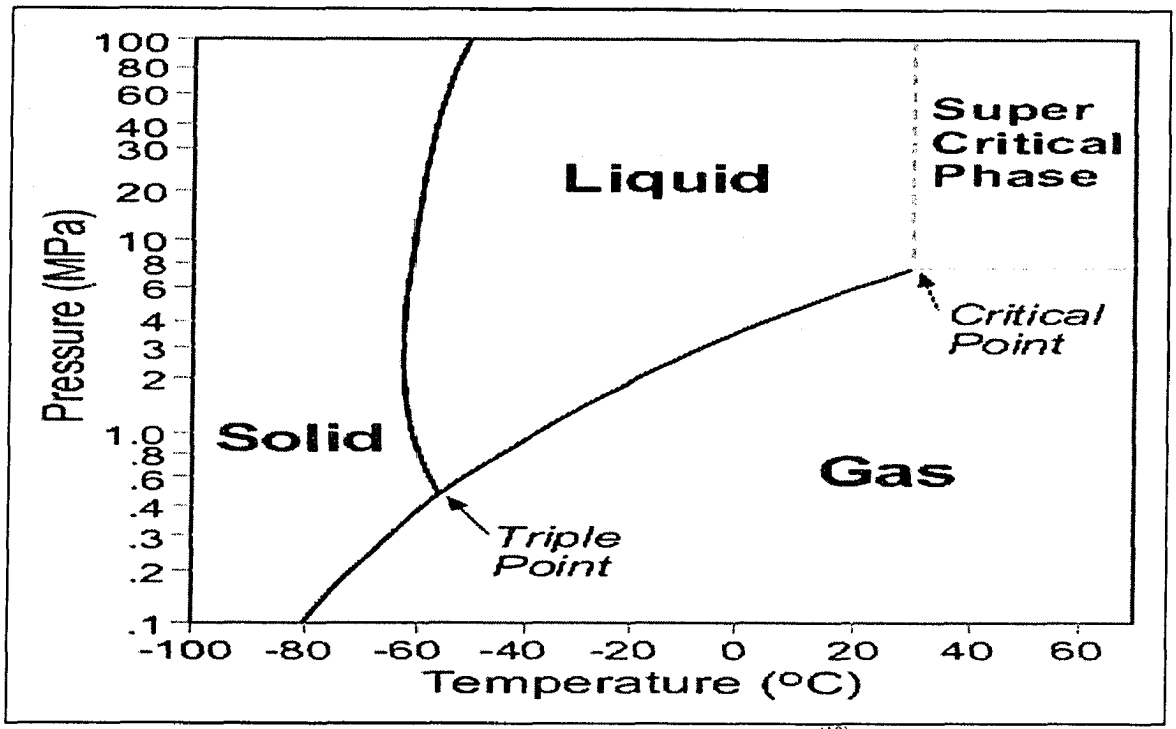

Figure 4 CO_2 Phase Diagram after Bachu [10]

The CO_2 is injected and stored in the intergranular pores of the reservoir rock. As dense phase CO_2 is still less dense than formation water, it will naturally rise to the top of the reservoir and a trap is required to ensure that it does not reach the surface; this is a natural feature of existing oil and gas reservoirs [10]. A proven trap, well known reservoir properties and only a limited requirement for exploration are all reasons for the storing of CO_2 in depleted hydrocarbon reservoirs. This represents a simpler and cheaper option than storage in aquifers. Estimates of the potential capacity of depleted oil reservoirs for storage of CO_2 have been derived from estimates of cumulative production and proven reserves of oil and natural gas. However, different assumptions are made in terms of the proportion of the volume of the depleted reservoir available for CO_2 storage, whether some of the gas is associated with oil, the proportion of reservoirs that could be used and the extent to which already depleted reservoirs could be used. An estimate of the potential storage capacity for CO_2, based on proven reserves, suggests a capacity approaching 200 Gigatonnes (Gt = 10^9 tonnes) would eventually become available. Around 70% of this capacity is associated with natural gas reservoirs. This figure could double if unproven reserves

Reproduced with permission of the copyright owner. Further reproduction prohibited without permission.

are taken into account, but much of this capacity is associated with large fields in the Middle East. In the steam flooded reservoir case, the hydrocarbons in the reservoir are replaced by steam. This steam condenses and becomes water in the reservoir. Then, after the economic producing life of the reservoir, by using the CO_2 solubility of water and hydrocarbons remaining in the reservoir, these fields can be used also as storage sinks.

2.4 Carbon Dioxide Flooding

To understand the importance of CO_2 injection and soaking prior to steam injection, it is necessary to explore the relations which exist between CO_2 gas and heavy oil. CO_2 has been a subject of interest in the oil industry for over 30 years. Originally, interest in CO_2 flooding arose because of its potential for enhanced oil recovery (EOR) [11].

Both laboratory studies and field applications have shown that CO_2 can be an efficient oil-displacing agent. The various mechanisms by which it can mobilize and displace oil in porous media have been of particular interest to the petroleum industry. These mechanisms include: (1) solution gas drive, (2) immiscible CO_2 drive, (3) hydrocarbon-CO_2 miscible drive, (4) hydrocarbon vaporization, (5) direct miscible CO_2 drive, and (6) multiple-contact dynamic miscible drive [12].

The importance of a given mechanism depends on whether the injected CO_2 is miscible or immiscible with the in-place oil. The main effects associated with immiscible CO_2 flooding are oil viscosity reduction, oil phase swelling, and solution gas–oil drive during pressure blow-down. The results obtained for immiscible CO_2 or gas flooding are affected primarily by the gas slug size, the number of slugs, the injection rates of the water and gas slugs for water alternating gas injection (WAG), the WAG ratio and WAG cycle, the reservoir operating pressure, the extent of phase equilibrium, and other factors related to rock–fluid interactions [13].

In miscible processes, as miscibility is approached, the oil and CO_2 phases (which now contain many of the intermediate hydrocarbon components) tend to flow together because of the low interfacial tension and the relative increase in the total volumes, of the combined CO_2 and oil phases, as compared to the water phase. However, the generation of miscibility between the oil and CO_2 is still considered to be the most important mechanism. Moreover, miscibility occurs in most CO_2/crude-oil systems, provided the pressure is high enough. High pressures are required to compress the CO_2 to a density at which it becomes a good solvent for the lighter hydrocarbons in the crude oil. The pressure at which miscibility first takes place is called the minimum miscibility pressure (MMP). Because of this minimum pressure requirement, reservoir depth is an important screening criterion, and CO_2 floods are carried out usually in reservoirs that are more than 762 m

Reproduced with permission of the copyright owner. Further reproduction prohibited without permission.

(2,500 ft) deep. Oil composition is also an important factor, as a high percentage of intermediate hydrocarbons (especially C_5 through C_{12}) can contribute to the mobility. Surveys show that the oil gravity exceeds 30°API for most active CO_2 floods [14].

Srivastava et al.'s laboratory studies [15] indicate that reservoirs suitable for CO_2 miscible flooding contain hydrocarbons that have CO_2 minimum miscibility pressures ranging from about 11.5 to 14.5 MPa. And, to reach a one-contact miscible state, the CO_2 concentration should be above 60 mol% for Weyburn oil. Moreover, the PVT data generated for the reservoir fluid-CO_2 mixtures show that viscosity reduction and oil swelling by CO_2 also contribute to oil recovery significantly.

Dong et al. [16] studied the effect of dissolved gas in the reservoir oil on the CO_2 MMP. According to their work, large amounts of dissolved gas or methane have a significant effect on the MMP. Higher gas-oil ratios, or dissolved gas, in the reservoir fluid caused higher CO_2 MMPs.

Recently, Yangmao et al. [17] conducted a laboratory CO_2 flood from which they collected experimental PVT data for a given reservoir. They demonstrated that by using the measured PVT properties, which included the bubble point pressure, the formation volume factor, the swelling factor, the solubility of the CO_2 and the viscosity of the reservoir oil , it was possible to obtain regression curves, which could be used to estimate the PVT behavior for any hydrocarbon during miscible CO_2 flooding. They found results similar to those of Srivastava et al. and Dong et al. for one-contact miscible concentrations of CO_2 (Shengli oil above 59 mol%) and higher bubble point pressures causing higher MMPs.

2.4.1 Enhanced Oil Recovery with Carbon Dioxide

In most CO_2-EOR projects, much of the CO_2 injected into the oil reservoir is only temporarily stored in the reservoir [5]. This is because the decommissioning of an EOR project usually involves the "blowing down" of the reservoir pressure to maximize oil recovery. Such "blowing down" of the reservoir results in most of the CO_2 being released to the atmosphere, with only a small, but significant amount of the injected CO_2 remaining dissolved in the immobile oil. The Weyburn Field in south-eastern Saskatchewan, Canada, is the only CO_2-EOR project to date that has been monitored specifically to understand CO_2 storage. In the case of the Weyburn Field, no blow-down phase is planned, thereby allowing for permanent CO_2 storage. Over the anticipated 25-year life of the project, it is expected that the injection of some 18 million tonnes of CO_2 from the Dakota Gasification Facility in North Dakota will produce around 130 million bbl of enhanced oil. This has been calculated to be equivalent to approximately 14 million tonnes

Reproduced with permission of the copyright owner. Further reproduction prohibited without permission.

of CO_2 being prevented from reaching the atmosphere. The 14 million tonnes include the CO_2 emissions from the generation of electricity required for the whole EOR operation [18].

Jeschke et al.[19] presented the results of a study of the CO_2 flooding potential of California oil reservoirs and listed possible sources of CO_2 for California enhanced oil recovery projects. They concluded that California has large quantities of oil in reservoirs which will probably respond well to CO_2 flooding. Two of these fields are the Wilmington Field Tar Sand and the Lost Hills field.

Some CO_2 injection projects do not achieve the MMP for their reservoir oils. In 1986, such an immiscible CO_2 flood was applied successfully to the Bati Raman [20] field in Turkey, which has an estimated 1.85 billion barrels of heavy oil reserves. Due to the low reservoir energy and to the unfavourable oil properties such as low gravity (12° API [0.986 g/cm^3]) and high viscosity (592 cp [0.592 Pa.s]), a poor primary recovery of the field's reserves (1.5% OOIP) was achieved by 1986. After starting immiscible CO_2 flooding, 5% of the field's reserves were produced by 2003. Subsequently, to increase the CO_2 sweep efficiency, polymer gel treatments were started, and the field currently continues to be produced.

Table 1 Reservoir and Fluid Characteristics for Wilmington, Weyburn and Bati Raman Fields

Field Name	Wilmington	Weyburn	Bati Raman
Zone	Tar	Midale Unit	Garzan
Lithology	Sand	Limestone	Limestone
CO_2 Injection Type	Immiscible	Miscible	Immiscible
Porosity, %	27	17.2	18
Average Permeability, md	700	15	58
Depth, m	701	1399	1310
Reservoir temperature, °C	49	61	54
Oil gravity, °API	14	29	12
Initial oil saturation, fraction	0.75	0.70	0.65
Average gross oil pay, m	91	15	64
Average net oil pay, m	43	7.83	50
Initial pressure, kPa	6800	14600	12400
Initial OIP, STB	69,465,000	176,185,000	1,850,000,000
Residual oil, STB	53,301,000	123,329,500	1,720,000,000
Oil density, kg/m^3	969	858	986
Discovery year	1961	1954	1961
Viscosity range in reservoir, cp	180 - 410	4.7	450 to 1000

Reproduced with permission of the copyright owner. Further reproduction prohibited without permission.

The reservoir and oil properties of these fields are given in Table 1 [20, 21, 22]. If one compares the CO_2 injection projects of the above examples, the Weyburn Field is different from the other fields, both with respect to the oil type and the CO_2 injection mechanism. In the Weyburn field, CO_2 has been injected at 12 MPa (miscible flooding) into a light oil reservoir (29 °API) at a depth of 1400 m. The Bati Raman Field immiscible CO_2 injection has been continued with gel treatment. In the California Wilmington Tar Sand reservoir, between 1982 and 1986, WAG injection has been applied.

The above examples of CO_2 flooding show that, whatever the injection (miscible or immiscible) or rock type (sandstone or limestone) or the fluid (heavy or light oil) characteristic of the reservoir, CO_2 is an indispensable tool for enhanced oil recovery.

2.5 Steam Flooding

Of all the enhanced oil recovery processes currently available, only the steam injection processes are widely used on a commercial basis in North America due to very high viscosity of the hydrocarbons in the reservoirs. The shallow and high oil saturation reservoirs are good candidates for these thermal processes [23]. Depths shallower than about 100 m may not permit good injectivity because the pressures required may exceed fracture gradients. Due to difficulty in insulation of the steam carrying pipes in the well bore, heat losses become important at depths greater than about 770 m and steam flooding is not considered at depths greater than 1500 m. There are two types of steam injection processes used for recovering heavy oils. Cyclic steam stimulation is for oil reservoirs having an oil gravity of less than 15° API, and continuous steam injection (steam flooding) is applied to reservoirs having oil gravities between 12-25° API [23].

The cyclic steam stimulation process involves a shut-in period of a few days following steam injection into the formation. Thereafter, the well is put back on production with very high oil-water ratios. The production rate declines with time with increasing water-oil ratios, but may still be well above the pre-stimulation rate, even after 6-12 months when considering a mobile heavy oil reservoir. Then, the treatment may be repeated. Many "cycles" may be conducted in this manner, depending on the reservoir production response. Three to five cycles are usually employed, although as many as 22 were used in one instance [24].

Steam flooding or steam drive is a process during which steam is used as the heat displacing agent, much like water in water flooding, usually on the basis of a suitable pattern. Steam is continuously introduced into a high permeability reservoir [23] to reduce the viscosity of the heavy oil and provide a driving force to displace the mobilized oil towards the producing wells. Because it is intended to displace the in-place heavy oil, much of which is loaded in the

Reproduced with permission of the copyright owner. Further reproduction prohibited without permission.

vicinity of the production wells where it is cold, the oil viscosity is expected to drop below 1000 cp at reservoir conditions.

During the steam flooding process, thermal energy is introduced into the reservoir by steam injection and condensation. The available heat is transferred to the oil bearing formation, the reservoir fluids, and some of the adjacent cap and base rock. Steam condenses to yield a mixture of steam and hot water flowing through the reservoir. The main effects present in steam flooding are the in-place oil viscosity reduction and its thermal expansion. Other thermal effects such as steam distillation, miscible drive, variation of relative permeabilities with temperature, and so on, play a secondary role in the oil recovery. Under ideal conditions, there is a "steam zone" in the vicinity of the injection well, which is at the steam temperature. The oil saturation here is very low, perhaps of the order of 20 %. Further ahead, there exists a "hot waterflood zone", where a high temperature displacement with the condensed water (hot waterflood) takes place. Still farther ahead, the formation is at the original formation temperature and cools the steam condensate where it acts as a cold waterflood. The oil recovery is the total amount displaced as these three consecutive zones propagate through the reservoir [24].

2.5.1 Steam-Assisted Gravity Drainage

Butler first emphasized the importance of gravity drainage as an oil production mechanism in 1981[25]. Steam-assisted gravity drainage (SAGD) is a special form of steam flooding, which has been used for recovering heavy oils for years, mostly in Canada, USA and Venezuela [26]. During this process, steam is continuously introduced into the reservoir through a horizontal injection well. A non-uniform chamber-like steam interface develops and expands, parallel to a horizontal production well which is located several meters below the horizontal injector. Mobilization of the heavy oil and condensation of the steam take place in the vicinity of the chamber interface. Movement of the oil and steam condensate towards the producer is due to gravitational forces (drainage) and takes place parallel to the interface [26].

The thermal energy of steam reduces the oil viscosity, and the horizontal wells provide a large reservoir contact area, resulting in increased recovery [27]. According to Butler, SAGD is feasible only when steam is injected above but close to a production well, which is completed at the base of the reservoir. The steam would then tend to rise, condense and drain together with the heated oil. The oil and condensate should be removed continuously from the production well. It was thought that, if these fluids were not removed too quickly, the tendency of the steam to flow directly to the production well and thus bypass the reservoir could be reduced or even eliminated. This is called the steam trap mechanism [26].

Reproduced with permission of the copyright owner. Further reproduction prohibited without permission.

Rose and Doe [28] also emphasized the attractive nature of this concept. The intention in developing the SAGD process was to devise a means where heavy oil or bitumen could be removed in a systematic manner in order to give a more complete recovery than is possible in conventional steam flooding processes, where the oil is moved by pushing it with the injected fluid. Gravity is already present throughout the reservoir, and by using it as the chief driving force to affect oil movement, it is possible to avoid the differential fingering that occurs when viscous oils (high density) are moved by pushing with less viscous oil (low density).

2.6 Carbon Dioxide with Steam Injection

The SAGD process has been used successfully for the commercial exploitation of the heavy oil and bitumen reservoirs in Canada. However, high SAGD production rates are associated with excessive energy requirements and the generation of large amounts of CO_2. For years, many researchers have been looking for ways to decrease the energy requirements as much as possible to make the operation more profitable and environmentally friendly. The addition or presence of CO_2 is one of the ways which can be used to decrease steam consumption during the flooding process. Some examples from the literature of how the addition of CO_2 to steam can be beneficial are given in the following paragraphs.

The effect of initial gas content on thermal EOR was investigated first by Frauenfeld et al. [29]. They conducted physical model experiments to study the effects of steam injection on EOR processes. For oils containing no initial CH_4 gas, co-injection of CO_2 was capable of improving oil recovery, as compared with that obtained with the injection of steam only. When an initial dissolved gas was present, co-injection of CO_2 was not favorable. The steam-only case gave better results than the steam/CO_2 case. However, injection of CO_2 or CH_4 slugs just before the injection of steam was beneficial in increasing oil recovery for experiments where an initial dissolved gas was present [29].

Metwally [30] conducted a laboratory program for the Lindbergh (Alberta) field to investigate the effect of CO_2 and CH_4 on the performance of steam processes. His results indicated that the presence of a non-condensable gas improved steam injectivity. Injectivity improvement was most pronounced when a CO_2 gas slug was injected prior to the injection of steam. However, the co-injection of a non-condensable gas with the steam did not improve recovery. This resulted in much higher residual oil saturations as compared to steam injection alone.

The effect of hydrocarbon gas injection on oil production during SAGD projects was investigated by Ito et al. using numerical simulation [31]. They concluded that oil production rates

Reproduced with permission of the copyright owner. Further reproduction prohibited without permission.

as well as the total oil production were significantly reduced when CH_4 gas was injected with steam during the early period of a SAGD operation. Because most of the injected gas migrated to the upper part of the leading edge of the steam chamber, vertical growth of the steam chamber was prevented, which caused a reduction in the ultimate oil recovery. However, if the gas injection was initiated during the later stages of the process, an improved steam-oil ratio was obtained without significantly reducing the oil production rates and the total oil production. In this case, the injected non-condensable gas migrated to the upper part of the reservoir but did not prevent the growth of the steam chamber, because the chamber had already grown to the desired size. Gas injection slowed down the growth of the steam chamber in the upper part of the reservoir and induced its lateral and downwards growth.

Canbolat [32] studied the effect of the initial presence of CO_2 in SAGD experiments. His results showed that the cumulative recoveries were almost the same but the cumulative steam-oil ratio (CSOR) was one quarter less in initially CO_2 flooded reservoir experiments. The benefits for the environment, from both GHG emission and water treatment points of view, were more pronounced in initially CO_2 flooded reservoirs.

Reproduced with permission of the copyright owner. Further reproduction prohibited without permission.

CHAPTER 3

STATEMENT OF THE PROBLEM

The reduction of GHG emissions is a growing concern of many industries. Following the solutions recommended by the Kyoto protocol, underground sequestration of CO_2 is a way to meet this goal as oil and gas fields offer huge CO_2 storage capacities while preserving the environment. Geological storage would be used to sequester CO_2 captured from anthropogenic sources, mainly power and large industrial plants.

The aim of this numerical work is to study one scenario for storing and sequestrating CO_2. Unlike the traditional proposals for the sequestration of CO_2 which are usually limited to exhausted reservoirs, the CO_2 is injected at reservoir pressure using horizontal well pairs, prior to steam injection into a virgin heavy oil reservoir. To enable complete distribution of the injected gas around the well bore, the system is shut in for some time. After producing oil by steam flooding to the economic limit of the project, sequestration then is carried out in order to store a maximum amount of CO_2. The source of CO_2 for this initial storage process and for sequestration in later stages can be done using the captured gas from steam generators on-site.

For this scenario, due to its success in the field for oil recovery, steam-assisted gravity drainage is selected as the steam flooding method. Lloydminister-type heavy oil reservoir properties are used in the numerical simulator. Reservoirs containing live and dead oil cases are tested.

The numerical procedure consists of two parts. One part is CO_2 storage and soaking before steam flooding. The second part is the sequestration of CO_2 after steam flooding. In the first part, CO_2 is injected into the reservoir at a constant rate for one year. The CO_2 is left to soak for one year. Then steam flooding is started and pursued until the economic producing limit of the reservoir is reached. The residual saturations of the reservoir fluids are determined at that stage. Then, in order to calculate the amount of CO_2 soluble in a depleted reservoir, the solubility curves generated experimentally for oil and water are used.

In the second part of the simulations, using the saturation values obtained from the first part, CO_2 is sequestrated in the steam flooded reservoir, neglecting the cooling time, until the injection pressure reaches the fracture pressure. Finally, the analytical results of CO_2 sequestration are compared with the numerical simulation results.

Reproduced with permission of the copyright owner. Further reproduction prohibited without permission.

CHAPTER 4

4.1 NUMERICAL SIMULATIONS

4.1.1 Numerical Model

The numerical simulations were performed using CMG's STARS™ [33]. The petrophysical parameters for a typical Lloydminster (Alberta) type heavy oil reservoir, which are taken from the literature, were used in the simulations [3, 4, 34, 35, 36]. The reservoir is assumed to be homogeneous and the other parameters are given in Table 2. The dead oil viscosity alteration versus temperature is presented in Figure 5.

Two cases were considered for this research. The first case was for dead Lloydminster oil, whereas the second was for live Lloydminster oil. In the live oil case, the reservoir oil has 10 % dissolved CH_4 in it.

The remaining parameters are assumed to be the same for each simulation.

Table 2 Lloydminster Reservoir and Fluid Characteristics for Dead Oil Case

Depth of reservoir top	750 m
Height of reservoir	25 m
Temperature of reservoir	21°C
Pressure of reservoir	3500 kPa
Porosity	32%
Permeability	2 Darcy
Viscosity of oil @ reservoir temperature	10,000 cp
Molecular weight of oil	325 g/mole
Initial saturation of heavy oil	0.80
Initial saturation of gas	0
Initial saturation of water	0.20
Compressibility of rock	7.4×10^{-6} 1/kPa
Overburden and underburden heat capacity of formation	2.3×10^{5} J/m^3-°C
Overburden and underburden thermal conductivity of rock	1.4×10^{4} J/m-d-°C

Reproduced with permission of the copyright owner. Further reproduction prohibited without permission.

Figures 6 and 7 represent the front and side views respectively of the reservoir under investigation. The length of the horizontal well was fixed at 500 m. Standard SAGD horizontal wells were used, with the producers located at the bottom of the reservoir, and the injectors located 5 m above the producers. The distance between the horizontal well pairs was varied from 80 to 120 m to see the effect of the injected CO_2 and steam on the performance of oil production. In order to achieve this, the reservoir in the numerical simulations was assumed to be 201 m wide (i direction), 25 m thick (k direction), and 500 m along the horizontal well (j direction). The total grid block number was 201x1x25 (i, j, k). A no flow boundary was used, but heat loss to the overburden was permitted. A sample data file of the simulator input with the dead oil case is given in Appendix A.

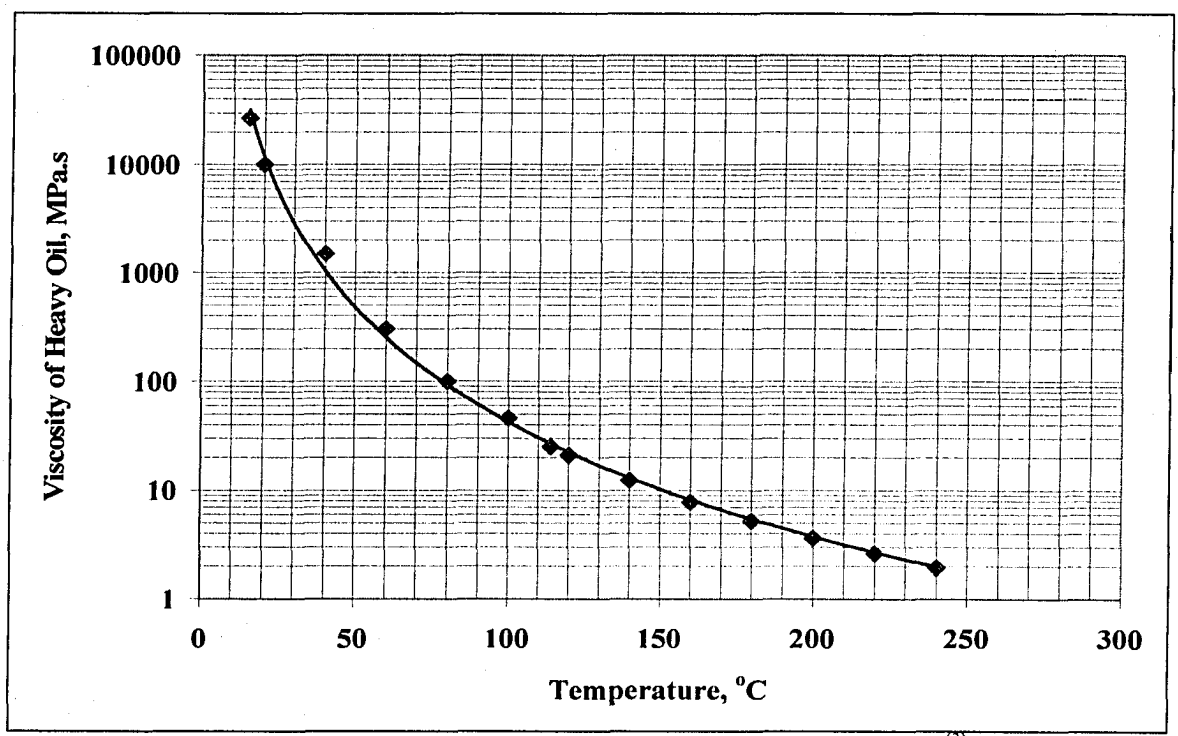

Figure 5 Crude Oil Viscosity versus Temperature (after Butler [3])

Reproduced with permission of the copyright owner. Further reproduction prohibited without permission.

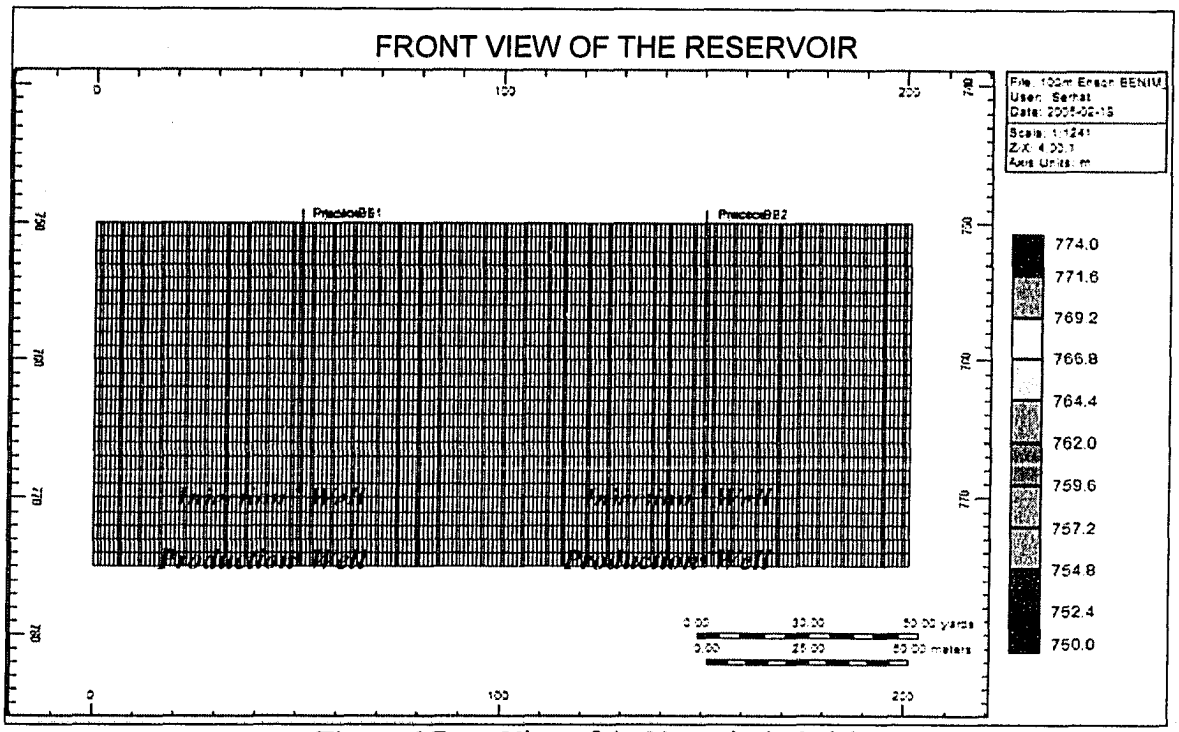

Figure 6 Front View of the Numerical Model

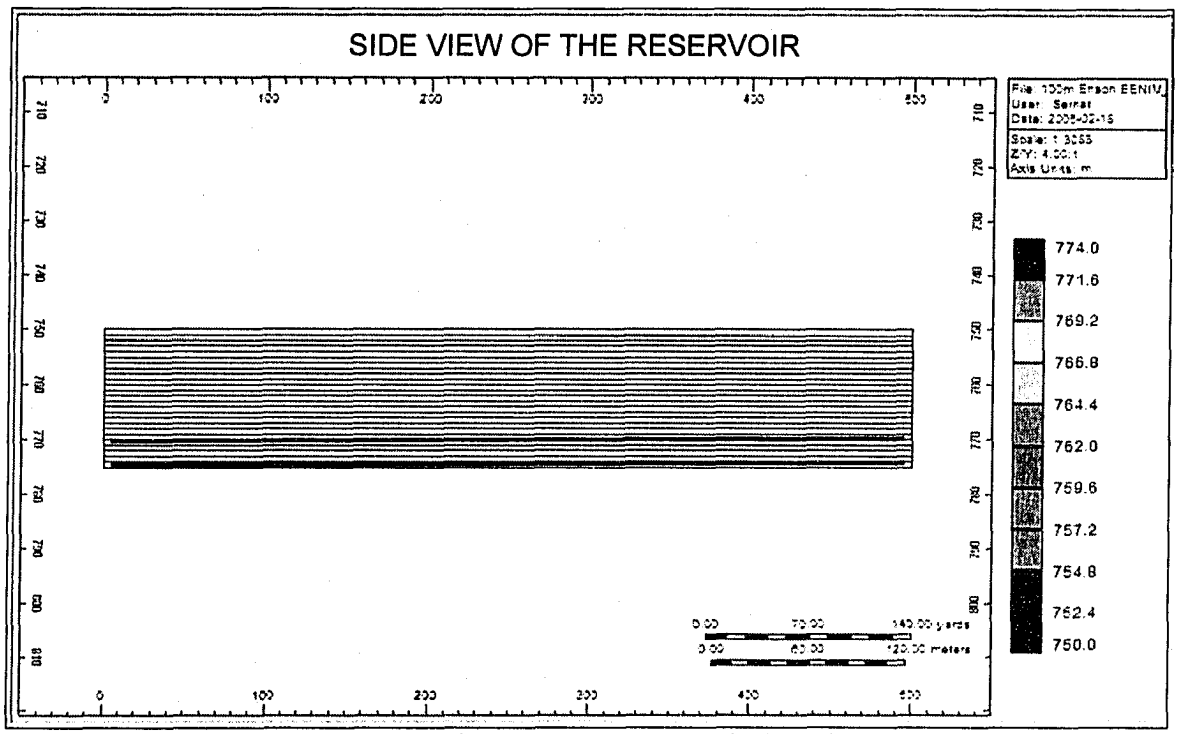

Figure 7 Side View of the Numerical Model

Reproduced with permission of the copyright owner. Further reproduction prohibited without permission.

4.2 Simulations Performed

The simulations were performed in two parts. In the first part, CO_2 was injected into the reservoir and soaked. Then the reservoir was steam flooded. The following procedure was used: one year of continuous CO_2 injection, followed by a one-year soaking period (see section 5.1.1 for optimum soaking time), followed by continuous steam injection until the economic production limit is reached.

After the end of the economic production life of a given reservoir, the simulations were stopped. Then, the residual saturations of the fluids in the reservoir were obtained, assuming that only heavy oil and water were present at the end of the steam injection process (neglecting the injected CO_2 prior to the steam flood and the fact that no more steam is present in the reservoir after cooling).

In the second part, the sequestration simulations were performed. The cooling time of the reservoir after steam injection was neglected. The maximum CO_2 injection was fixed at 2000 sm^3/day (3.72 tonnes/day) to provide a long time with respect to the key storage criteria (see section 2.3.1) [9].The injection temperature was 21°C and the depth of reservoir was 750 m. In the simulation data file, injection of CO_2 was carried out until the fracture pressure of 6500 kPa was reached (assuming a fracture pressure of 7000 kPa, plus a safety factor of 500 kPa).

4.2.1 Reservoir with Dead Oil

In the first case, the reservoir had dead oil with initial oil saturation (S_o) value of 80% and an initial water saturation (S_w) value of 20% respectively. The reservoir pore volume was calculated to be 804,000 sm^3, containing 643,200 sm^3 of original-oil-in-place and a water volume of 160,800 sm^3.

To find the optimum conditions for CO_2 storage, simulations were run using the base SAGD case for various injection rates at various separation distances, varying from 80 to 120 m, between the two injection-production well pairs. Using different steam injection rates, CO_2 storage was also tested at these distances with varying CO_2 injection rates varying from 50 to 700 sm^3/day.

4.2.2 Reservoir with Live Oil

The simulations were carried out changing the oil type, which was now a live oil containing dissolved CH_4. The reservoir had the same initial S_o and S_w values as the dead oil case (see section 4.2.1) However, different from the dead oil case, the oil had 10% dissolved CH_4 in it. The simulations were carried out using the same steam injection rate and well pairs distance, as

Reproduced with permission of the copyright owner. Further reproduction prohibited without permission.

determined in the dead oil case. The reservoir pore volume was calculated to be 804,000 sm^3, containing 643,200 sm^3 of original-oil-in-place (having 10% dissolved CH_4 gas) and a water volume of 160,800 sm^3.

The CO_2 storage and injection effect as well as the ensuring oil recovery due to the presence of CH_4 were investigated in the reservoir at different pressures. The critical rate of CO_2 injection into the gas saturated reservoir needed to be determined as the solubility of CH_4 in the heavy oil is a function of pressure.

The aforementioned sequestration procedure was applied.

4.3 Sequestration Calculations with Solubility Effects

Solubility of one substance in another depends fundamentally upon the ease with which the two molecular species are able to mix. The solubility of CO_2 in fresh water is a function of temperature, pressure and salinity. The amounts of CO_2 that can be dissolved in fresh water are estimated by making use of available experimental work in the literature [37, 38, 39]. A series of solubility curves are used to generate a relational database table of solubility of CO_2 in fresh water at different pressure and temperature combinations (Figure 8). The lower water temperature provides higher CO_2 solubility.

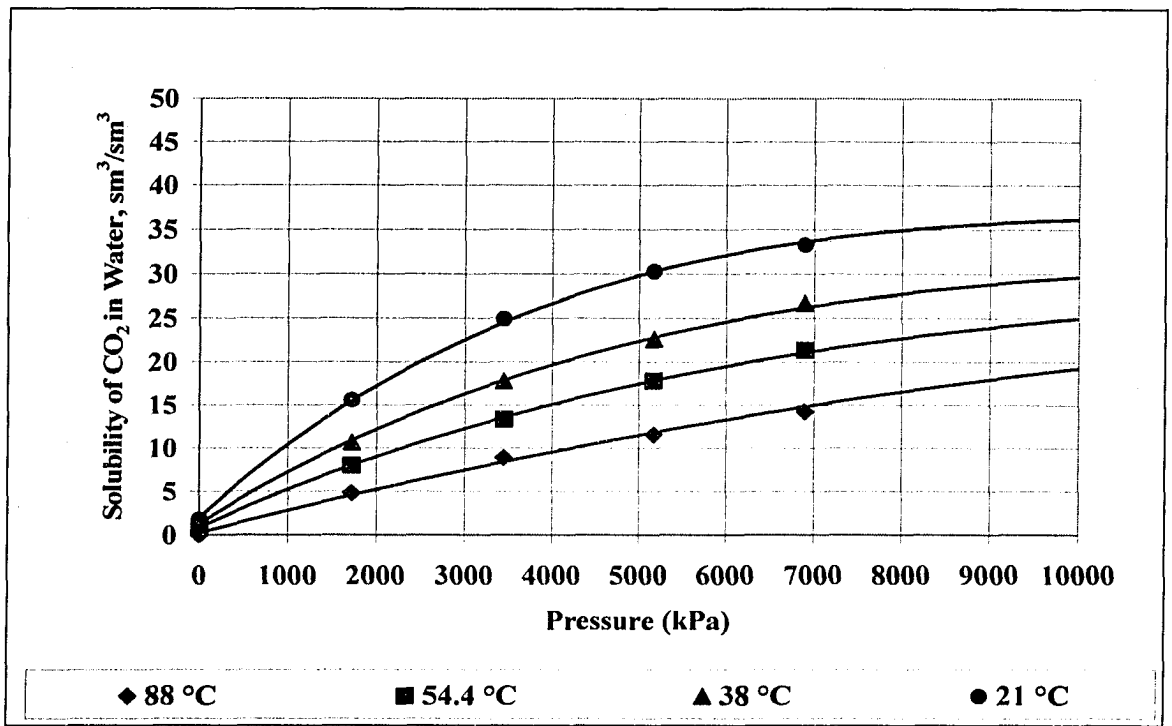

Figure 8 CO_2 Solubility Curves in Fresh Water [37, 38, 39]

Reproduced with permission of the copyright owner. Further reproduction prohibited without permission.

For immiscible (low pressure) applications, the major effect would be the solubility of CO_2 in crude oil. Solubility is a strong function of pressure and to a lesser extent of temperature and oil composition. Solubility increases with pressure and decreases with temperature and reduced API gravity. CO_2 is more soluble in hydrocarbon as a gas rather than as a liquid. The CO_2 solubility decreases as the bubble point pressure of the crude oil increases, requiring higher CO_2 injection pressures. The solubility of CO_2 decreases with increasing concentration of methane [40]. CO_2 is soluble in water to a much less extent than in crude oil. The solubility of CO_2 gas in heavy oil (14 -17 °API) at moderate pressure (4-6 MPa) and temperature (20-25 °C) is approximately 50-100 sm^3/sm^3 which results in a 10-20 % increase in the oil volume [40]. The solubility of CO_2 in Lloydminster oil at different pressures and 21 °C is given in Figure 9 [41].

After running the simulations, the saturation values at the economic limit of oil recovery, which is assumed to be when the cumulative steam-oil ratio (CSOR) exceeds a value of 6, the volumes of the fluids (oil, water, gas) remaining in the reservoir are calculated. Then, assuming the reservoir has returned to its original temperature (neglecting the cooling period after steam flooding the reservoir), and using Figures 8 and 9, the amount of CO_2 that can be dissolved in the reservoir fluids [37, 38, 39, 41] is found.

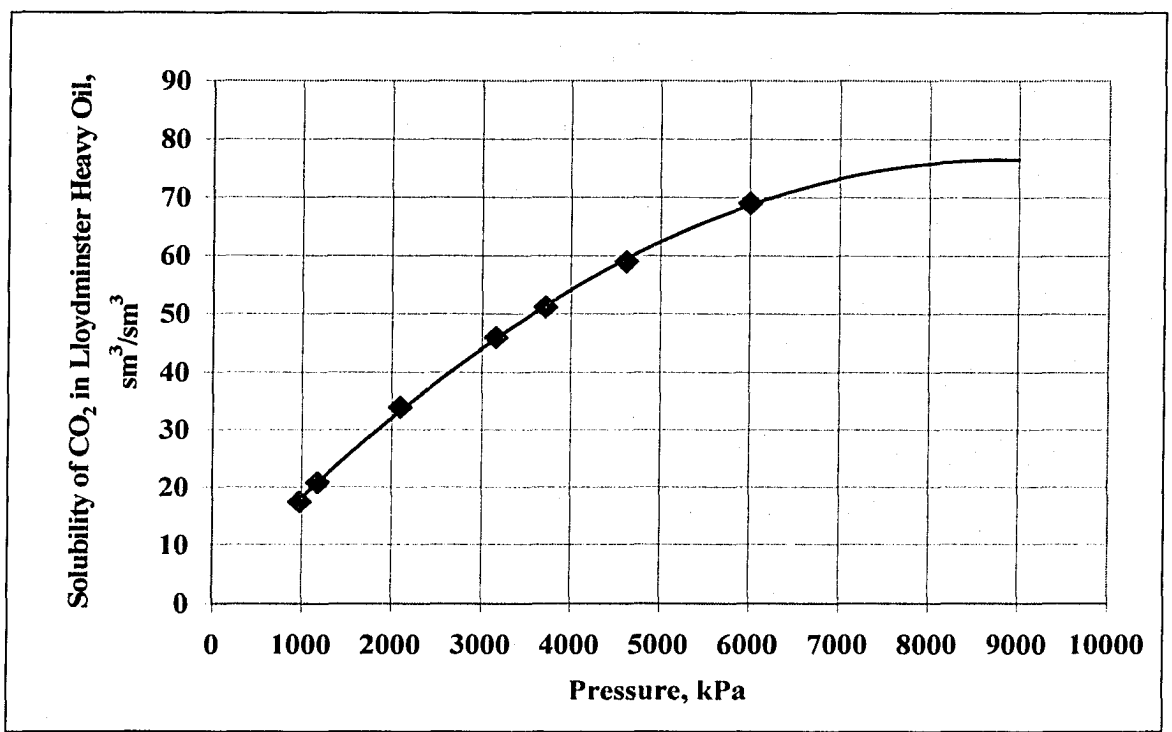

Figure 9 CO_2 Solubility in Crude Oil at 21°C [41]

Reproduced with permission of the copyright owner. Further reproduction prohibited without permission.

CHAPTER 5

RESULTS AND DISCUSSIONS

5.1 Carbon Dioxide Injection Prior to Steam Injection

5.1.1 Reservoir with Dead Oil

Currently, the commonly accepted distance between two well pairs employed by industry is 100 m [3, 42]. To determine the optimal steam injection rate, simulations were run using the base SAGD case with various injection rates and for various separation distances between the two injection-production well pairs.

In the simulations, the distance in the reservoir between two injection-production well pairs was varied from 80 to 120 m. The reservoir pressure was set to 3500 kPa initially. The injection pressure of steam was 3510 kPa at a steam temperature of 242 °C. Three different steam injection rates were tested. The oil recoveries obtained as a function of well pair separation distance and steam injection rate are shown in Figure 10. The recoveries were similar to each other for all conditions.

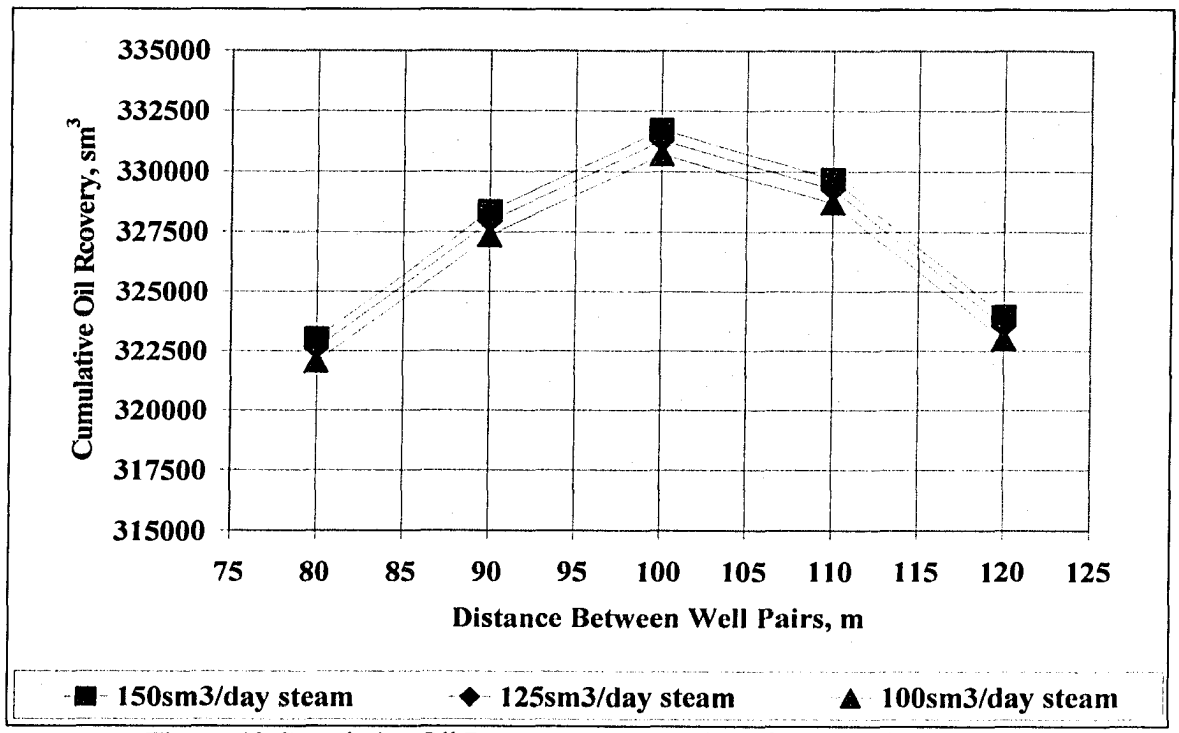

Figure 10 Cumulative Oil Recovery as a Function of Steam Injection Rate

Reproduced with permission of the copyright owner. Further reproduction prohibited without permission.

Figure 11 shows the CSOR and Figure 12 shows the CWOR under the same conditions. The lowest CSOR was found to be 6.5 sm^3/sm^3 at a steam injection rate of 100 sm^3/day/well. Moreover, the lowest produced CWOR values occurred at that same rate rather than at rates of 125 and 150 sm^3/day/well (Figure 12). Also, at this rate, the cumulative oil recovery was virtually at the peak when the distance between the well pairs was 100 m (Figure 10).

Finally, considering that the lowest CSOR and CWOR are a good indication for optimal conditions, and having the highest recovery, 100 sm^3/day/well was selected as the optimum steam injection rate for the simulations.

The optimal CO_2 soaking period was found after determining the optimal steam injection rate. Using four CO_2 injection rates with a 100 sm^3/day/well steam injection rate in the dead oil case at 3500 kPa reservoir pressure, the maximum volume of CO_2 stored was determined as a function of time. Figure 13 shows the results of the simulations where the maximum CO_2 storage amount was determined to be one year prior to steam flooding. At the end of one year (12 months), 100 % of the injected CO_2 was stored for all injection rates. This value was used for all the soaking simulations and was assumed constant (one year for each run).

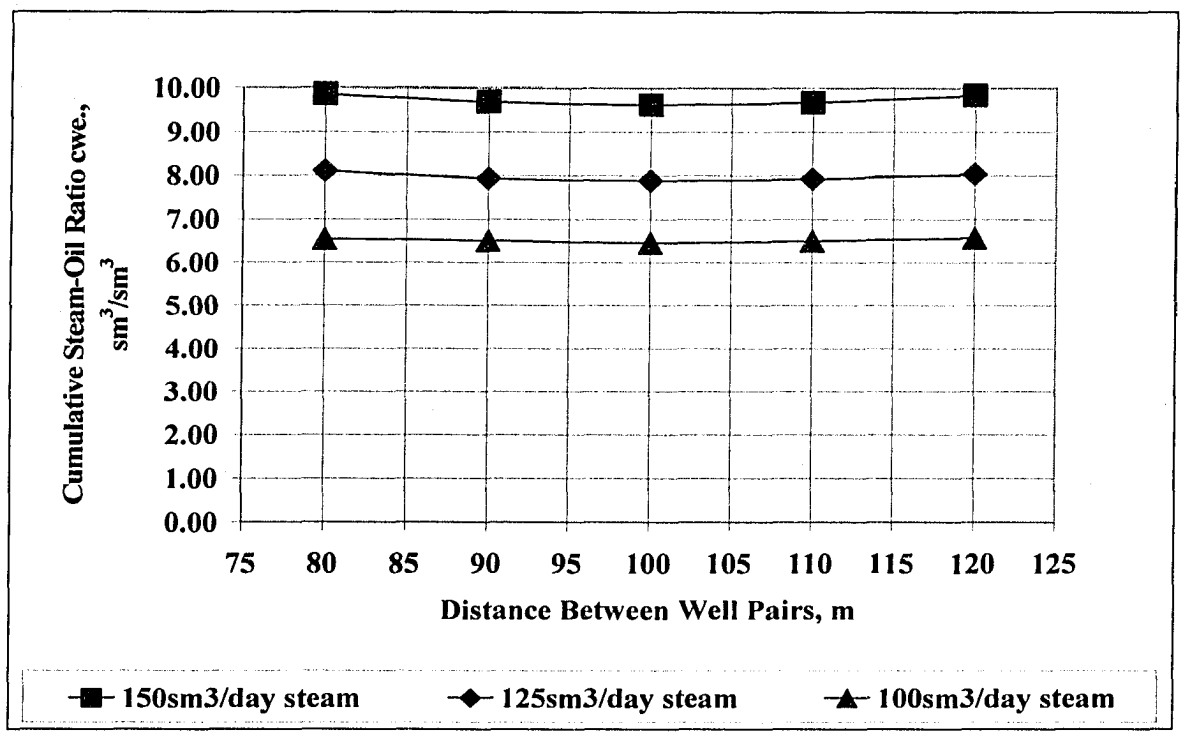

Figure 11 Cumulative Steam-Oil Ratio as a Function of Steam Injection Rates

Reproduced with permission of the copyright owner. Further reproduction prohibited without permission.

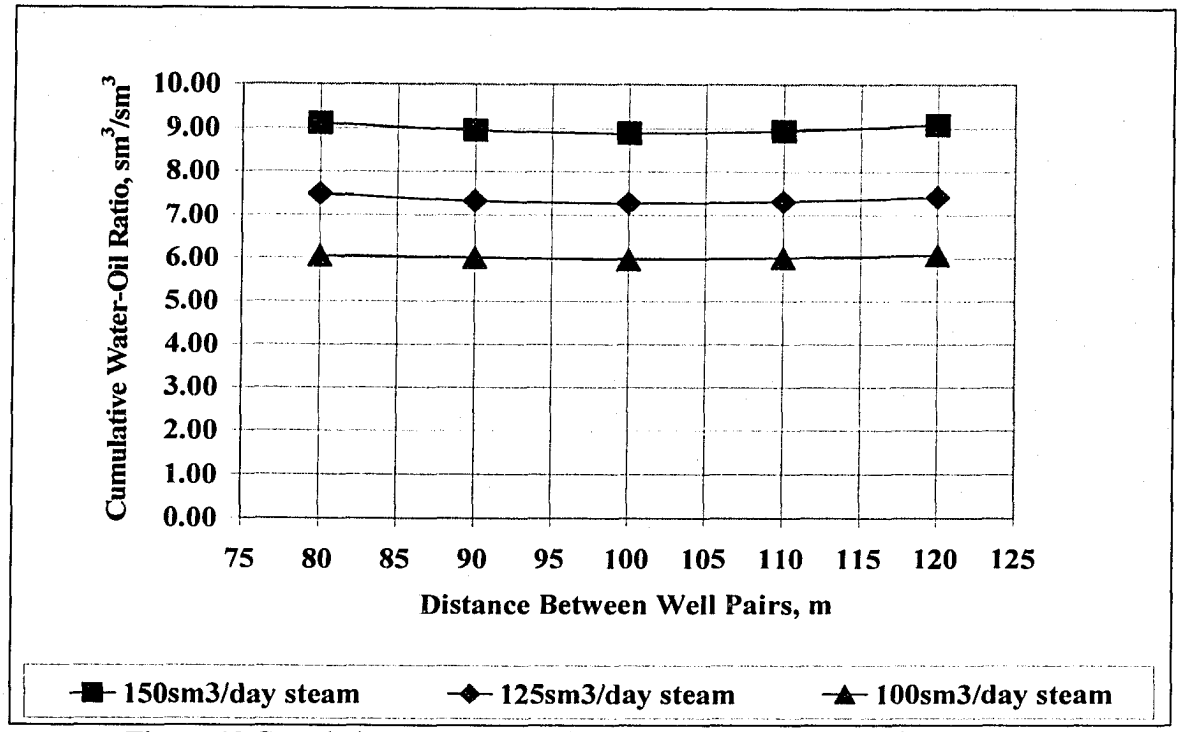

Figure 12 Cumulative Water-Oil Ratio as a Function of Steam Injection Rates

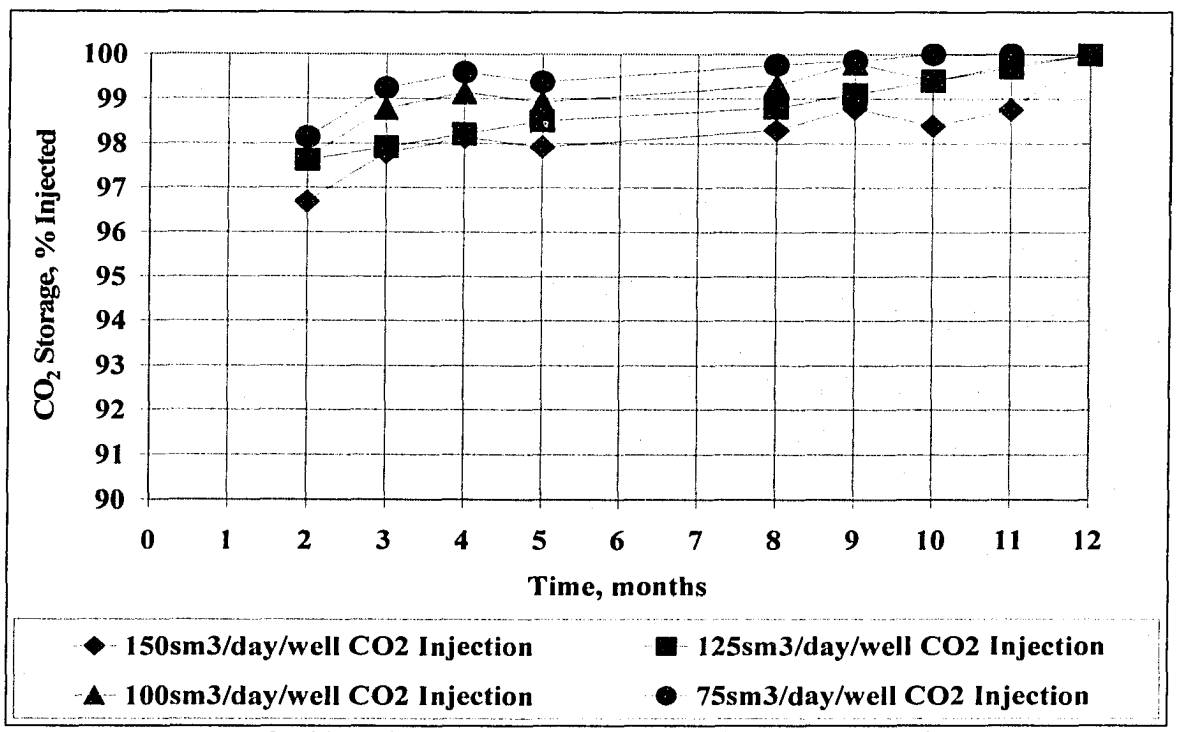

Figure 13 Soaking Time Optimization as a Function of CO_2 Injection Rates

Reproduced with permission of the copyright owner. Further reproduction prohibited without permission.

Although one of the aims of this study was to store a maximum amount of CO_2 prior to the steam flood, the effect of soaking time on production was also analyzed. In order to see the difference in the produced CO_2 between the soaking and no soaking cases, simulations were carried out at the 100 sm^3/day/well steam injection rate with various CO_2 injection rates. At 3500 kPa reservoir pressure and a well pair separation distance of 100 m in the dead oil case, steam flooding simulations were run for one year of CO_2 injection at different rates, with and without soaking. The soaking of CO_2 provided better storage percentage with respect to the no soaking cases (Figure 14). The increased CO_2 injection rates decreased the storage of CO_2 during the producing life of the reservoir in either case except at the rates of 75 and 100 sm^3/day/well (0.14 and 0.19 tonne/day/well) with soaking. The comparison of CSOR is shown for the soaking and no soaking cases in Figure 15. Due to soaking, more of the CO_2 dissolved in the oil, causing a reduction in viscosity and swelling of the oil, both of which contributing to improve the flow properties [43]. Therefore, less steam was used. That is why the produced water was less with soaking (Figure 16). However, the cumulative oil recoveries at different CO_2 injection rates for the no soaking cases were higher than the one year soaking cases (Figure 17), despite the higher values of steam-oil ratio (Figure 15).

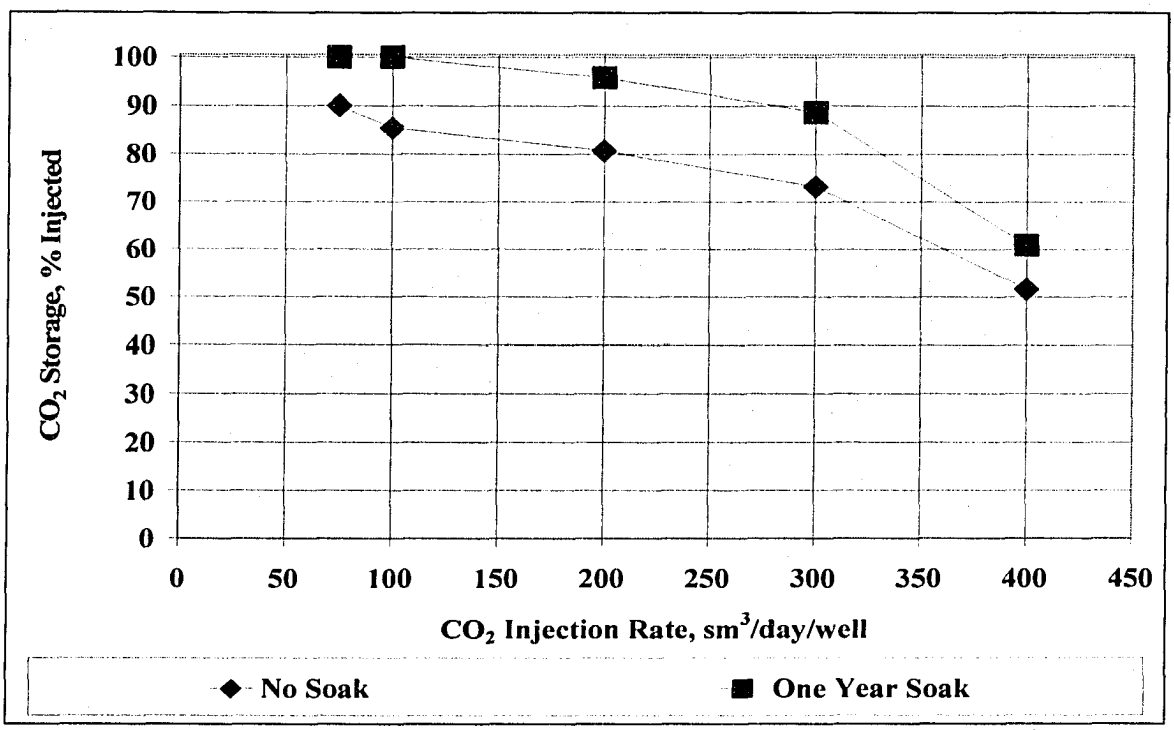

Figure 14 Comparison of Storage percent of CO_2 Soaking and No Soaking at Different CO_2 Injection Rates

Reproduced with permission of the copyright owner. Further reproduction prohibited without permission.

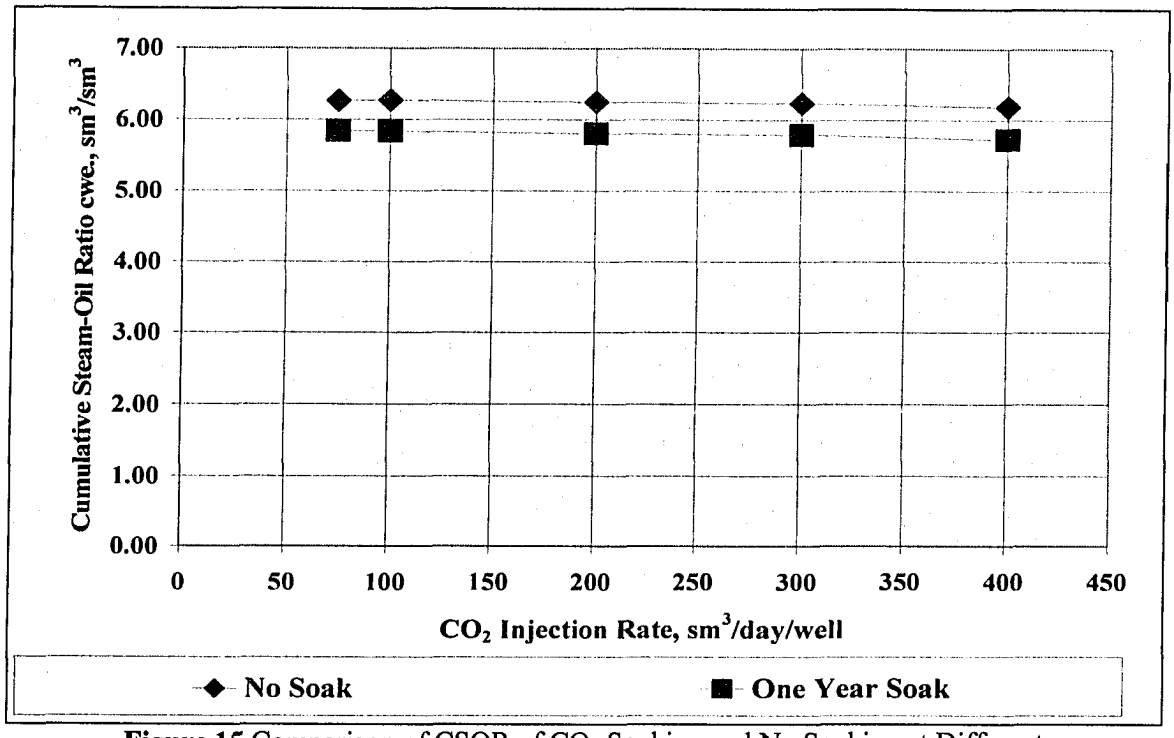

Figure 15 Comparison of CSOR of CO_2 Soaking and No Soaking at Different CO_2 Injection Rates

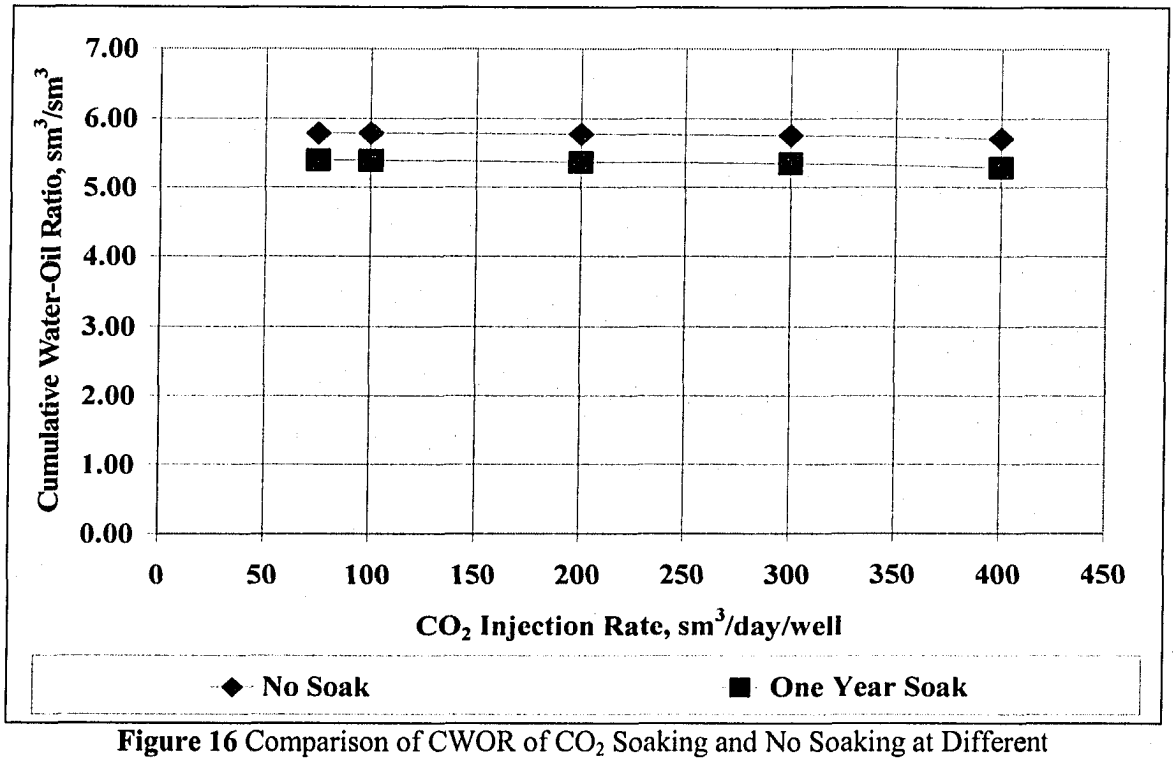

Figure 16 Comparison of CWOR of CO_2 Soaking and No Soaking at Different CO_2 Injection Rates

Reproduced with permission of the copyright owner. Further reproduction prohibited without permission.

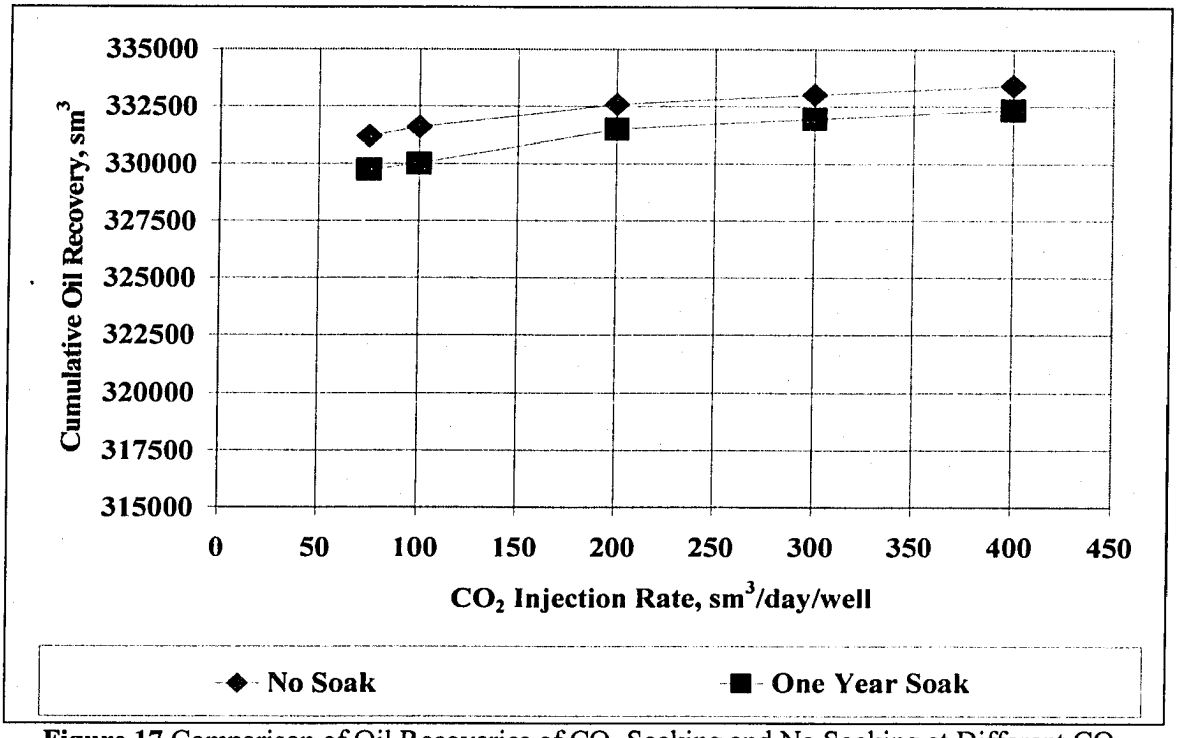

Figure 17 Comparison of Oil Recoveries of CO_2 Soaking and No Soaking at Different CO_2 Injection Rates

After finding the optimum soaking time of one year, a series of simulations were run in order to investigate the effect of various CO_2 injection rates on the previously tested steam injection rates of 100, 125 and 150 sm^3/day/well (Figure 18). The process used, as mentioned earlier, was one year of continuous CO_2 injection, followed by one year of soaking, followed by continuous steam injection until the economic production limit of the reservoir was reached. An analysis of the results obtained showed that, for a fixed injection rate of CO_2, the cumulative recovery of oil was virtually independent of the rate at which steam was injected, as shown in Figure 18.

It can be seen from Figure 18 that the cumulative oil recovery increases with the increased CO_2 injection rate, which is directly proportional to the amount of CO_2 stored in the reservoir. The incremental recovery occurs at higher injection rates, due to more swelling of CO_2 in the oil causing more viscosity reduction [12, 13]. Besides, the trapped gas effect might be dominant for establishing a solution gas drive mechanism during oil recovery [44]. The oil recovery curves for the simulations of well pairs separated by 80, 90, 110 and 120 m are given in Appendix B.

Reproduced with permission of the copyright owner. Further reproduction prohibited without permission.

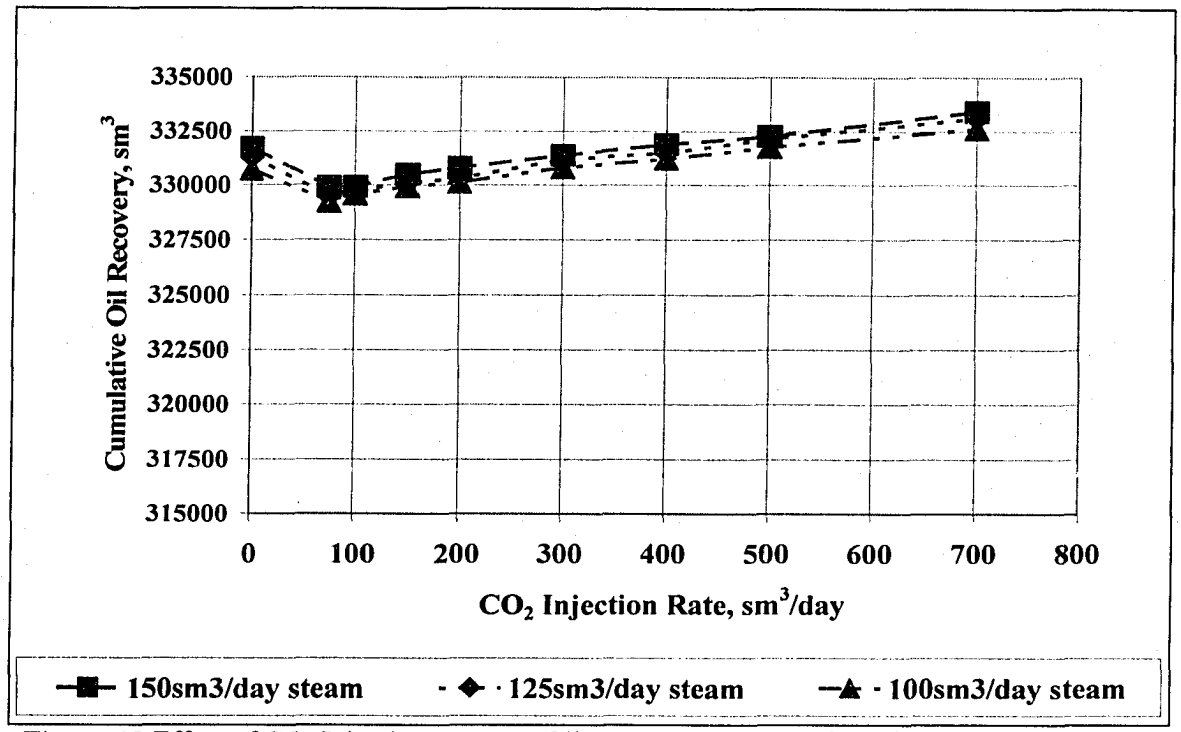

Figure 18 Effect of CO_2 Injection Rates on Oil Recovery as a Function of Steam Injection Rate

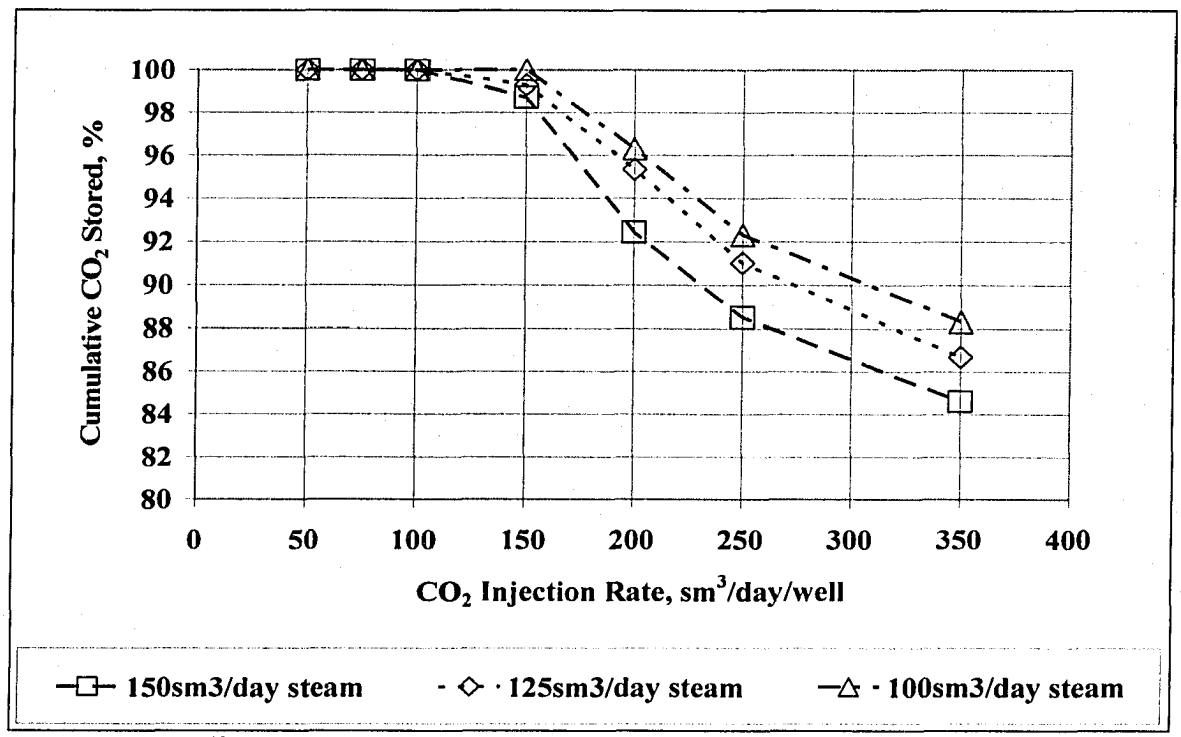

Figure 19 Effect of CO_2 Injection Rates on Storage as a Function of Steam Injection Rate

Reproduced with permission of the copyright owner. Further reproduction prohibited without permission.

Figure 19 shows the effect of initial CO_2 injection rate on the storage capacity of the reservoir during its economic producing life. Higher amounts of CO_2 injected into the reservoir caused less storage of CO_2 in the reservoir, but more swelling of the mobile oil, resulting in higher recoveries (Figure 18). Hundred percent storage occurred at all steam injection rates when CO_2 was injected at a rate of 100 sm^3/day/well (0.19 tonne/day/well). The percent CO_2 storage amounts for the simulations of well pairs separated by 80, 90, 110 and 120 m are given in Appendix C.

5.1.2 Reservoir with Live Oil

Additional simulations were carried out changing the oil type from dead to live, which has an initially dissolved CH_4 gas content of 10% in the oil. The simulations were carried out based on the same parameters used in the dead oil case. A distance of 100 m between two injection-production well pairs, and a steam injection rate of 100 sm^3/day/well were used in the simulations.

Figure 20 shows how the CO_2 injection rate affects the oil recovery from a reservoir having an initial reservoir pressure of 3500, 3000, 2500 and 2000 kPa, respectively. Except for the 2000 kPa reservoir pressure case, the injection rate of CO_2 increases the cumulative recovery of the oil only slightly, although the pressure in the reservoir is increased. At 2000 kPa reservoir pressure, the cumulative recovery of oil is highest.

Due to the optimum operating conditions reached at this pressure, the recoveries increased with increasing CO_2 injection rates, although the process has a two-year production delay before the start of steam injection. This is the result of the CO_2 displacing a slug of heavy oil not produced by steam, probably the incremental recovery from oil swelling, and the trapped gas effect resulting from CO_2 addition. The optimum steam to CO_2 ratio should also maximize the oil recovery [44].

Figure 21 shows the cumulative CH_4 recovery curves at different pressures. Higher reservoir pressures resulted in higher CH_4 recovery. Unlike the oil recovery, CH_4 recovery increased with increasing pressure, due to presence of high volume of dissolved gas initially in the oil. The CO_2 injection rate had virtually no effect on the gas recovery at each pressure considered.

Reproduced with permission of the copyright owner. Further reproduction prohibited without permission.

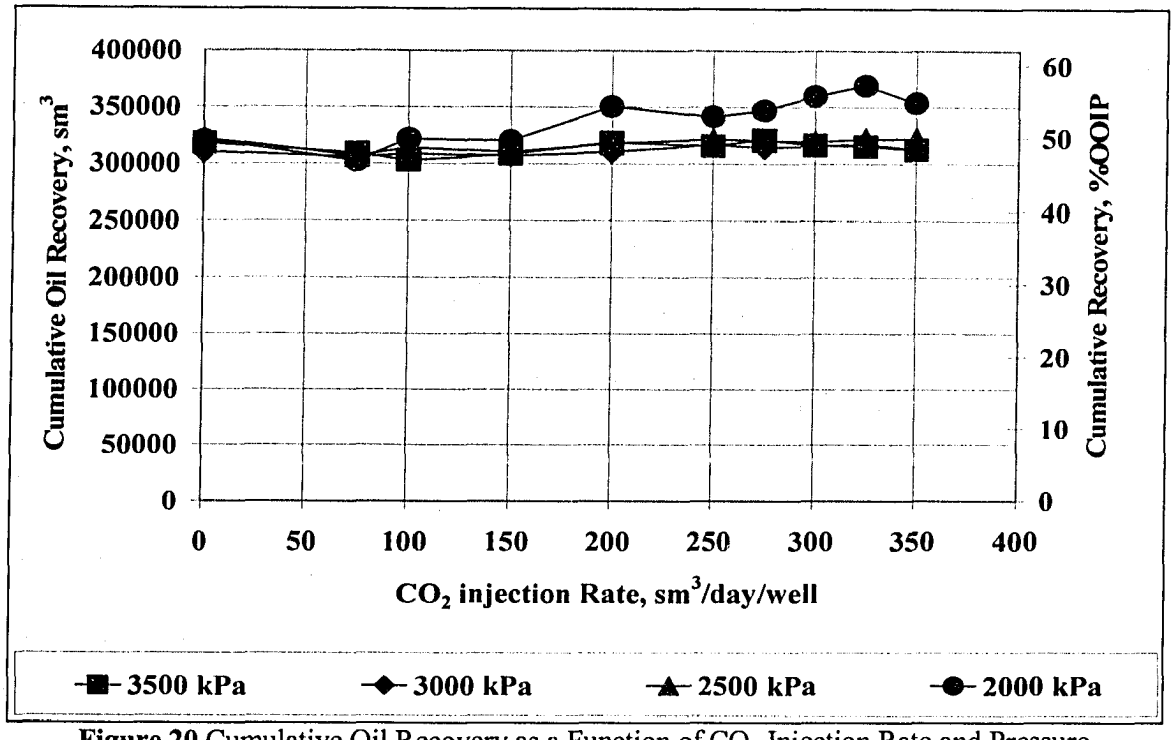

Figure 20 Cumulative Oil Recovery as a Function of CO_2 Injection Rate and Pressure

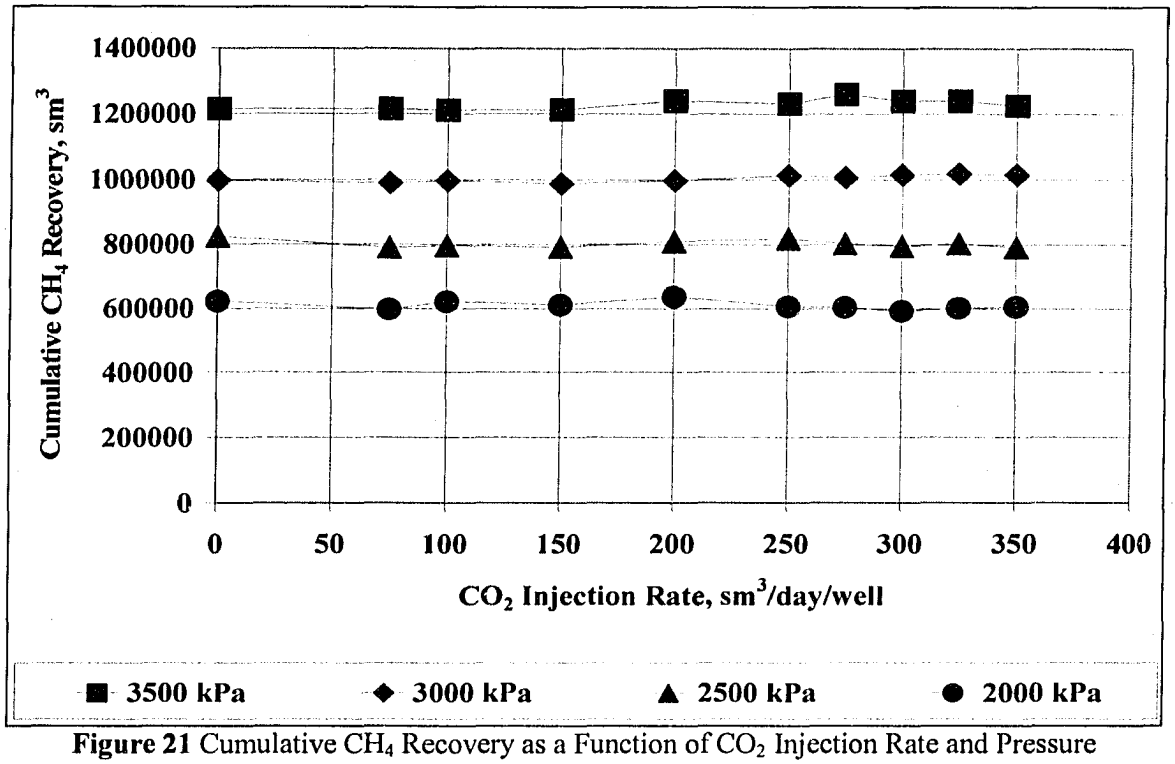

Figure 21 Cumulative CH_4 Recovery as a Function of CO_2 Injection Rate and Pressure

Reproduced with permission of the copyright owner. Further reproduction prohibited without permission.

From a storage point of view, it can be seen that, for all pressures and CO_2 injection rates up to 150 sm^3/day/well (0.28 tonne/day/well), all the injected CO_2 could be stored in the reservoir (Figure 22). However, the storage percent of cumulative CO_2 was higher with increased pressure. In the simulations that were run at 3500 and 3000 kPa pressures, all injection rates of CO_2 up 250 sm^3/day/well (0.47 tonne/day/well) indicated 100 % storage. The CO_2 storage trends in the initially gas saturated reservoir oil are similar to the no gas saturated reservoir oil case studied earlier.

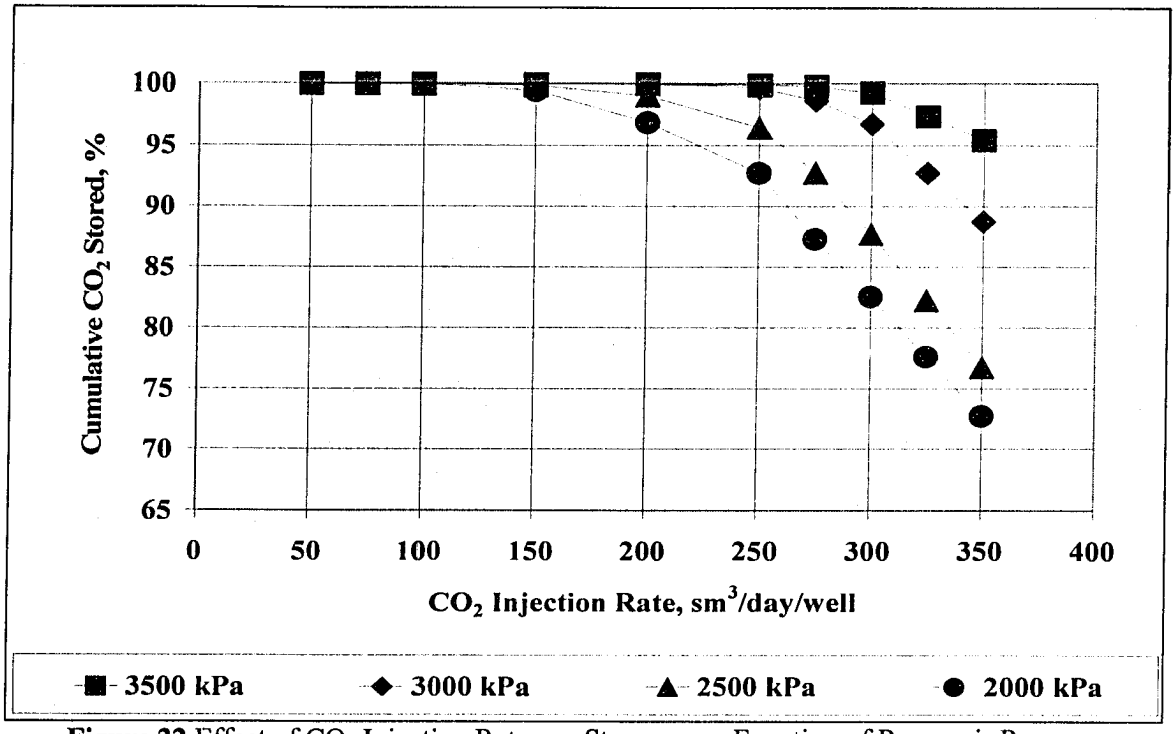

Figure 22 Effect of CO_2 Injection Rates on Storage as a Function of Reservoir Pressure

The injected CO_2 increased the amount of gas volume in the reservoir around the well bore. Due to decreasing heat loss to the under- and overburden, the CSOR for all pressures studied decreased. The steam necessary to heat the oil for viscosity reduction was less than that of the dead oil case at 100 sm^3/day/well steam injection rate (see Figure 11) at all pressures studied. The CSOR value was around 6 sm^3/sm^3 without CO_2 injection prior to the steam flood. However, a one-quarter decrease was realized on CSOR when CO_2 was injected at a rate of 350 sm^3/well/day prior to the steam flood. Moreover, at 2000 kPa pressure, the decrease was more pronounced (Figure 23).

The CWOR values were also much similar to the CSOR values (Figure 24), meaning that less water was produced together with the oil.

Reproduced with permission of the copyright owner. Further reproduction prohibited without permission.

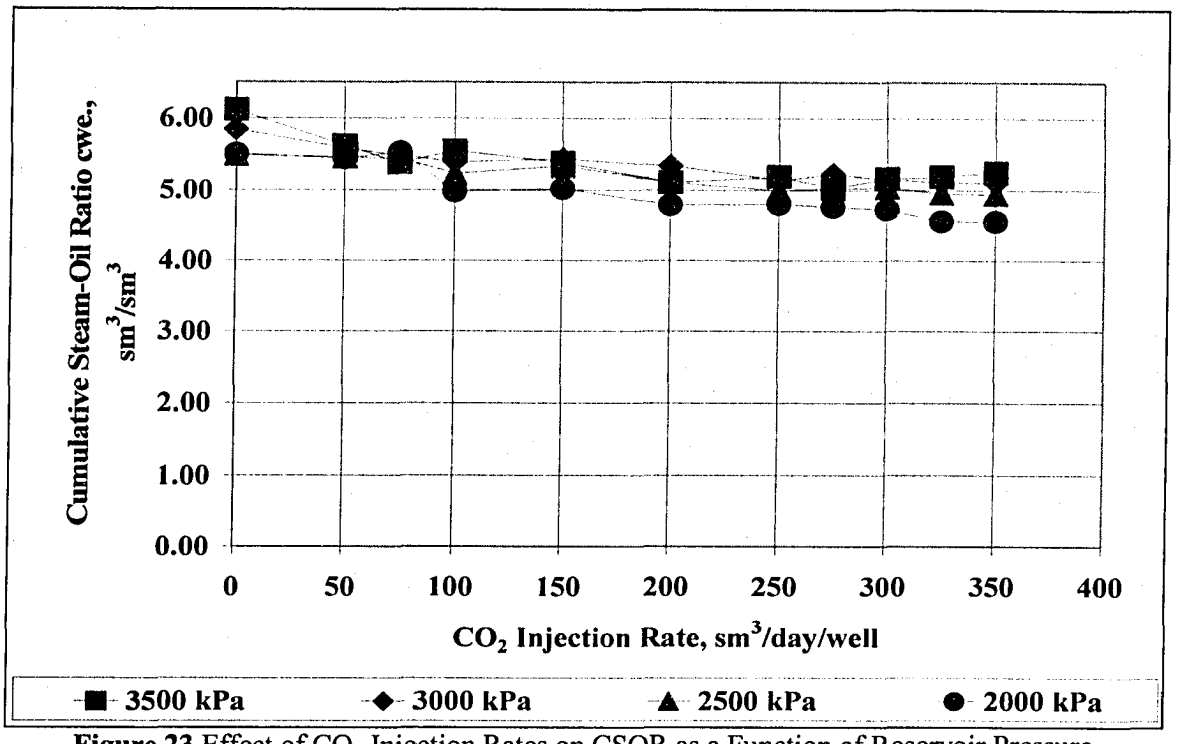

Figure 23 Effect of CO_2 Injection Rates on CSOR as a Function of Reservoir Pressure

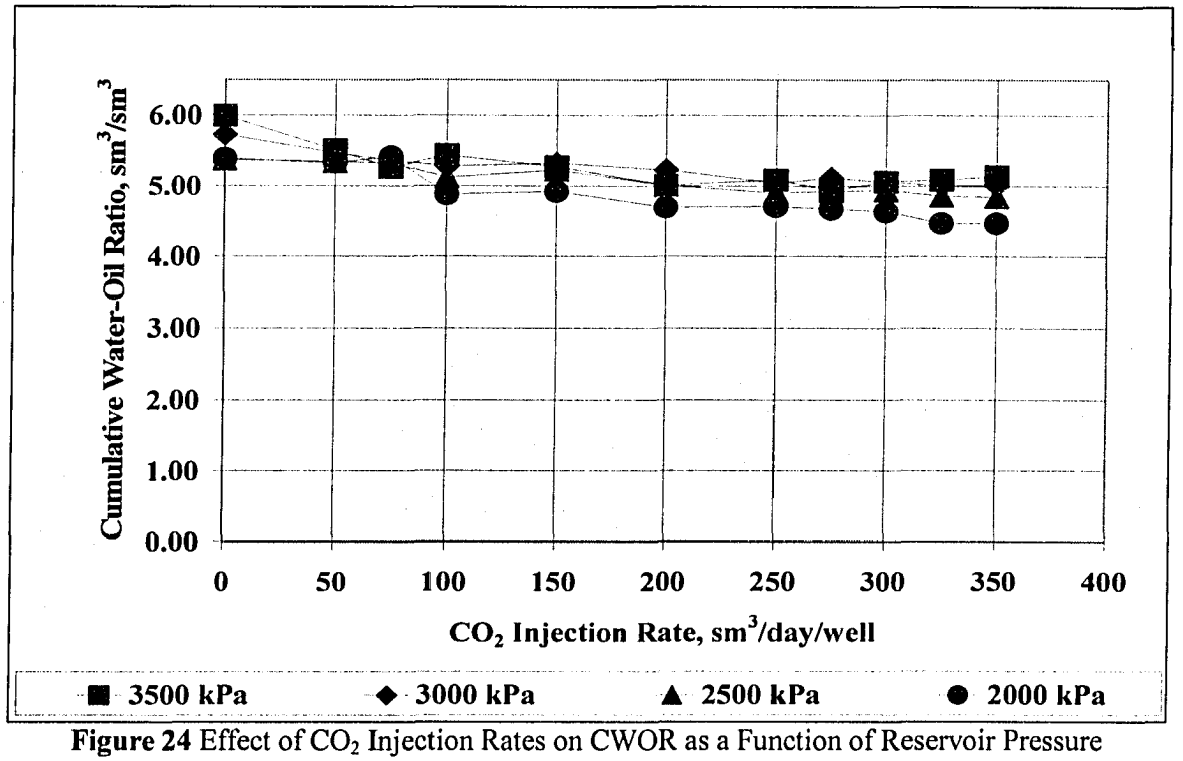

Figure 24 Effect of CO_2 Injection Rates on CWOR as a Function of Reservoir Pressure

Reproduced with permission of the copyright owner. Further reproduction prohibited without permission.

5.1.3 Comparison of the Dead and Live Oil Cases

In the previous sections, the storage and the effect of CO_2 injection prior to steam flooding have been analyzed separately. However, the steam injection performance is also affected by the oil type. In order to show the effect of oil type, the simulations with the same operating conditions are compared.

In these simulations, the distance between the well pairs was taken as 100 m. The steam and CO_2 injection rates were set at 100 sm^3/day/well at a pressure of 3500 kPa. The cumulative recovery of both oil types is given in Figure 25, with and without CO_2 injection. The oil recovery rate for the live oil was higher than that of the dead oil. The results showed that the dissolved CH_4 gas in the oil enabled higher recovery rates and significantly more oil production in the first 20 years (7300 days) of the life of the reservoir.

Most of the cumulative oil recovery (83%) occurred in the first 20 years of the production life of the reservoir (Figure 25). The remaining oil (17%) was recovered in the second half of the production life. This is similar to what was reported by Frauenfeld et al. [29]. Also, at this pressure in the dead oil case, two years of production delay was compensated for at the end of the production life of the reservoir, whereas it did not in the live oil case.

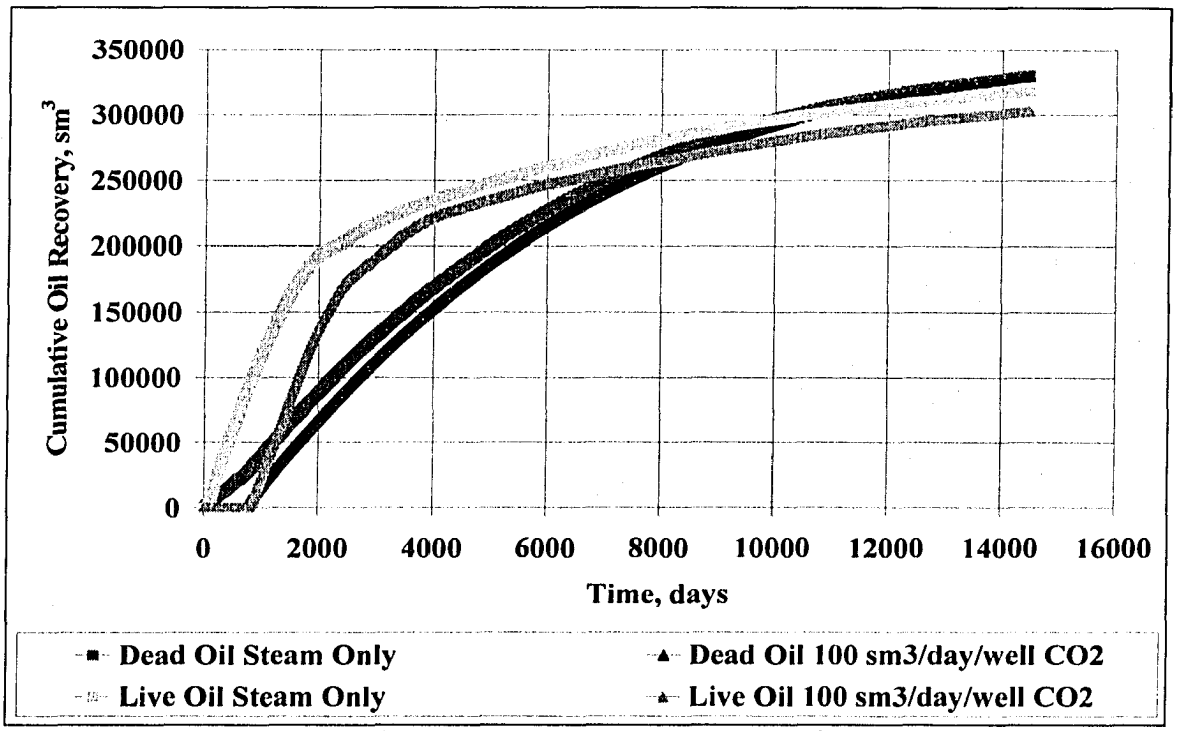

Figure 25 Comparison of Cumulative Oil Recoveries of Reservoirs with Dead and Live Oil at 3500 kPa Pressure

Reproduced with permission of the copyright owner. Further reproduction prohibited without permission.

The temperature profiles showing the formation of the steam chamber were analyzed to explain the higher rates of oil production in the live oil case. The live oil steam chamber grows faster than that of the dead oil (Figures 26 and 27) after six months and one year, respectively. There was less heat loss in the live oil case than in the dead oil case so that the growth of the steam chamber is faster in the live oil.

The effect of the addition of CO_2 on temperature profiles are given in Appendix D. In the live oil case, the addition of CO_2 expanded the steam chamber laterally, whereas it had no significant effect in dead oil case (Figures D1 to D7 in Appendix D). The steam chamber temperatures in the live oil case were higher than those in the dead oil case, indicating that the heat losses were smaller, therefore resulting in higher production rates (Figures D.5, D.6 and D.7).

In addition, the CSOR curve shown in Figure 28 has lower values in the live oil case. This shows that less steam is required for recovering the same amount of oil in the reservoir having live oil rather than dead oil, which is beneficial for the process. That is why the produced CWOR are smaller in both cases (Figure 29). The dead and live oil cases are compared at the other reservoir pressures of interest (3000, 2500 and 2000 kPa) in Appendix E. The lower reservoir pressures of 3000, 2500 and 2000 kPa for the dead oil cases gave better or similar oil recovery results in the long run (after 3650 days [10 years]) compared to the 3500 kPa reservoir. This is due to the displacing effect of the CO_2 slug where the incremental heavy oil is not produced by steam, but by oil swelling and the trapped gas effects from CO_2 injection [44]. After 10 years of production, the CSOR continuously increased until reaching a value of 6 sm^3/sm^3 which was the constraint imposed to stop the simulations (Figure 28).

Reproduced with permission of the copyright owner. Further reproduction prohibited without permission.

Reproduced with permission of the copyright owner. Further reproduction prohibited without permission.

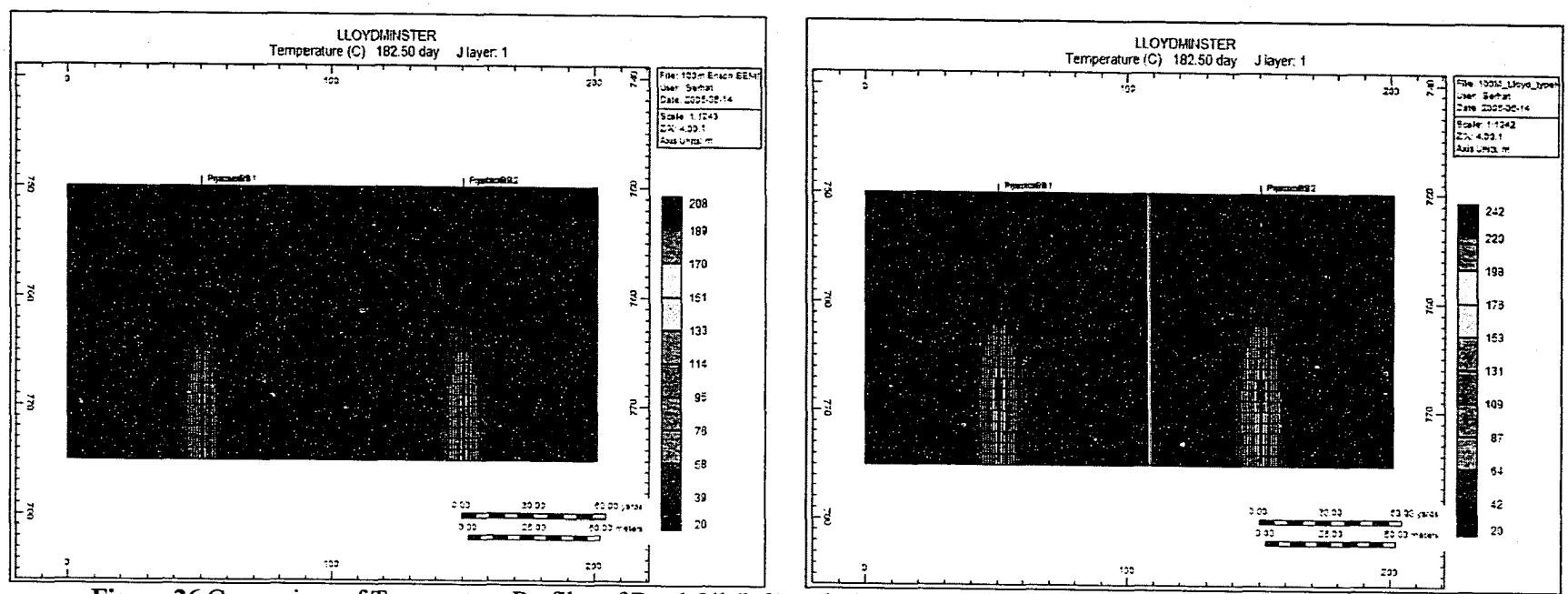

Figure 26 Comparison of Temperature Profiles of Dead Oil (left) and Live Oil (right) Reservoirs after 6 Months of Steam Flooding

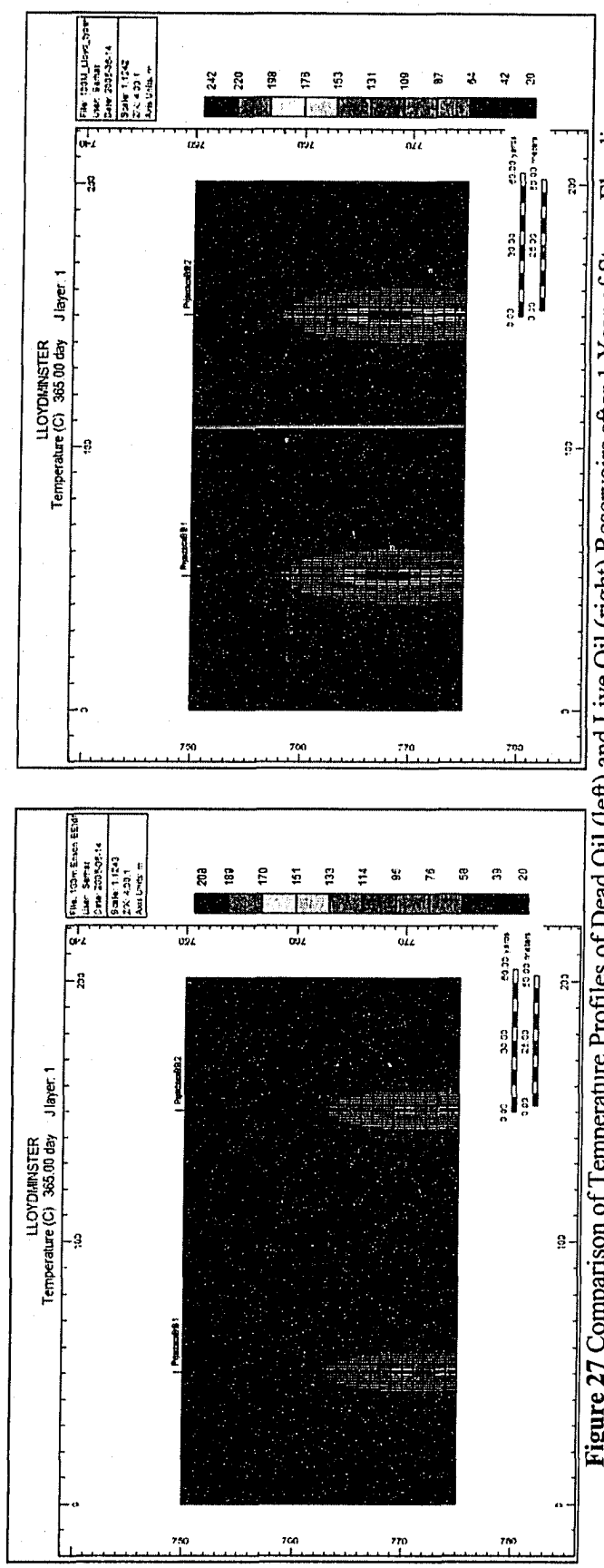

Figure 27 Comparison of Temperature Profiles of Dead Oil (left) and Live Oil (right) Reservoirs after 1 Year of Steam Flooding

Reproduced with permission of the copyright owner. Further reproduction prohibited without permission.

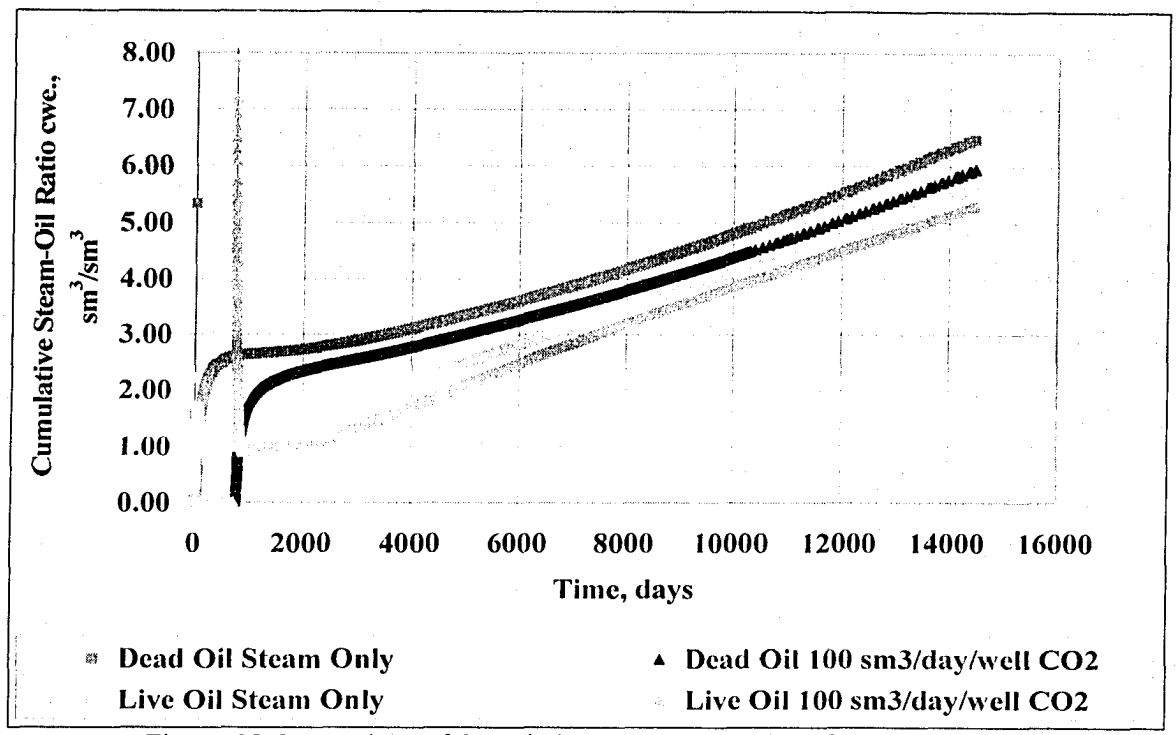

Figure 28 Comparison of Cumulative Steam-Oil Ratios of Reservoirs with Dead and Live Oil at 3500 kPa Pressure

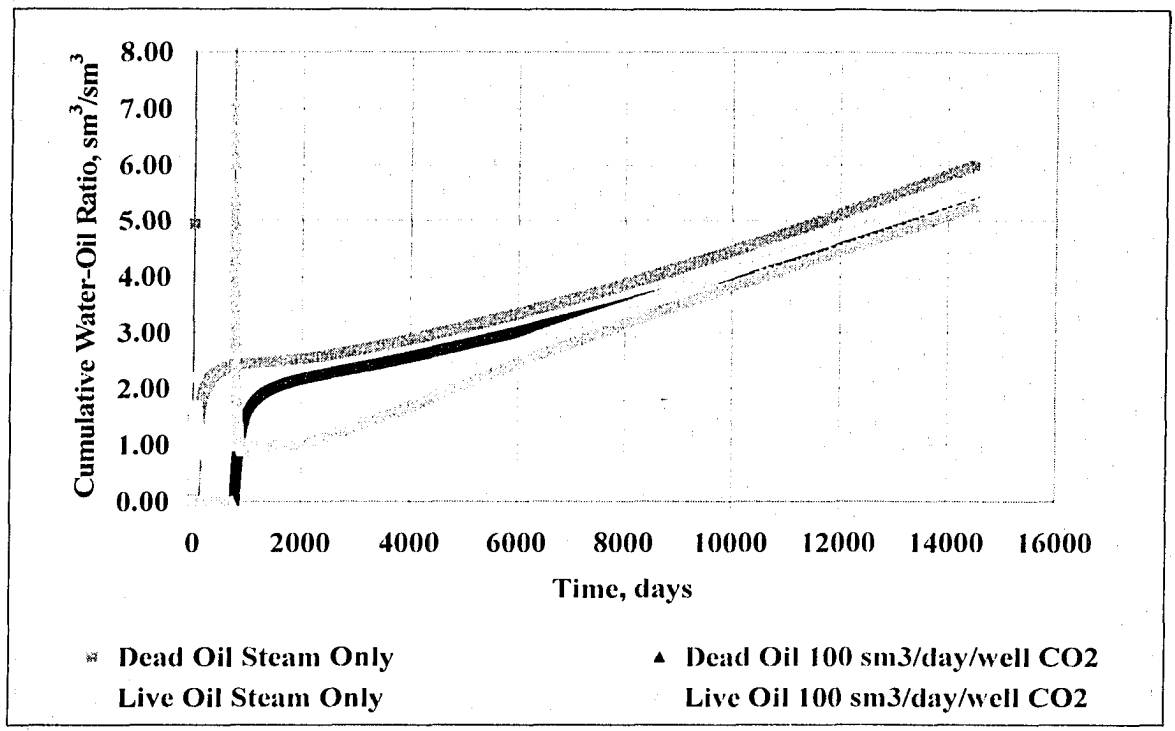

Figure 29 Comparison of Cumulative Water-Oil Ratios of Reservoirs with Dead and Live Oil at 3500 kPa Pressure

Reproduced with permission of the copyright owner. Further reproduction prohibited without permission.

5.1.4 Economic Analysis of the Dead and Live Oil Cases

The proposed scheme has a two-year production delay, the first year for injecting CO_2 and the second one for soaking. The simulation results, especially in the dead oil and lower reservoir pressure cases have shown that the higher CO_2 injection rates eliminated this delay in the later stages (after 11 years) of the producing life of the reservoir (Figures E.1 to E.6 in Appendix E).

As mentioned in Section 2.2, the cost of CO_2 recovery from flue gas adds \$37.80/sm^3 [6] to the oil production cost. The most recent SAGD supply cost available in the literature was that of the Surmont project which was reported to be \$29.36/sm^3 [45]. The decrease in the CSOR was around 5% for the CO_2 injection prior to steam flooding process. This is the only positive cost for the application providing +\$0.44/sm^3 (the steam cost is 30% of the total production cost) towards the profit from the sale of oil. The economics of this study with and without CO_2 injection is given in Table 3. As can be seen from the table, the \$37.36/sm^3 difference is the cost of a cleaner environment. With today's oil prices hovering around \$315/sm^3 (\$50/bbl), the increase in production costs may not be the main concern for the companies. However, a two-year delay in production and associated costs would be the main reason for their hesitation in applying this process. In those two years, the cumulative oil production was found to be 25,600 sm^3 (see section 5.1.3) resulting in \$7,312,384 loss from the net profit.

In the live oil cases, the dissolved CH_4 gas in the oil enabled higher recovery rates. With respect to Figure 25, at 3500 kPa reservoir pressure, two years of cumulative recovery was 86,702 sm^3, causing a loss of \$24,765,674 from the net profit. If one analyzed the economics of such a study with live oil, the lost amount of production would be the main reason for an unwillingness to apply this process.

Table 3 Simple Economics Calculation of a Project with and without CO_2 Injection

	With CO_2 Injection	**Without CO_2 Injection**
Oil Price, \$/sm^3	315.00	315.00
Production Cost with SAGD, \$/sm^3	-29.36	-29.36
CO_2 Capture and Injection Cost, \$/sm^3	-37.80	--
Decrease CSOR, \$/sm^3	+0.44	--
Net Profit from Oil \$/sm^3	248.28	285.64
Loss Production Cost for two years Dead Oil, \$	7,312,384	--
Loss Production Cost for two years Live Oil, \$	24,765,674	--

Reproduced with permission of the copyright owner. Further reproduction prohibited without permission.

5.2 Carbon Dioxide Sequestration After Steam Injection

5.2.1 Reservoir with Dead Oil

The simulations were stopped at the end of the economic production life of a given project, where typically 50% of the OOIP was recovered. At that point, the residual saturations of the fluids in the reservoir were calculated, assuming that only heavy oil and water were present (the injected CO_2 was negligible, less than 0.1 PV [136 tonnes]). Figure 30 shows the oil recovery from the SAGD operation at the optimal conditions described earlier. The residual saturation values, at the end of each run, are given in Table 4 at each distance between the well pairs.

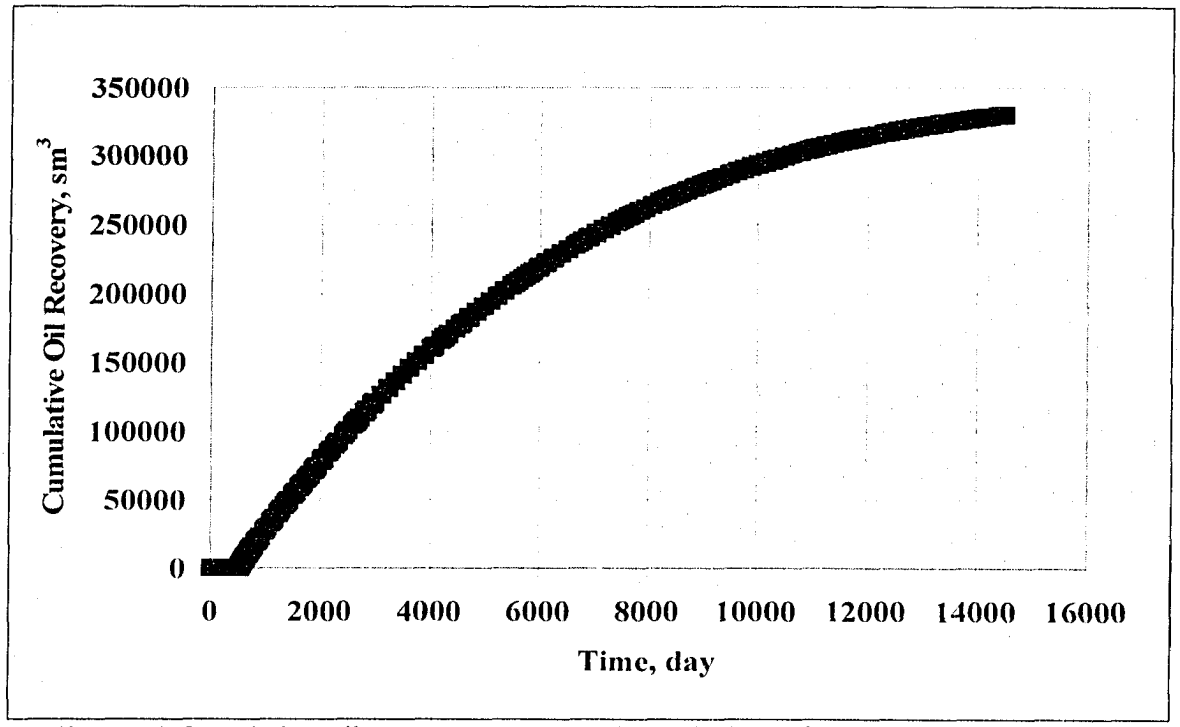

Figure 30 Cumulative Oil Recovery to Economic Producing Life of Reservoir at Optimum Conditions for CO_2 and Steam Injection Rates

Before the sequestration simulations, the amount of CO_2 that can be dissolved in the reservoir was calculated analytically by using Figures 8 and 9 with the residual fluid saturations. The residual water and oil saturations at a well pair separation of 100 m at the end of the numerical simulation were found to be S_{wr}=0.61 and S_{or}=0.39, respectively. The volumes of the residual water and oil in the reservoir were calculated, using the PV of the reservoir (804,000 sm^3), to be 488,832 and 315,168 sm^3, respectively. The solubility ratio of CO_2 in water was 33 sm^3/sm^3 (Figure 8) and that in oil was 71.5 sm^3/sm^3 (Figure 9) at 6500 kPa and 21°C. The amount

Reproduced with permission of the copyright owner. Further reproduction prohibited without permission.

of CO_2 soluble in the reservoir fluids was found to be 38,671,707 sm^3 (72,014 tonnes) in the reservoir for the optimal oil recovery case. The solubility results of the different well pair spacings are given in Table 5. The analytical calculations showed that more CO_2 can be dissolved in the reservoir oil if more hydrocarbons are left in the reservoir.

Table 4 Simulation Results at 100 sm^3/day/well CO_2 Injection Prior to 100 sm^3/day/well Steam Flooding

Simulation #	Distance Between Well Pairs (m)	Oil Recovery % OOIP	Residual Oil S_{or}	Residual Water S_{wr}
1	80	50	0.40	0.60
2	90	50	0.40	0.60
3	100	51	0.39	0.61
4	110	50	0.40	0.60
5	120	48	0.41	0.59

Table 5 CO_2 Sequestration Results of a Dead Oil Reservoir at Different Well Pair Distance after Steam Flooding by Analytical Calculations

Distance Between Well Pairs (m)	Σ Oil Remaining in the Reservoir (sm^3)	Σ Water Remaining in the Reservoir (sm^3)	Amount of CO_2 Soluble in Oil (sm^3)	Amount of CO_2 Soluble in Water (sm^3)	Total CO_2 Soluble in the Model (tonne)
80	321,600	482,400	23,010,480	15,909,313	72,476
90	321,600	482,400	23,010,480	15,909,313	72,476
100	315,168	488,832	22,550,270	16,121,437	72,014
110	321,600	482,400	23,010,480	15,909,313	72,476
120	328,032	475,968	23,470,690	15,697,188	72,938

In the sequestration simulations, two horizontal wells were used to inject CO_2 into the steam flooded reservoir. Using the residual saturations after each run at the different well pair spacings and neglecting the reservoir cooling time, the CO_2 was injected continuously from each well at a rate of 2000 sm^3/day (3.72 tonnes/day/well), until the fracture pressure was reached, which was determined to be 6500 kPa (see earlier, 500 kPa safety factor).

Reproduced with permission of the copyright owner. Further reproduction prohibited without permission.

The CO_2 sequestration graph is shown in Figure 31, which was obtained using CMG STARS™ [33]. The dashed line shows the continuous injection of CO_2 from the two wells at a rate of 2000 sm^3/day/well (3.72 tonnes/day/well). The smooth line, with the vertical ending shows the bottom hole pressure in the reservoir during injection. The vertical ending shows when the fracture pressure of 6500 kPa is reached. Besides, the phase diagram of the CO_2 (Figure 4) shows that, CO_2 gas becomes liquid after if the temperature increases beyond 21 °C and the pressure beyond 6500 kPa. This may also be a limiting factor in sequestering more gas because of the phase change of CO_2 from gas to liquid.

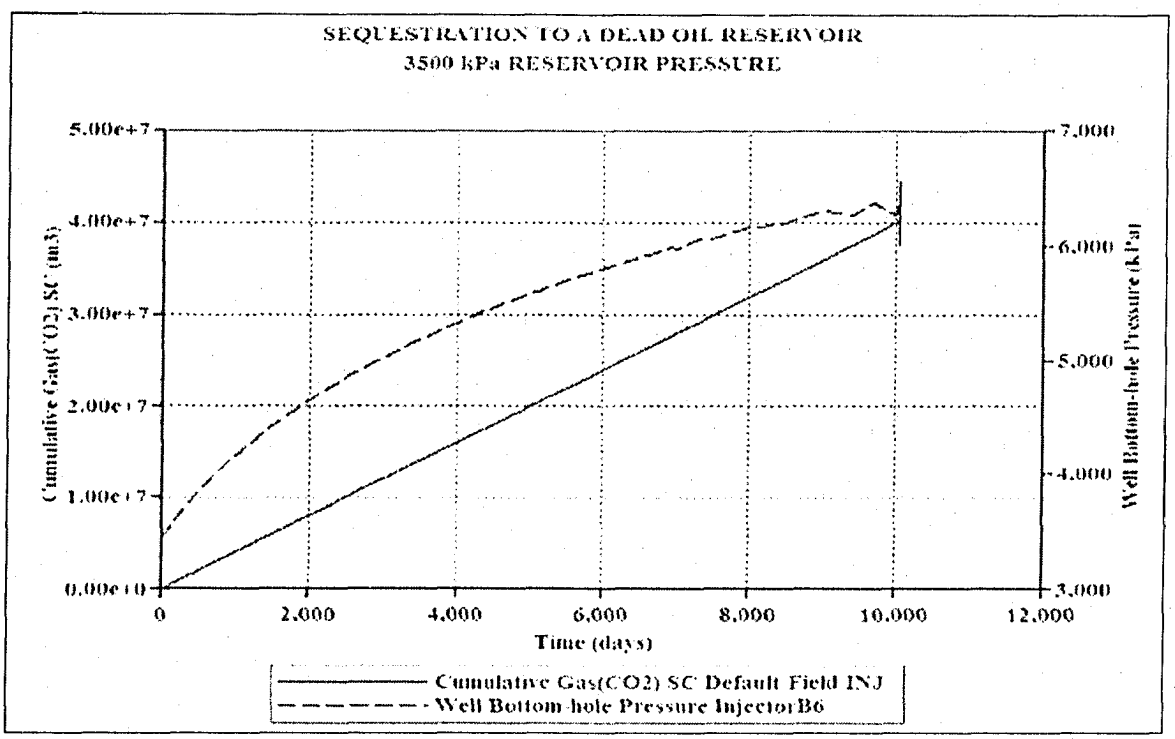

Figure 31 CO_2 Sequestration in Dead Oil Reservoir at 3500 kPa Reservoir Pressure from CMG STARS™

The results of the numerical modeling for CO_2 sequestrations were almost same as those obtained using analytical calculations. The total amount of CO_2 storage capacity for the each SAGD pattern was found to be around 72,000 tonnes which confirmed the results found by Law [4]. The numerical and analytical sequestration results are both given in

Table 6 for comparison. The analytical calculations show sequestration values similar to the numerical results, as shown in Figure 32.

Reproduced with permission of the copyright owner. Further reproduction prohibited without permission.

Table 6 Comparison of CO_2 Sequestration Results after Steam Flooding in a Dead Oil Reservoir

Distance between Well Pairs (m)	Total CO_2 Sequestrated Numerically (tonne)	Total CO_2 Soluble Analytically (tonne)
80	77,162	72,476
90	75,815	72,476
100	74,919	72,014
110	75,216	72,476
120	75,216	72,938

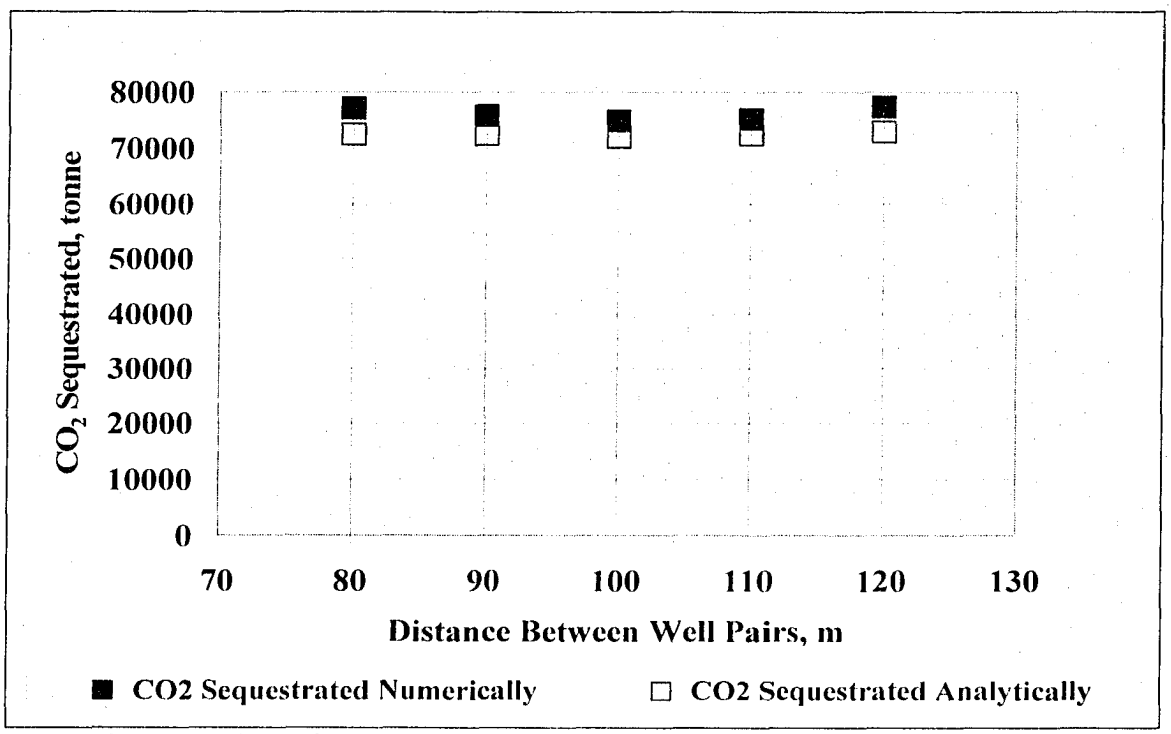

Figure 32 Comparison of Numerical and Analytical CO_2 Sequestration Calculations in Dead Oil

5.2.2 Reservoir with Live Oil

The simulations were stopped after reaching the economic producing life of the live oil case after forty years. The residual saturations were calculated after each run at different reservoir pressures at the selected CO_2 and steam injection rates (100 sm^3/day/well). The oil recoveries ranged from 52.5 to 55 % OOIP, depending on the pressure. The residual oil saturations (S_{or}) were around 0.38 to 0.36 and the residual water saturations (S_{wr}) 0.62 to 0.64 as pressure decreased (Table 7). The injected CO_2 gas was neglected during the residual fluid calculations.

Reproduced with permission of the copyright owner. Further reproduction prohibited without permission.

The amount of CO_2 that can be dissolved in the reservoir was calculated analytically by using the same procedure as for the residual fluid saturation calculations described in Section 5.2.1. The residual water and oil saturations at 3500 kPa at the end of the numerical simulation were found to be S_{wr}=0.62 and S_{or}=0.38, respectively. The volumes of the residual water and oil in the reservoir calculated using the PV of the reservoir (804,000 sm^3), were 498,840 sm^3 and 305,160 sm^3 respectively. The solubility ratio of CO_2 in water is taken as 33 sm^3/sm^3 (Figure 8) and that in oil as 71.5 sm^3/sm^3 at 6500 kPa and 21°C (Figure 9). The amount of CO_2 soluble in the reservoir fluids at 3500 kPa was found to be 38,285,702 sm^3 (71,296 tonnes) for the optimal oil recovery case. The solubility results at the different reservoir pressures are given in Table 8.

Table 7 Simulation Results to the Economic Producing Life of a Live Oil Reservoir at Different Pressures

Simulation #	Reservoir Pressure (kPa)	Oil Recovery % OOIP	S_{or} Residual Oil	S_{wr} Residual Water
1	3500 kPa	52.55	0.38	0.62
2	3000 kPa	53.21	0.37	0.63
3	2500 kPa	53.81	0.37	0.63
4	2000 kPa	54.91	0.36	0.64

Table 8 CO_2 Sequestration Results of a Live Oil Reservoir at Different Pressures of Steam Flooding by Analytical Calculations

Reservoir Pressure (kPa)	Σ Oil Remaining in the Reservoir (sm^3)	Σ Water Remaining in the Reservoir (sm^3)	Amount of CO_2 Soluble in Water (sm^3)	Amount of CO_2 Soluble in Oil (sm^3)	Total CO_2 Soluble in the Model (tonne)
3500 kPa	305,160	498,840	21,834,214	16,451,488	71,296
3000 kPa	300,930	503,070	21,531,517	16,591,010	70,992
2500 kPa	297,052	506,948	21,254,054	16,718,901	70,713
2000 kPa	290,020	513,980	20,750,923	16,950,809	70,208

The CO_2 sequestration simulations were run in the live oil reservoir with the same constraints as in the dead oil case. The fracture pressure was assumed constant at 6500 kPa, and CO_2 was injected at a rate of 2000 sm^3/day/well (3.72 tonnes/day/well). The results were comparable to the dead oil case, but the dominant factor affecting the storage of CO_2 was again the residual saturations after the steam flood (Table 9).

Reproduced with permission of the copyright owner. Further reproduction prohibited without permission.

The sample sequestration graph of a live oil reservoir is given in Figure 33 for a reservoir pressure of 3500 kPa. The smooth line shows the sequestrated CO_2 volume and the dashed line, with the vertical ending shows the bottom hole pressure in the reservoir. This vertical line indicates when the fracture pressure of 6500 kPa was reached. At this point

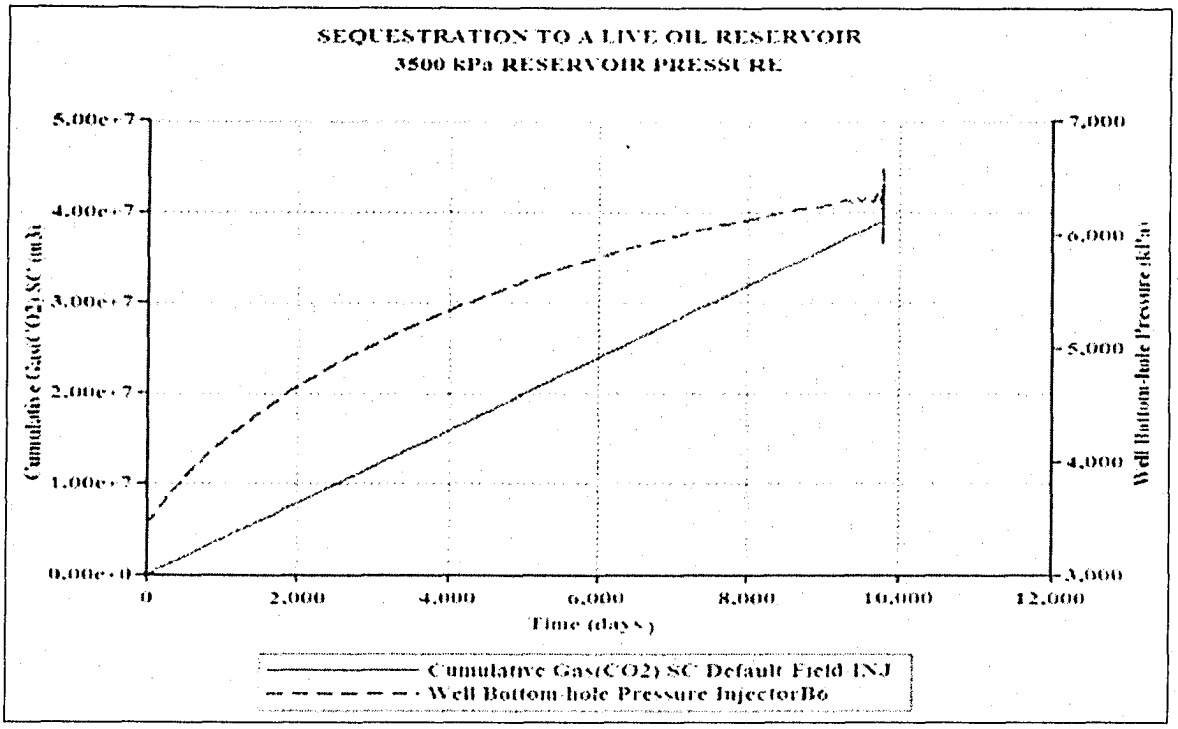

Figure 33 CO_2 Sequestration in Live Oil Reservoir at 3500 kPa Pressure from CMG STARS™

Table 9 Comparison of CO_2 Sequestration Results after Steam Flooding in a Live Oil Reservoir

Reservoir Pressure (kPa)	Total CO_2 Sequestrated Numerically (tonne)	Total CO_2 Soluble Analytically (tonne)
3500 kPa	73,962	71,296
3000 kPa	73,753	70,992
2500 kPa	73,228	70,713
2000 kPa	72,689	70,208

The comparison of the analytical and numerical sequestration results are given in Figure 34. About 71,000 tonnes of CO_2 could be sequestrated in a reservoir having live oil with the aforementioned properties.

Reproduced with permission of the copyright owner. Further reproduction prohibited without permission.

In the steam flooded dead and live oil reservoirs, the analytical and numerical calculations showed that both reservoirs can be used for sequestration purposes, depending on the residual fluids at the end of the production period. The results of less CO_2 storage and less oil recovery leads to more CO_2 sequestration over a longer time period (see Figures 30 and 32). These storage values were also confirmed the results of the study carried out by Law [4].

Given the volume of oil contained in heavy oil and bitumen reservoirs in Alberta, for each SAGD pattern defined in this study, 71,000 to 73,000 tonnes of CO_2 could be sequestrated (equivalent to about 50 PV of reservoir volume).

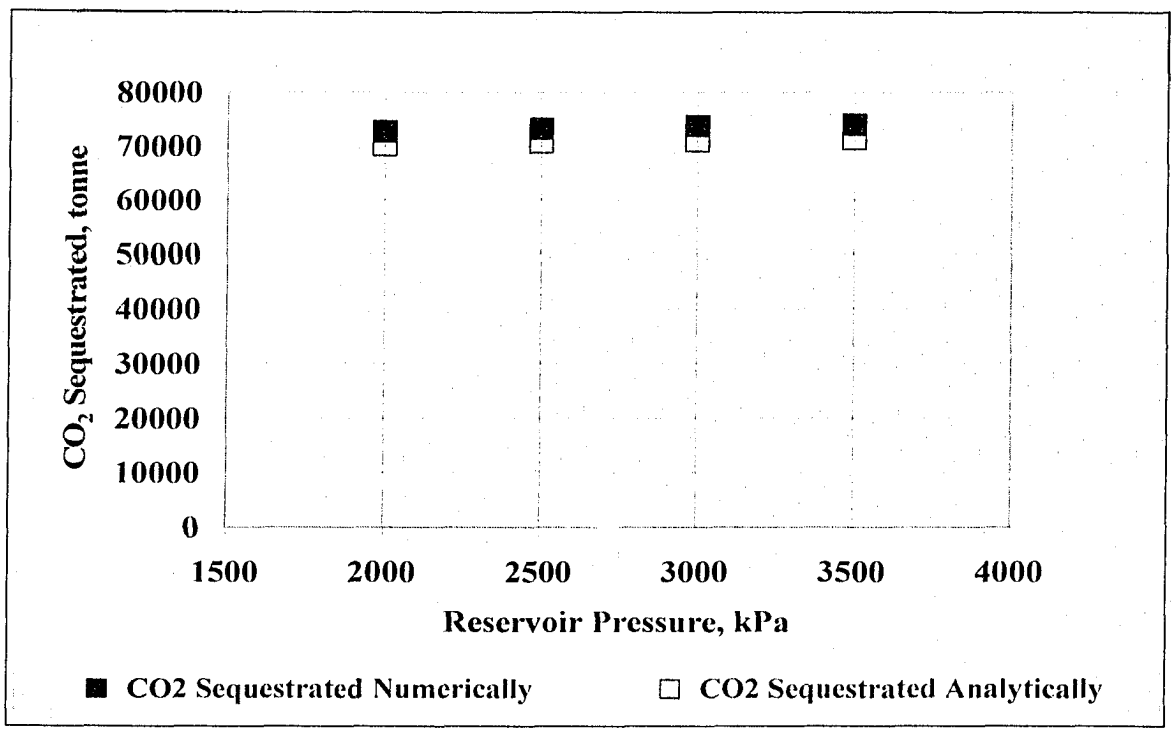

Figure 34 Comparison of Numerical and Analytical CO_2 Sequestration Calculations in Live Oil

Reproduced with permission of the copyright owner. Further reproduction prohibited without permission.

CHAPTER 6

CONCLUSIONS AND RECOMMENDATIONS FOR FUTURE WORK

6.1 CONCLUSIONS

The following conclusions can be drawn from this numerical study of the effect of CO_2 gas storage prior to steam flooding and CO_2 sequestration after the economic producing life of the reservoir. Two cases were considered for this study: reservoirs containing dead oil and live oil.

- During this numerical study, CO_2 was always injected into the heavy oil reservoir immiscibly because of the fracture pressure limitations (depth limitations).
- All of the injected CO_2 was stored, when injected at a rate of 100 sm^3/day/well (0.19 tonne/day/well), prior to a steam flood using an injection rate of 100 sm^3/day/well in a reservoir having dead oil.
- The optimum well pair separation distance for this model was 100 m.
- Injecting CO_2 prior to steam flooding decreased the CWOR and CSOR, either with or without a CO_2 soaking period.
- With CO_2 injection at the optimum rate in the dead oil case, storage of 100% of the CO_2 and decrease in the CSOR by 5% were realized, which produced a reduction in the amount of water that needed to be treated and in the GHG released to the atmosphere.
- The cumulative oil recoveries increased with the increased amount of CO_2 injected prior to the steam flooding, but the initial storage percentage decreased.
- The CO_2 storage trend in the live oil reservoir was similar to that in the dead oil reservoir at all pressures with an injection rate of 150 sm^3/day/well (0.28 tonne/day/well). The injected CO_2 was completely stored in the reservoir.
- The reservoir was tested at four different pressures for the live oil case. Increased injection rate of CO_2 increased the cumulative recovery of oil, as the reservoir pressure decreased.
- Higher reservoir pressures caused higher CH_4 recovery in the live oil case. However, the magnitude of the CO_2 injection rate had no effect on gas recovery prior to steam flooding.
- Two-year delay of production at 3500 kPa reservoir pressure decreases the net profit of such a scheme by approximately $7,312,384 in the dead oil case and $24,765,674 in the live oil case, respectively.

Reproduced with permission of the copyright owner. Further reproduction prohibited without permission.

- The cost of the CO_2 addition decreases the profit of the proposed scheme by $ 37.36/sm^3, which is a huge cost for oil companies, even at today's high oil prices.
- The analytical and numerical calculations undertaken in this study showed that, for each SAGD patterns defined, having both dead and live oil cases, 71,000 to 73,000 tonnes of CO_2 (equivalent to about 50 PV of reservoir) could be sequestrated after steam flooding, depending on the residual fluids at the end of production period. This represents a huge sink for future CO_2 sequestration and will provide an opportunity to reduce greenhouse gas emissions.

6.2 RECOMMENDATIONS FOR FUTURE WORK

There are still questions to be answered to fully study and understand the effect of CO_2 gas storage prior to steam flooding.

- Experimental verification of the numerical simulation results is strongly recommended.
- This can be done by scaling the numerical model to a laboratory model. The experimental work has to be carried out to observe and quantify the effect of CO_2 storage before steam flooding and to determine the optimum soaking time in both live and dead oil cases.
- Injecting CO_2 prior to steam and without soaking would be better for the project at least to halve the present loss form the net profit.
- New technologies should be developed to reduce the cost of CO_2 capture, transportation and compression to bring down the overall cost for the proposed process, keeping in mind that the steam flooded Alberta heavy oil and bitumen reservoirs represent a huge sink for CO_2 sequestration.

Reproduced with permission of the copyright owner. Further reproduction prohibited without permission.

REFERENCES

1 AEUB, Alberta's Reserves 2002 and Supply/Demand Outlook 2004-2013, *Statistical Series 2004-98, June 2004.*

2 NATURAL RESOURCES CANADA, Canada's Emissions Outlook: An Update, prepared for the Analysis and Modelling Group, National Climate Change Process, *December 1999.*

3 BUTLER, R.M., JIANG, Q. and YEE, C.-T., Steam and Gas Push (SAGP)—2; Mechanism Analysis and Physical Model Testing, *Journal of Canadian Petroleum Technology, 39 (4), pp. 52-61, April 2000.*

4 LAW, D., Disposal of Carbon Dioxide, a Greenhouse Gas for Pressure Maintenance in a Steam-Based Thermal Process for Recovery of Heavy Oil and Bitumen, SPE 86958, *SPE International Thermal Operations and Heavy Oil Symposium and Western Regional Meeting, Bakersfield, California, USA, March 16-18, 2004.*

5 HERZOG, H., DRAKE, E. and ADAMS. E., CO_2 Capture, Reuse and Storage Technologies for Mitigating Global Climate Change: a White Paper. *Massachusetts Institute of Technology, Energy Laboratory Report under DOE Order DE-AF22-96PC01257, Cambridge, MA 02139. 1997.*

6 DUNBAR, R.B. and SLOAN T.W., Does Nuclear Energy Have a Role in the Development of Canada's Oil Sands?, *Canadian International Petroleum Conference, Calgary, AB, Canada, June 10-12, 2003.*

7 CHAPEL, D.G and MARIZ, C.L., Recovery of CO_2 from flue Gases: Commercial Trends, *Canadian Society of Chemical Engineers Annual Meeting, and October 4-6, 1999.*

8 HERZOG, H. and GOLOMB, D., Carbon Capture and Storage From Fossil Fuel Use, *Massachusetts Institute of Technology, Laboratory* for *Energy and the Environment, Chapter Contribution to Encyclopaedia of Energy, 2004.*

9 HENDRIKS C. A. and BLOK K., Underground Storage of Carbon Dioxide, *Energy Conversion. Management, 34(9-11), 949-957, 1993.*

Reproduced with permission of the copyright owner. Further reproduction prohibited without permission.

10 BACHU, S., Sequestration of CO2 in Geological Media: Criteria and Approach for Site Selection in Response to Climate Change; *Energy Conversion and Management, Volume 41, pp. 953-970, 2000.*

11 EDWARDS, K., CO_2 in Alberta—A Vision of the Future; *Journal of Canadian Petroleum Technology, Volume 39, No. 9, pp. 48-53, September 2000.*

12 HELM, L.W. and JOSENDAL, V.A., Mechanisms of Oil Displacement by Carbon Dioxide; SPE 4736, *Journal of Petroleum Technology, pp. 1427-1438, November 1974.*

13 MUNGAN, N., An Evaluation of Carbon Dioxide Flooding, SPE 21762, *SPE Western Regional. Meeting, Long Beach, California, USA, pp. 113–122. March 20–22, 1991.*

14 KOVSCEK, A.R., Screening Criteria for CO_2 Storage in Oil Reservoirs, *Petroleum Science and Technology, Volume 20, No. 7 & 8, pp. 841–866, 2002.*

15 SRIVASTAVA, R.K., HUANG, S.S. and DONG, M., Laboratory Investigation of Weyburn Miscible Flooding, *Journal of Canadian Petroleum Technology, Volume 39, No. 2, pp. 41-51, February 2000.*

16 DONG, M., HUANG, S.S., and SRIVASTAVA, R.K., Effect of Solution Gas in Oil on CO_2 Minimum Miscibility Pressure, *Journal of Canadian Petroleum Technology, 39 (11), pp. 53-61, November 2000.*

17 YONGMAO, H., ZENGGUI, W. YUEMING, C. and XIANGJIE, L., Laboratory Investigation of CO_2 Flooding, SPE 88883, *28th Annual SPE International Technical Conference and Exhibition, Abuja, Nigeria, August 2-4, 2004.*

18 WHITE, D.J., BURROWES, G., DAVIS, T., HAJNAL, Z., HIRSCHE, K., HUTCHEON, I., MAJER, E., ROSTRON, B. and WHITTAKER, S., Greenhouse Gas Sequestration in Abandoned Oil Reservoirs: The International Energy Agency Weyburn Pilot Project, *The Geological Society of America, Volume 14, No.7, pp. 4-10, February 2004.*

19 JESCHKE, P.A. SCHOELING, L. and HEMMINGS, J., CO_2 Flood Potential of California Oil Reservoirs and Possible CO_2 Sources, SPE 63305, *2000 SPE/AAPG Western Regional Meeting, Long Beach, California, June 19-23, 2000.*

Reproduced with permission of the copyright owner. Further reproduction prohibited without permission.

20 KARAOGUZ, K.O., TOPGUDER, N.N., LANE, R.H., KALFA, U. and CELEBIOGLU, D., Improved Sweep In Bati Raman Heavy-Oil CO_2 Flood: Bullhead Flowing Gel Treatments Plug Natural Fractures, SPE 89400, *SPE/DOE 14th Symposium on Improved Oil Recovery, Tulsa, Oklahoma, USA, April 17-21, 2004.*

21 HUANG, S.S. and DYER, S.B., Miscible Displacement in the Weyburn Reservoir: A Laboratory Study *Journal of Canadian Petroleum Technology, Volume 32, No.7 pp. 42-52, September 1993.*

22 ADVANCED RESOURCES INTERNATIONAL, INC., Basin Oriented Strategies for CO_2 Enhanced Oil Recovery: Onshore California Oil Basins, *U.S. Department of Energy Office of Fossil Energy – Office of Oil and Natural Gas, March 2005.*

23 TABER, J.J. and MARTIN, F.D., Technical Screening Guides for the Enhanced Recovery, SPE 12069, *58th Annual Technical Conference and Exhibition, San Francisco, California, USA, October 5-8, 1983.*

24 FAROUQ ALI, S.M., Heavy Oil Recovery - Principles, Practicality, Potential, and Problems, SPE 4935, *The Rocky Mountain Regional Meeting of the Society of Petroleum Engineers of AIME, May 15-16, 1974.*

25 BUTLER, R.M., Horizontal Wells for the Recovery of Oil, Gas and Bitumen; *Petroleum Society Monograph No.2, Canadian Institute of Mining, Metallurgy & Petroleum, Calgary, AB, 1994*

26 BUTLER, R.M., Thermal Recovery of Oil and Bitumen; GravDrain`s Blackbook, *GravDrain Inc., Calgary, AB, Canada, pp. 285-359, 1997.*

27 BUTLER, R.M. AND YEE, C.T., A Theoretical Study of Steam Condensation in The Presence of Non-Condensable Gases in Porous Solids, *AOSTRA Journal of Research 3 (1), 1986.*

28 ROSE P.E. and DOE, M.D., Steam Assisted Gravity Drainage in Oil Sand Reservoirs Using a Combination of Vertical and Horizontal Wells, *Butterworth Heinemann Fuel, 74 (8): 1180-84, 1995.*

Reproduced with permission of the copyright owner. Further reproduction prohibited without permission.

29 FRAUENFELD, T.W.J., RIDLEY, R.K. and NGUYEN D.M., Effect of Initial Gas Content on Thermal EORs Applied to Oil Sands, *Journal of Petroleum Technology, pp. 333-338, March 1988.*

30 METWALLY, M., Effect of Gaseous Additives on Steam Processes for Lindenberg Field Alberta, *Journal of Canadian Petroleum Technology., Volume 29, No.6 pp. 26-30, (Nov-Dec) 1990.*

31 ITO, Y., ICHIKAWA, M. and HIRATA, T., The Effect of Gas Injection on Oil Recovery During SAGD Projects, *CSPG and Petroleum Society Joint Convention, Digging Deeper, Finding a Better Bottom Line, in Calgary, AB, Canada, June 14 – 18, 1999.*

32 CANBOLAT, S., A Study of Steam Assisted Gravity Drainage Performance in the Presence of Non-Condensable Gases, *M.Sc. Thesis. Middle East Technical University, Ankara Turkey, December 2001.*

33 Computer Modeling Group (CMG) LTD., CMG STARS Advanced Process and Thermal Reservoir Simulator, *Version 2004.10, Calgary, AB, Canada, 2004.*

34 KISMAN, K.E. and YEUNG, K.C., Numerical Study of the SAGD Process in the Burnt Lake Oil Sands Lease, SPE 30276, *International Heavy Oil Symposium, Calgary, AB, Canada, June 19-21, 1995.*

35 SAYEGH, S.G. and MAINI, B.B., Laboratory Evaluation of the CO_2 Huff-n-Puff Process for Heavy Oil Reservoirs, *Journal of Canadian Petroleum Technology, pp. 78-76, May-June 1990.*

36 ADAMS, D.M., Experiences with Water Flooding Lloydminister Heavy Oil Reservoirs, *Journal of Canadian Petroleum Technology, pp. 1643-1650, August 1982.*

37 CRAWFORD, H.R., NEILL, G.H., BUCY, B.J., and CRAWFORD, P.B., Carbon Dioxide: A Multipurpose Additive for Effective Well Stimulation, *Journal of Petroleum Technology, 237, March 1963.*

38 HOLM, L.W., CO_2 Slug and Carbonated Water Oil Recovery Processes, *Producers Monthly, 6, September 1963.*

Reproduced with permission of the copyright owner. Further reproduction prohibited without permission.

39 JARRELL, P.M., FOX, C.E., STEIN, M.H., and WEBB, S L., Practical Aspects of CO_2 Flooding, *SPE Monograph 22, 220pp, 2002.*

40 MANGALSINGH, D. AND JAGAI, T., A Laboratory Investigation of the Carbon Dioxide Immiscible Process, SPE 36134, *4th Latin American and Caribbean Petroleum Engineering Conference, Port of Spain, Trinidad & Tobago, April 23-26, 1996.*

41 FRAUENFELD, T.W.J., KISSEL, G. and ZHOU, S., PVT and Viscosity Measurements for Lloydminister-Aberfeldy and Cold Lake Blended Oil Systems, SPE 79018, *International Thermal Operations and Heavy Oil Symposium and International Horizontal Well Technology Conference, Calgary, AB, Canada, November 4-7, 2002.*

42 DONNELLY, J.K., The Best Process for Cold Lake: CSS vs. SAGD, *Journal of Canadian Petroleum Technology, 39(8), pp. 5-7, August 2000.*

43 JHA, K.N., A Laboratory Study of Heavy Oil Recovery with Carbon Dioxide, *The Annual Technical Meeting of the South Saskatchewan Section, Petroleum Society of Canadian Institute of Mining , Metallurgy and Petroleum Comference, Regina, SK, Canada September 15-17, 1985.*

44 HORNBROOK M.W., DEGHANI K., QADEER S.,OSTERMANN R.D., and OGBE D.O., Effects of CO_2 Addition to Steam on Recovery of West-Sak Crude Oil, *SPE 18753, SPE Reservoir Engineering, 273-286, August 1991.*

45 SINGH, S., DU PLESSIS, M.P., ISAACS, E.E. and KERR, R., Cost Analysis of Advanced Technologies for the Production of Heavy Oil and Bitumen in Western Canada, 1999-2003, *World Energy Council Report, 2004.*

Reproduced with permission of the copyright owner. Further reproduction prohibited without permission.

APPENDICES

Reproduced with permission of the copyright owner. Further reproduction prohibited without permission.

Appendix A Data File for the Simulator

```
** 4/12/2005, 6:54:53 PM, canbolat
RESULTS SIMULATOR STARS 200410

**=========INPUT/OUTPUT CONTROL===============================
**checkonly    ** check well data without running simulation
*TITLE1  'LLOYDMINSTER'
*TITLE2  'DUAL SAGD Wells'
*TITLE3  'Data file: STEAM INJECTION'

*INUNIT *SI EXCEPT 6 1 **$ darcy instead of md
*OUTUNIT *SI EXCEPT 6 1 **$ darcy instead of md

*WRST *TIME
*OUTPRN *GRID *NONE
*OUTPRN *ITER *BRIEF
OUTSRF GRID PRES SG SO SW TEMP VPOROS X Y
OUTSRF WELL DOWNHOLE
OUTSRF WELL LAYER ALL
OUTSRF WELL COMPONENT ALL
*OUTPRN *WELL *WELLCOMP
*OUTPRN *ITER *NEWTON
*PRNTORIEN  2  0


GRID CART 201 1 25
KDIR UP
DI CON 1.
DJ CON 500.
DK CON 1.
DTOP
 201*750.

NINEPOINT IK
**$
**$ Property: NULL Blocks  Max: 1  Min: 1
**$  0 = null block, 1 = active block
NULL CON            1
**$ RESULTS PROP POR  Units: Dimensionless
POR CON 0.32
**$ RESULTS PROP PERMI  Units: darcy
PERMI CON 2.
PERMJ EQUALSI
**$ RESULTS PROP PERMK  Units: darcy
PERMK CON 2.
**$
**$ Property: Pinchout Array  Max: 1  Min: 1
**$  0 = pinched block, 1 = active block
PINCHOUTARRAY CON            1
END-GRID
ROCKTYPE 1
PRPOR 3500.
CPOR 7.4E-006
CTPOR 0
```


Reproduced with permission of the copyright owner. Further reproduction prohibited without permission.

```
ROCKCP 2.3E+06
THCONR 6.E+05
THCONW 5.3E+04
THCONO 1.1E+04
THCONG 139
HLOSST 21.
HLOSSTDIFF 0.1
HLOSSPROP OVERBUR 2.3E+06 1.4E+05
UNDERBUR 2.3E+06 1.4E+05


**$ Model and number of components
MODEL 3 3 2 1
COMPNAME 'WATER' 'OIL' 'CO2'
CMM 0.018 0.329 0.04401
PCRIT 22048 797 7376
TCRIT 374.15 588 31.05
KV1 1.1816000E+07 5.718929E+06
KV4 -3.81644E+03 -4.933E+03
KV5 -2.2702E+02 -1.164E+02
PRSR 101.325
TEMR 20
PSURF 1.01325E+2
TSURF 20
**$ Surface conditions
SURFLASH W O G
CPG1 0.0E+0 8.41E+2 0
CPL1 0.0E+0 1.060E+3 0
HVAPR 0 9813
MOLDEN 1.8E+3 2E+3
CP 0.0E+0 5.5E-7
CT1 0.0E+0 8.0E-4
CT2 0.0E+0 0.0E+0


**Temp(C)     Water         Oil
** ------------------------------------------------------------
VISCTABLE
**$  temp
15       0       26971
20       0       10024
40       0       1500
60       0       300
80       0       100
100      0       46
114      0       25
120      0       21
140      0       12
160      0       8
180      0       5
200      0       4
220      0       3
240      0       2
260      0       1
```


Reproduced with permission of the copyright owner. Further reproduction prohibited without permission.

```
** ============== ROCK-FLUID PROPERTIES ==============

*ROCKFLUID

*RPT 1 *WATWET *STONE2
*SWT
**  SW        KRW        KROW
**  ----------------------------------
0.187000  0.000000  0.800000  0.000000
0.250000  0.012300  0.197500  0.000000
0.350000  0.047400  0.080900  0.000000
0.450000  0.126900  0.025600  0.000000
0.550000  0.169200  0.005000  0.000000
0.600000  0.184100  0.000300  0.000000
0.650000  0.280000  0.000000  0.000000

*SLT
**  S1KRG     KROG
** ----------------------------------
0.187000  1.000000  0.000000  0.000000
0.250000  0.197500  0.012300  0.000000
0.350000  0.080900  0.047400  0.000000
0.450000  0.025600  0.129600  0.000000
0.550000  0.005000  0.289200  0.000000
0.650000  0.000300  0.564100  0.000000
0.900000  0.000000  0.800000  0.000000

**$ RESULTS PROP KRTYPE  Units: Dimensionless
**$ RESULTS PROP Minimum Value: 1  Maximum Value: 1
KRTYPE CON 1.

**============== INTIAL CONDITIONS ==============
*INITIAL
*VERTICAL *ON
**$ Data for PVT Region 1
**$ ------------------------------------
*INITREGION 1
*REFDEPTH 775.
*REFPRES 3500.

**$ RESULTS PROP SW  Units: Dimensionless
**$ RESULTS PROP Minimum Value: 0.2  Maximum Value: 0.2
SW CON 0.20
**$ RESULTS PROP PRES  Units: kPa
**$ RESULTS PROP Minimum Value: 1500  Maximum Value: 1500
PRES CON 3500.
**$ RESULTS PROP SO  Units: Dimensionless
**$ RESULTS PROP Minimum Value: 0.8  Maximum Value: 0.8
SO CON 0.80
**$ RESULTS PROP TEMP  Units: C
**$ RESULTS PROP Minimum Value: 18  Maximum Value: 18
TEMP CON 21.
**$ RESULTS PROP SG  Units: Dimensionless
**$ RESULTS PROP Minimum Value: 0  Maximum Value: 0
SG CON 0
**$ RESULTS PROP MFRAC_OIL 'OIL'  Units: Dimensionless
MFRAC_OIL 'OIL' CON 1.
```


Reproduced with permission of the copyright owner. Further reproduction prohibited without permission.

```
**========== Numerical Control ==============
*NUMERICAL

RUN



TIME 0

DTWELL 0.0001

**$
WELL  'InjectorB3'  FRAC  1.
INJECTOR UNWEIGHT 'InjectorB3'
INCOMP  GAS  0.  0.  0.  1.
TINJW  20.
OPERATE  MAX  STG  100.  CONT REPEAT
**$      rad  geofac  wfrac  skin
GEOMETRY  J  0.11  0.249  1.  0.
PERF  GEO  'InjectorB3'
**$ UBA      ff  Status  Connection
    51 1 6  1.  OPEN    FLOW-FROM  'SURFACE'

**$
WELL  'InjectorB4'  FRAC  1.
INJECTOR UNWEIGHT 'InjectorB4'
INCOMP  GAS  0.  0.  0.  1.
TINJW  20.
OPERATE  MAX  STG  100.  CONT REPEAT
**$      rad  geofac  wfrac  skin
GEOMETRY  J  0.11  0.249  1.  0.
PERF  GEO  'InjectorB4'
**$ UBA      ff  Status  Connection
    151 1 6  1.  OPEN    FLOW-FROM  'SURFACE'


**$ RESULTS PROP UHTR  Units: J/day-C
**$ RESULTS PROP Minimum Value: 0  Maximum Value: 0

UHTR CON 0


TIME 31.5

TIME 61.5

TIME 91.5

TIME 121.5

TIME 151.75

TIME 182.5

TIME 212.75

TIME 243
```


Reproduced with permission of the copyright owner. Further reproduction prohibited without permission.

```
TIME 273.75

TIME 365

SHUTIN 'InjectorB4'

SHUTIN 'InjectorB3'

TIME 548

TIME 730

DTWELL 0.001



**$
WELL  'InjectorB1'  FRAC  1.
INJECTOR MOBWEIGHT EXPLICIT 'InjectorB1'
INCOMP  WATER  1.  0.
TINJW  242.
QUAL  0.95
OPERATE  MAX  BHP  3510.  CONT REPEAT
OPERATE  MAX  STW  100.  CONT REPEAT
**$       rad  geofac  wfrac  skin
GEOMETRY  J  0.11  0.249  1.  0.
PERF  GEO  'InjectorB1'
**$ UBA      ff  Status  Connection
    51 1 6  1.  OPEN    FLOW-FROM  'SURFACE'


**$
WELL  'InjectorB2'  FRAC  1.
INJECTOR MOBWEIGHT EXPLICIT 'InjectorB2'
INCOMP  WATER  1.  0.
TINJW  242.
QUAL  0.95
OPERATE  MAX  BHP  3510.  CONT REPEAT
OPERATE  MAX  STW  100.  CONT REPEAT
**$       rad  geofac  wfrac  skin
GEOMETRY  J  0.11  0.249  1.  0.
PERF  GEO  'InjectorB2'
**$ UBA      ff  Status  Connection
    151 1 6  1.  OPEN    FLOW-FROM  'SURFACE'
**$
WELL  'ProducerB1'  FRAC  1.
PRODUCER 'ProducerB1'
OPERATE  MIN  BHP  3500.  CONT REPEAT
OPERATE  MIN  STEAMTRAP  5.  CONT REPEAT
**$       rad  geofac  wfrac  skin
GEOMETRY  J  0.11  0.249  1.  0.
PERF  GEO  'ProducerB1'
**$ UBA      ff  Status  Connection
    51 1 1  1.  OPEN    FLOW-TO  'SURFACE'
```


Reproduced with permission of the copyright owner. Further reproduction prohibited without permission.

```
WELL  'ProducerB2'  FRAC  1.
PRODUCER 'ProducerB2'
OPERATE  MIN  BHP  3500.  CONT REPEAT
OPERATE  MIN  STEAMTRAP  5.  CONT REPEAT
**$          rad  geofac  wfrac  skin
GEOMETRY  J  0.11  0.249  1.  0.
PERF  GEO  'ProducerB2'
**$ UBA      ff  Status  Connection
    151 1 1  1.  OPEN    FLOW-TO  'SURFACE'


TIME 731

TIME 913

TIME 1095

:
:
:
:

TIME 13928

TIME 14110

TIME 14293

TIME 14475


STOP

RESULTS SPEC 'Permeability J'
RESULTS SPEC SPECNOTCALCVAL 0
RESULTS SPEC REGION 'All Layers (Whole Grid)'
RESULTS SPEC REGIONTYPE 0
RESULTS SPEC LAYERNUMB 0
RESULTS SPEC PORTYPE 1
RESULTS SPEC EQUALSI 0 1
RESULTS SPEC STOP
RESULTS WPD END
```


Reproduced with permission of the copyright owner. Further reproduction prohibited without permission.

Appendix B Oil Recovery Curves with CO_2 Injection

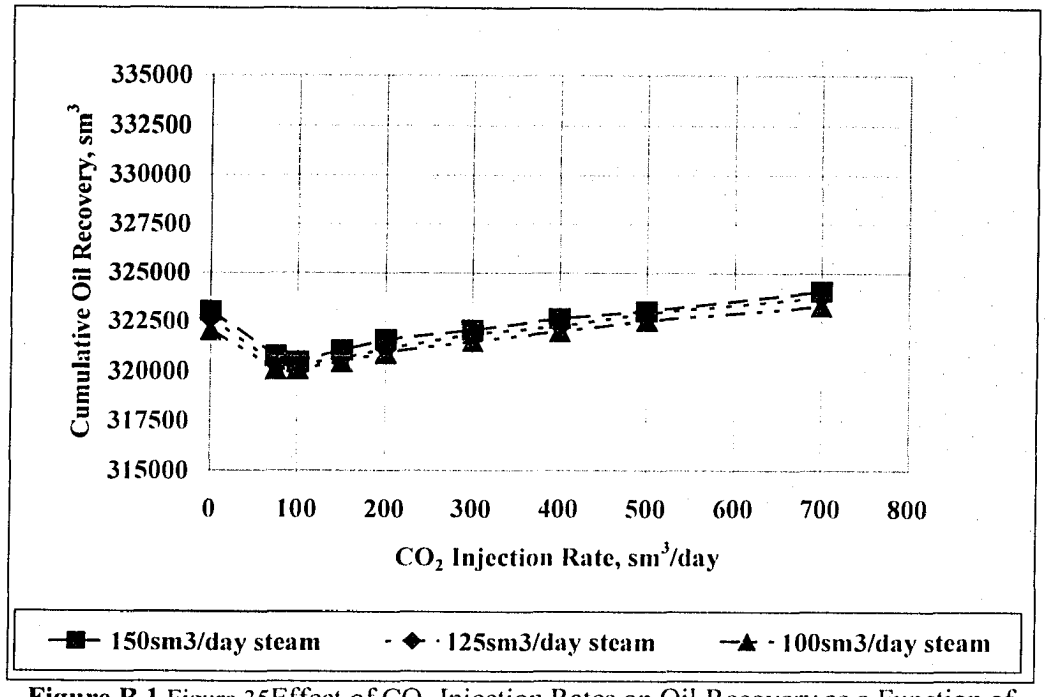

Figure B.1 Figure 35Effect of CO_2 Injection Rates on Oil Recovery as a Function of Steam Injection Rate for Well Pair Spacing of 80 m

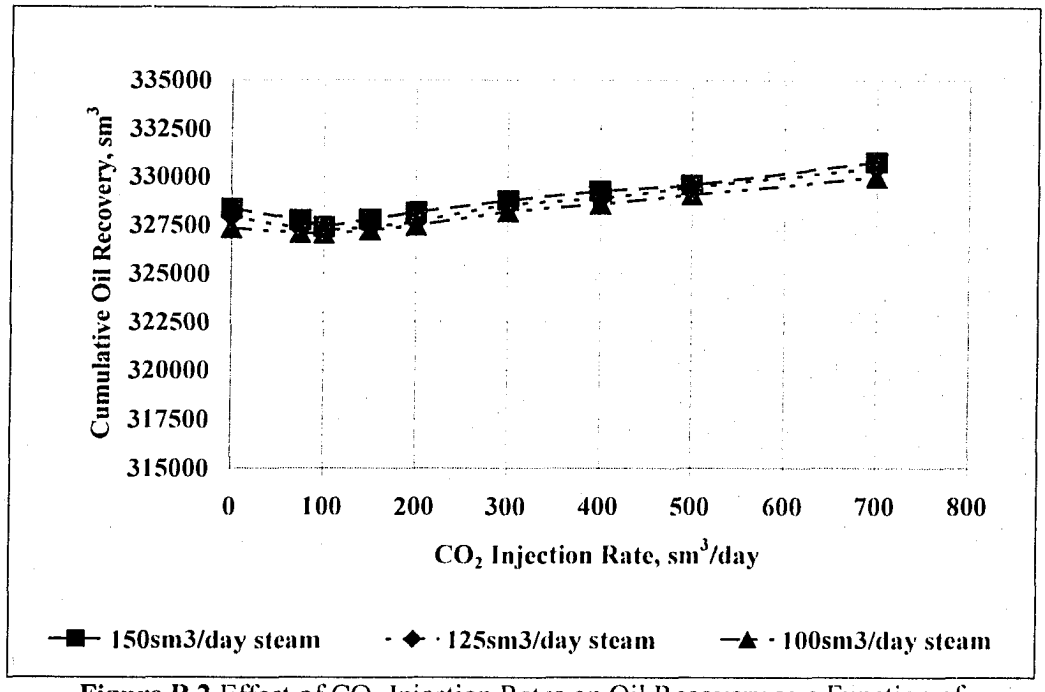

Figure B.2 Effect of CO_2 Injection Rates on Oil Recovery as a Function of Steam Injection Rate for Well Pair Spacing of 90 m

Reproduced with permission of the copyright owner. Further reproduction prohibited without permission.

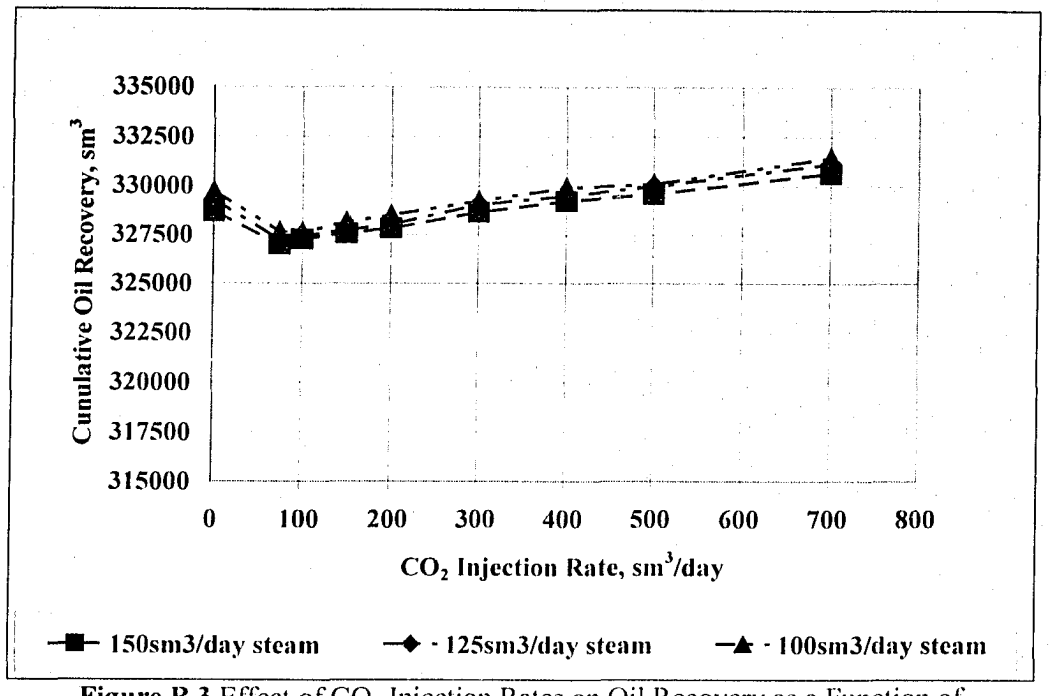

Figure B.3 Effect of CO_2 Injection Rates on Oil Recovery as a Function of Steam Injection Rate for Well Pair Spacing of 110 m

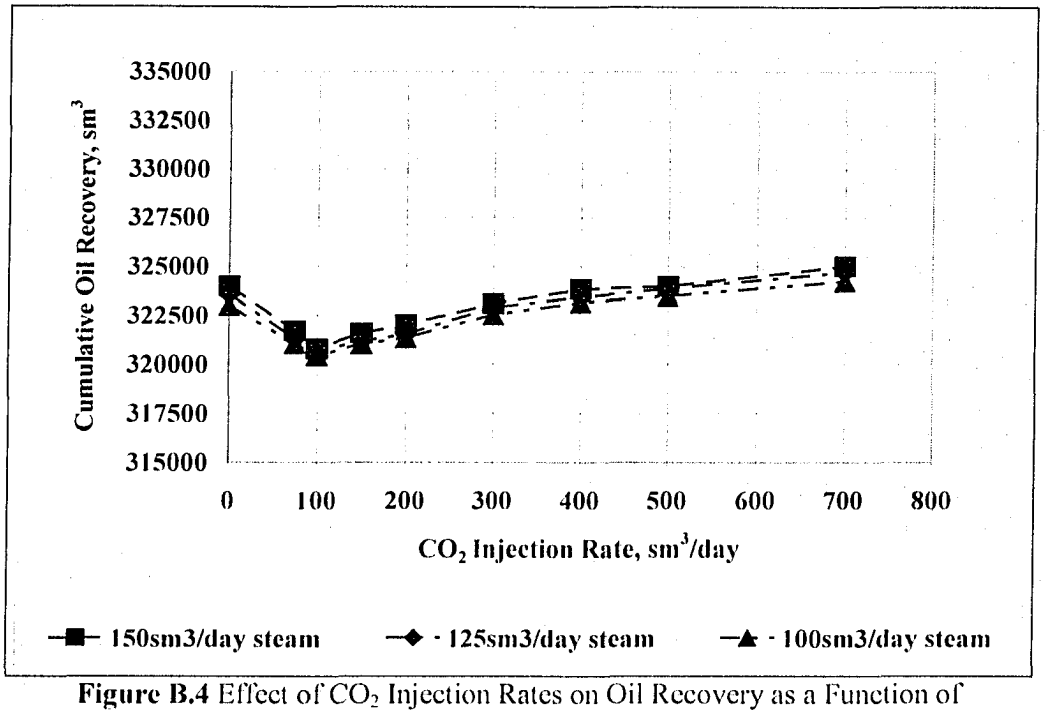

Figure B.4 Effect of CO_2 Injection Rates on Oil Recovery as a Function of Steam Injection Rate for Well Pair Spacing of 120 m

Reproduced with permission of the copyright owner. Further reproduction prohibited without permission.

Appendix C CO_2 Storage percent at Different Well Pair Distances

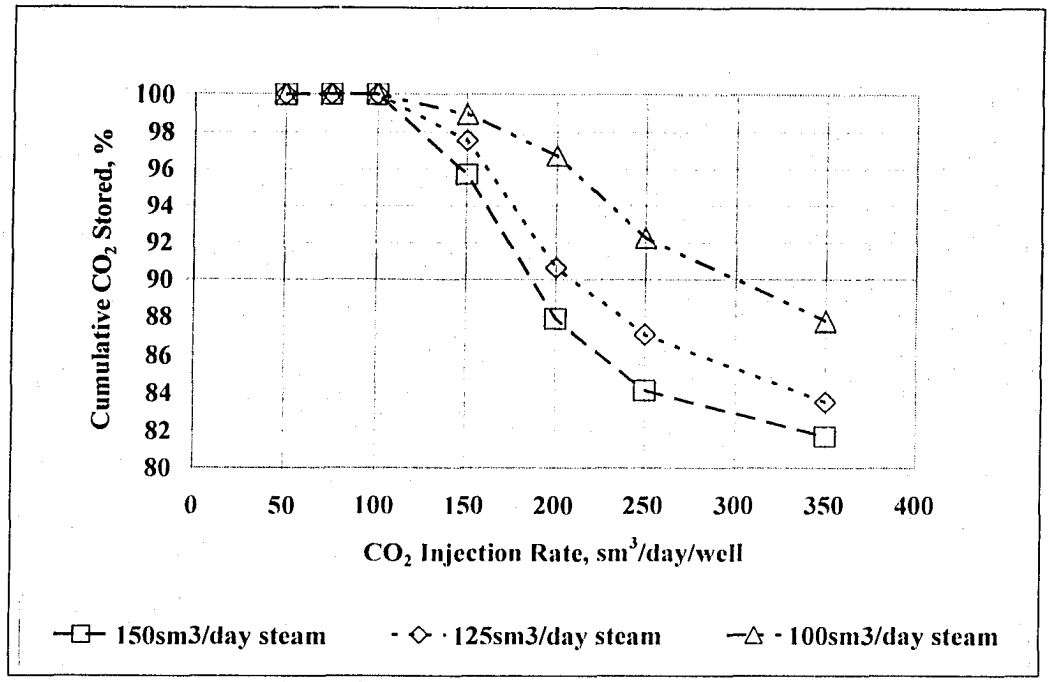

Figure C.1 Effect of CO_2 Injection Rates on Storage as a Function of Steam Injection Rate for Well Pair Spacing of 80 m

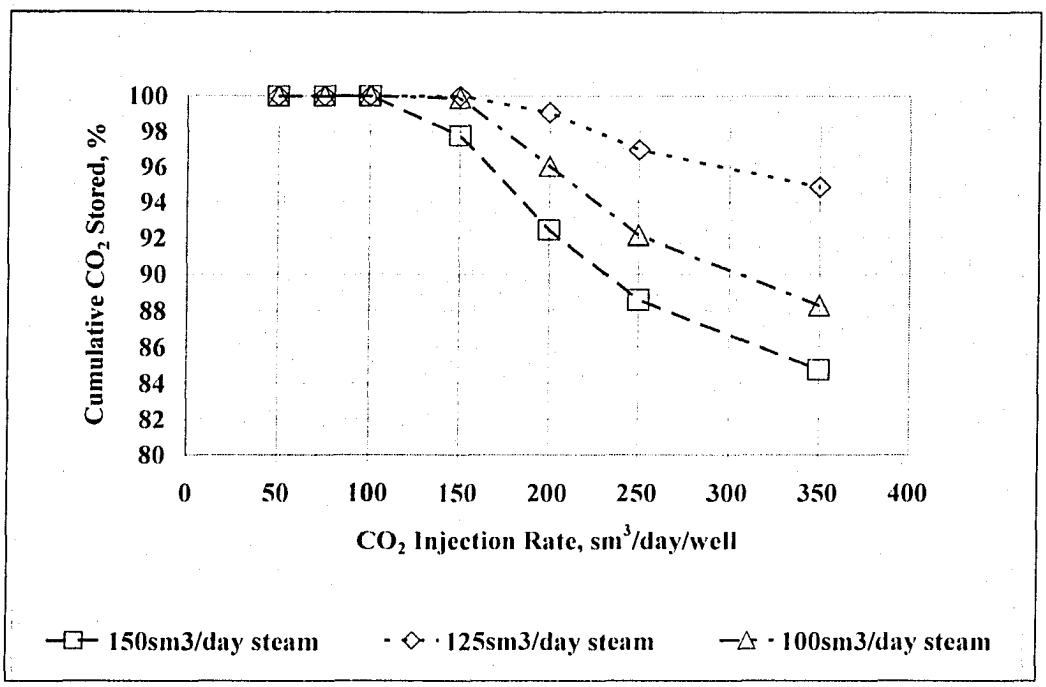

Figure C.2 Effect of CO_2 Injection Rates on Storage as a Function of Steam Injection Rate for Well Pair Spacing of 90 m

Reproduced with permission of the copyright owner. Further reproduction prohibited without permission.

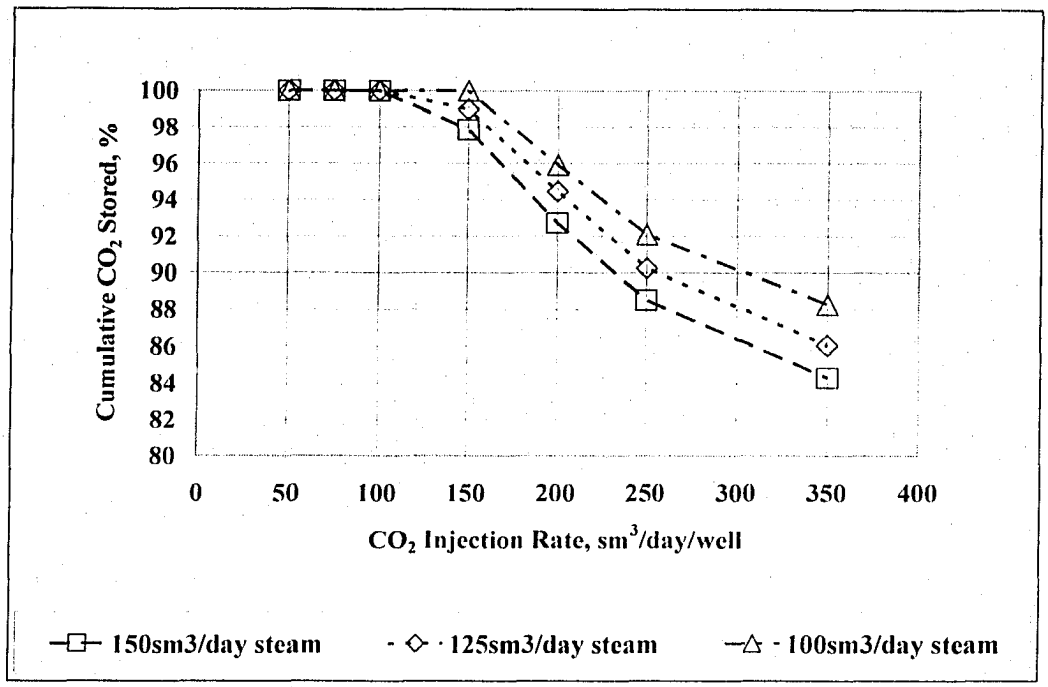

Figure C.3 Effect of CO_2 Injection Rates on Storage as a Function of Steam Injection Rate for Well Pair Spacing of 110 m

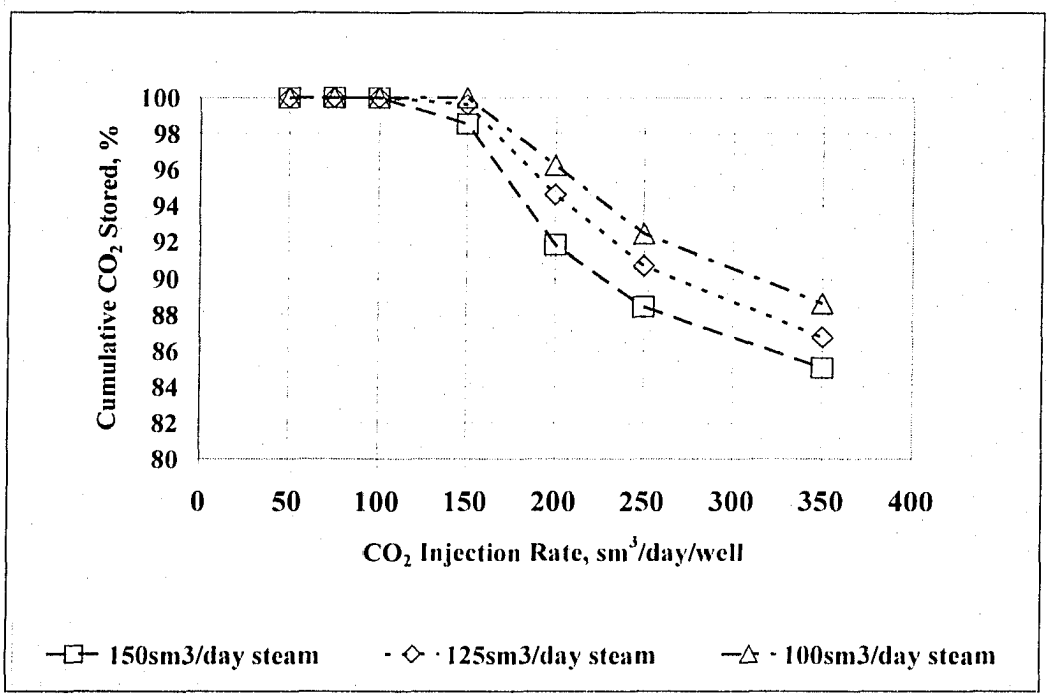

Figure C.4 Effect of CO_2 Injection Rates on Storage as a Function of Steam Injection Rate for Well Pair Spacing of 120 m

Reproduced with permission of the copyright owner. Further reproduction prohibited without permission.

Reproduced with permission of the copyright owner. Further reproduction prohibited without permission.

Appendix D Comparison of Temperature Profiles with and without CO_2 Injection

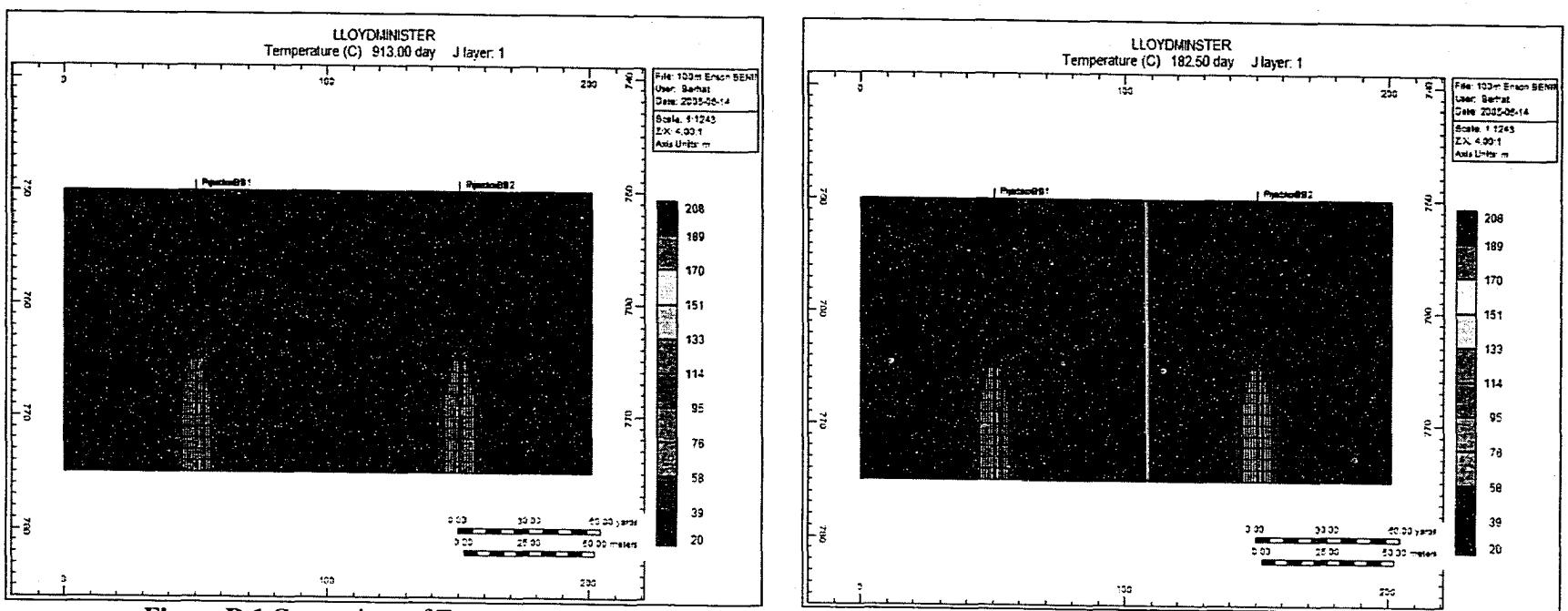

Figure D.1 Comparison of Temperature Profiles in Dead Oil with (left) and without (right) CO_2 Injection after 6 Months of Steam Flooding

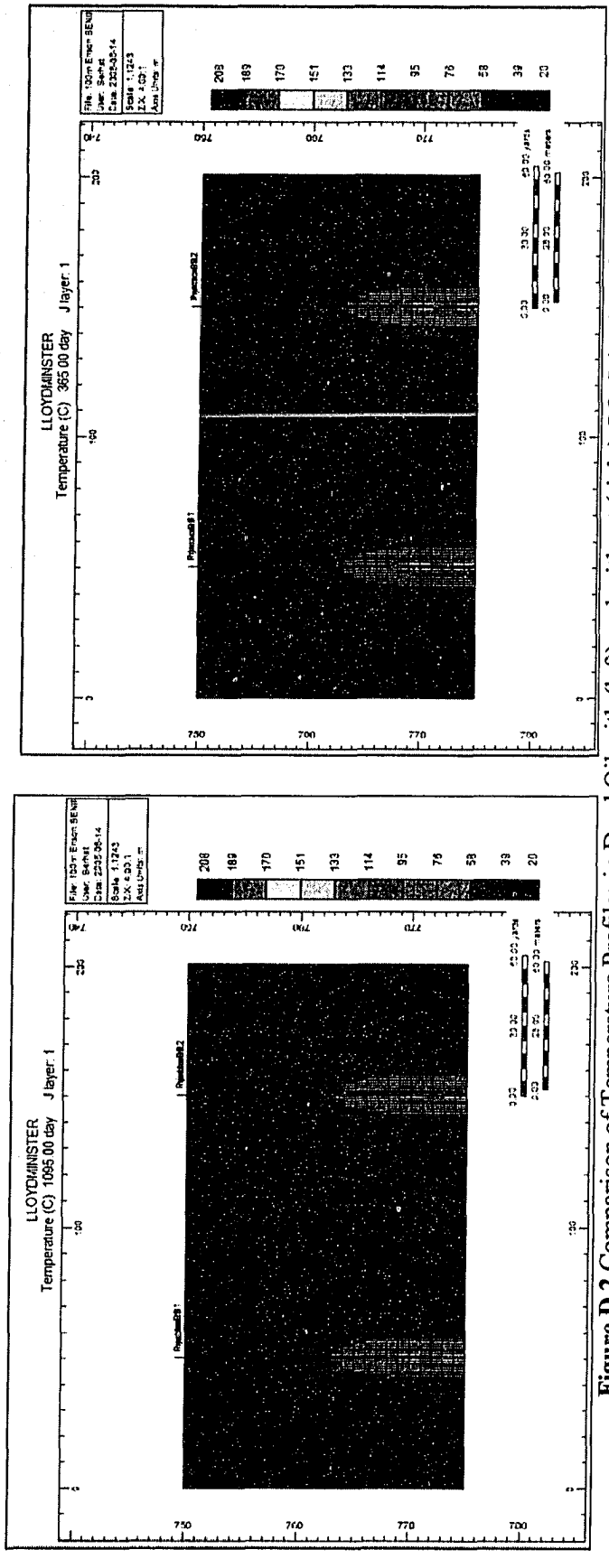

Figure D.2 Comparison of Temperature Profiles in Dead Oil with (left) and without (right) CO_2 Injection after 1 Year of Steam Flooding

Reproduced with permission of the copyright owner. Further reproduction prohibited without permission.

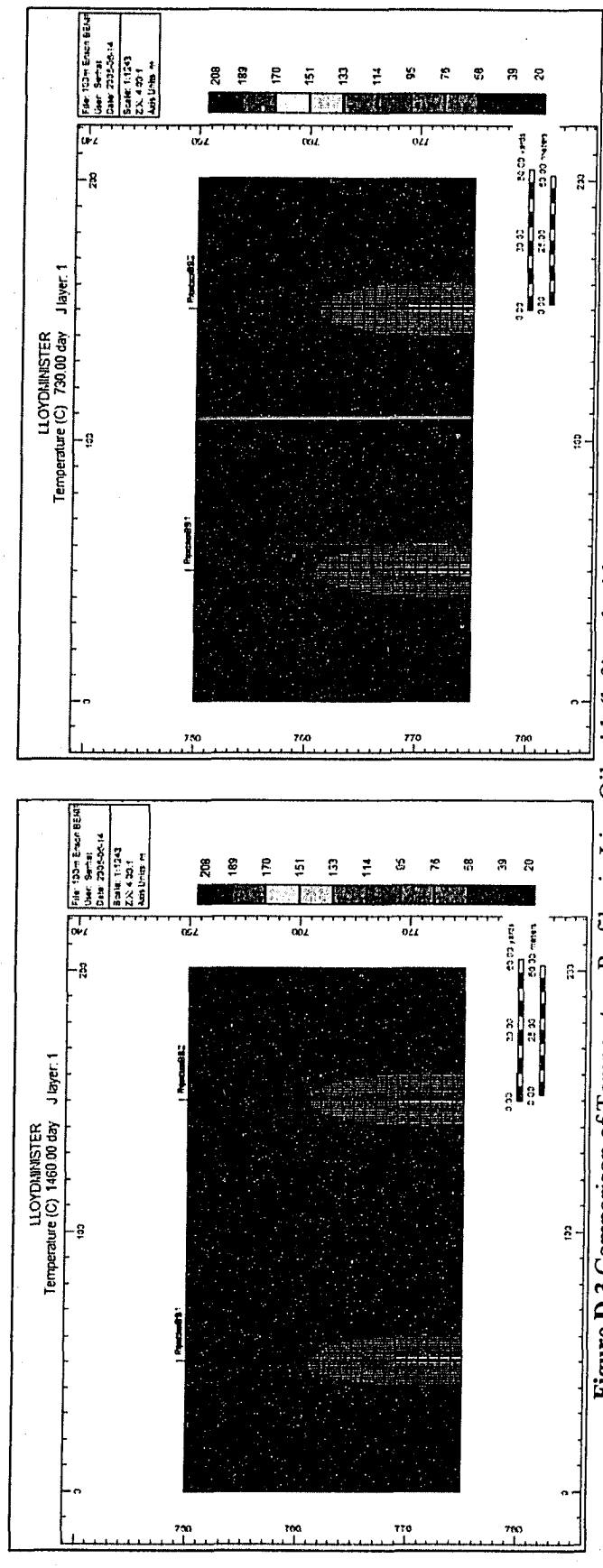

Figure D.3 Comparison of Temperature Profiles in Live Oil with (left) and without (right) CO_2 Injection after 2 Years of Steam Flooding

Reproduced with permission of the copyright owner. Further reproduction prohibited without permission.

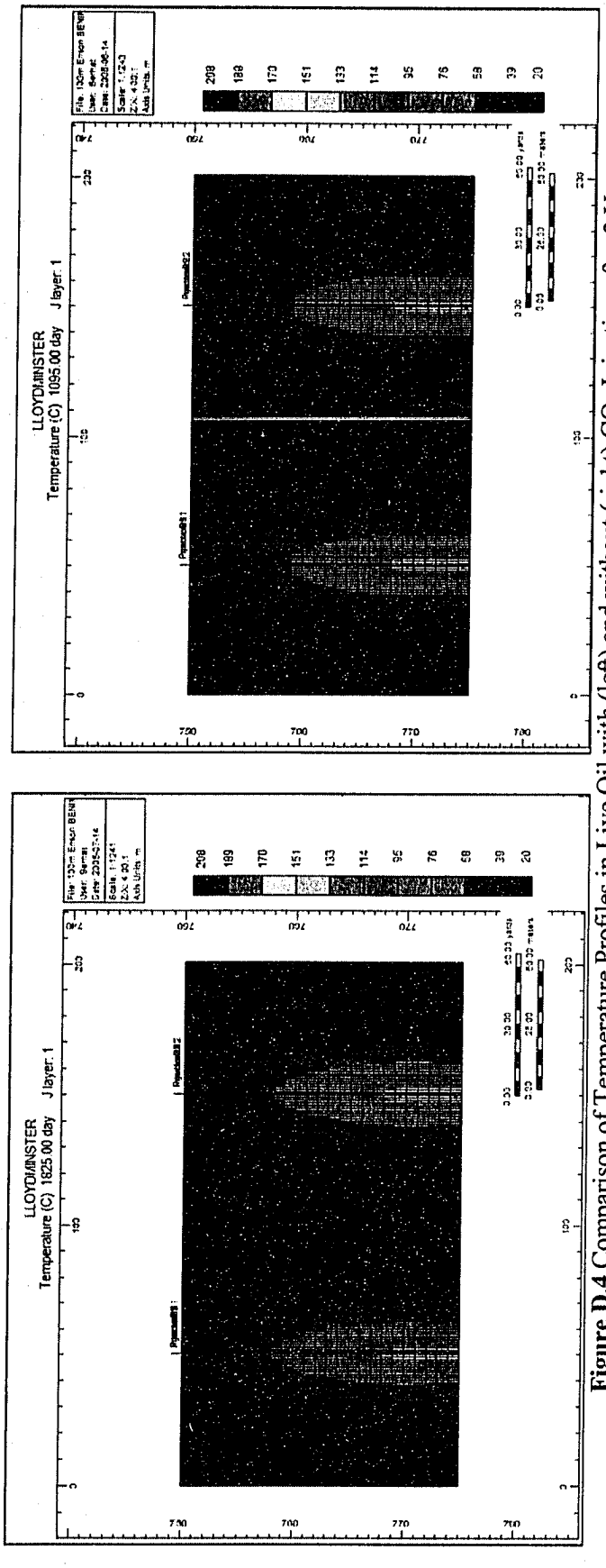

Figure D.4 Comparison of Temperature Profiles in Live Oil with (left) and without (right) CO_2 Injection after 3 Years of Steam Flooding

Reproduced with permission of the copyright owner. Further reproduction prohibited without permission.

Reproduced with permission of the copyright owner. Further reproduction prohibited without permission.

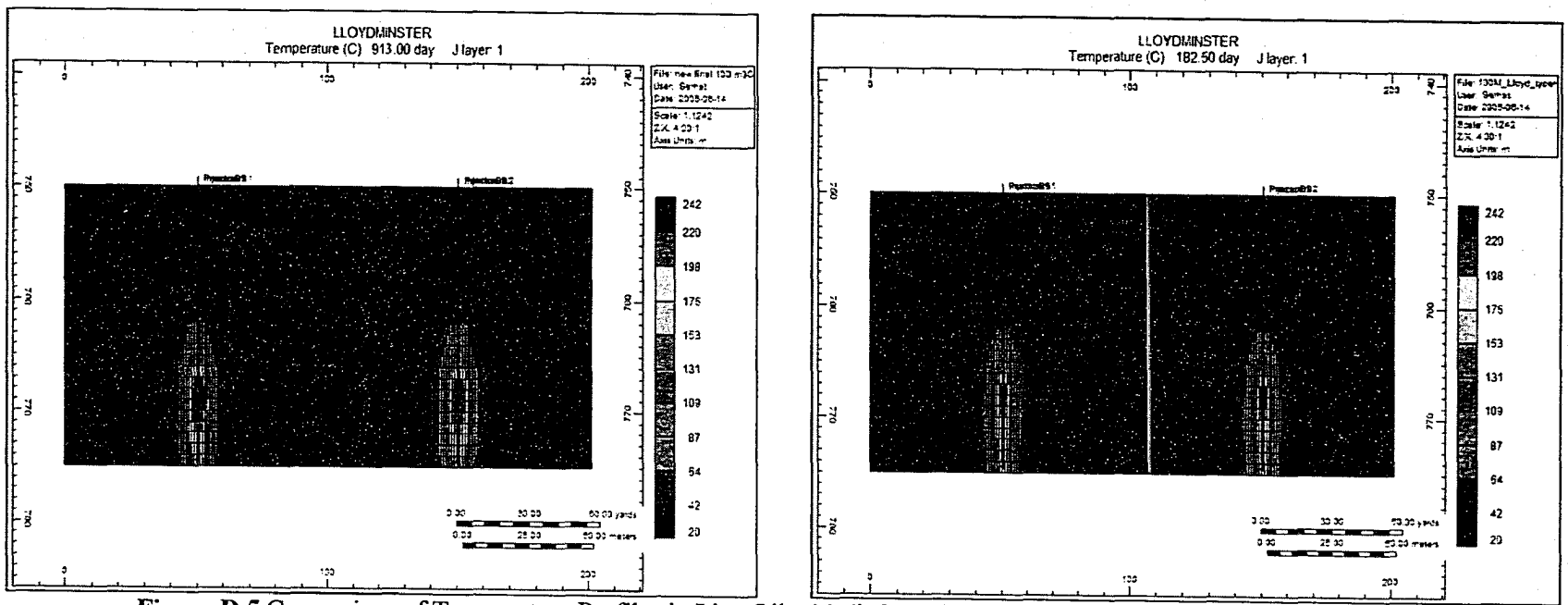

Figure D.5 Comparison of Temperature Profiles in Live Oil with (left) and without (right) CO_2 Injection after 6 Months of Steam Flooding

Reproduced with permission of the copyright owner. Further reproduction prohibited without permission.

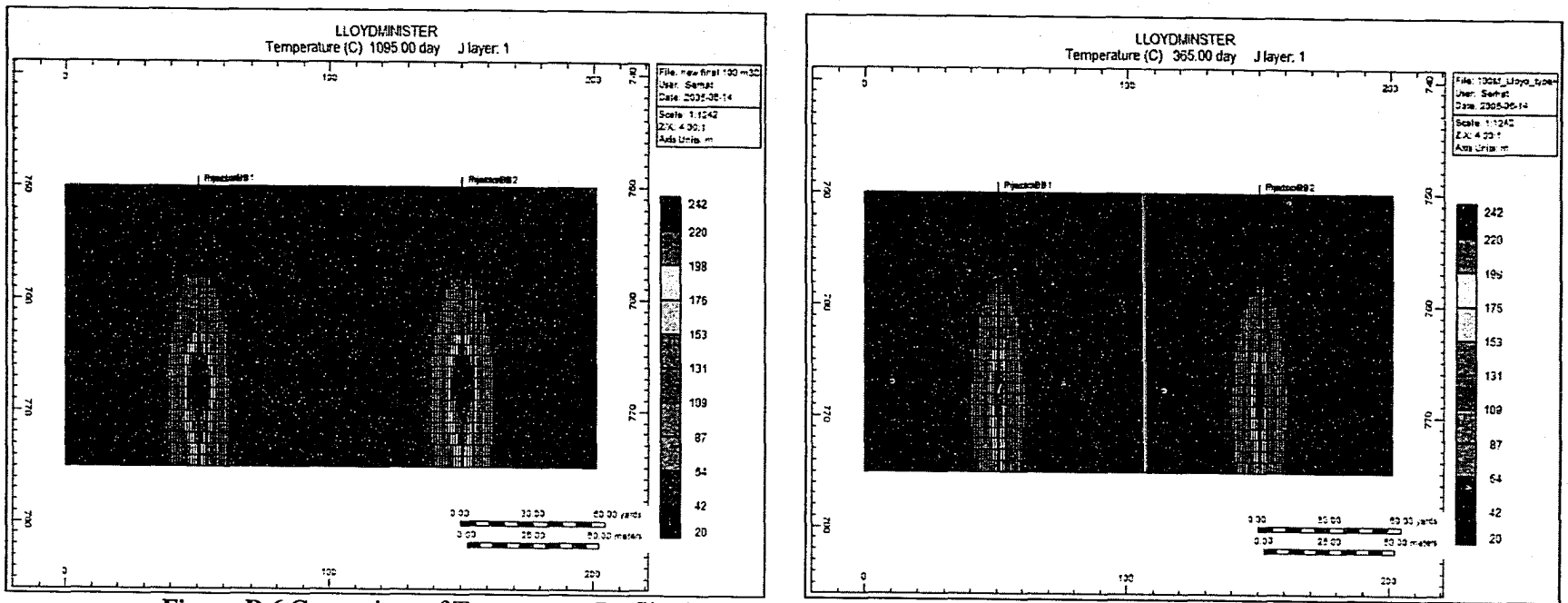

Figure D.6 Comparison of Temperature Profiles in Live Oil with (left) and without (right) CO_2 Injection after 1 Year of Steam Flooding

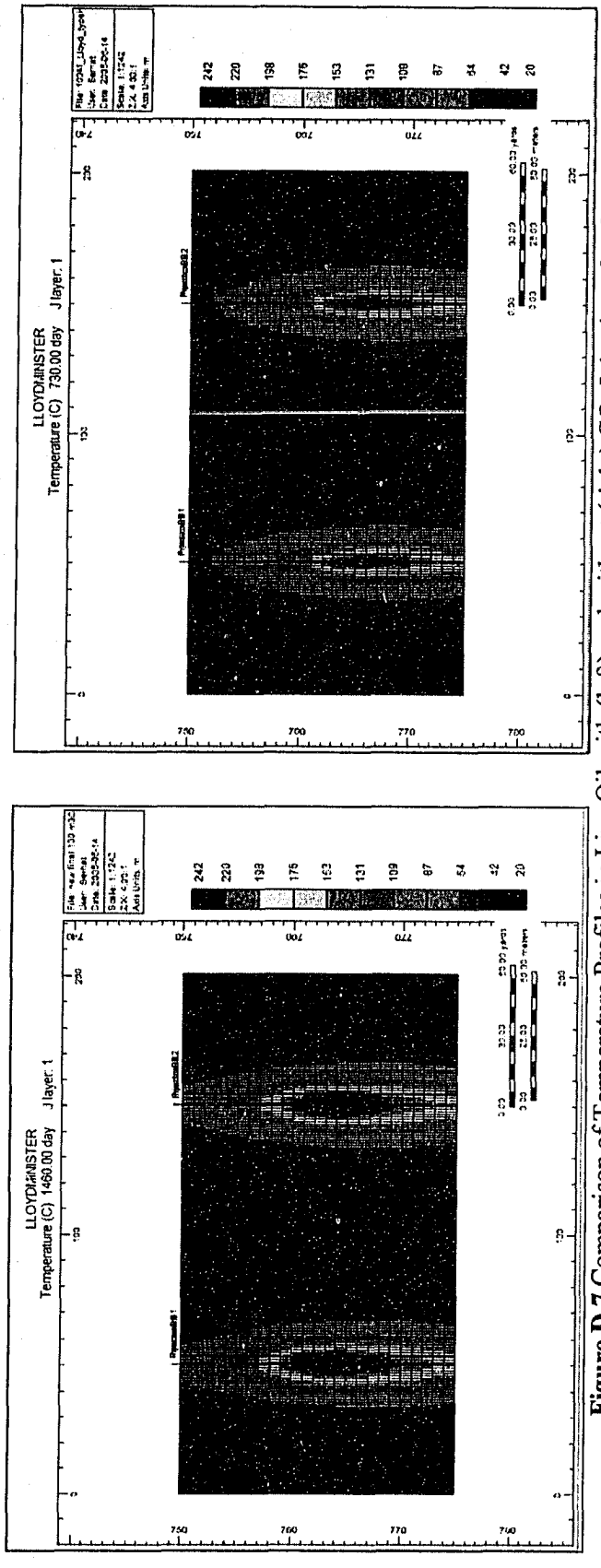

Figure D.7 Comparison of Temperature Profiles in Live Oil with (left) and without (right) CO_2 Injection after 2 Years of Steam Flooding

Reproduced with permission of the copyright owner. Further reproduction prohibited without permission.

Appendix E Comparison of Dead and Live Oil Reservoirs

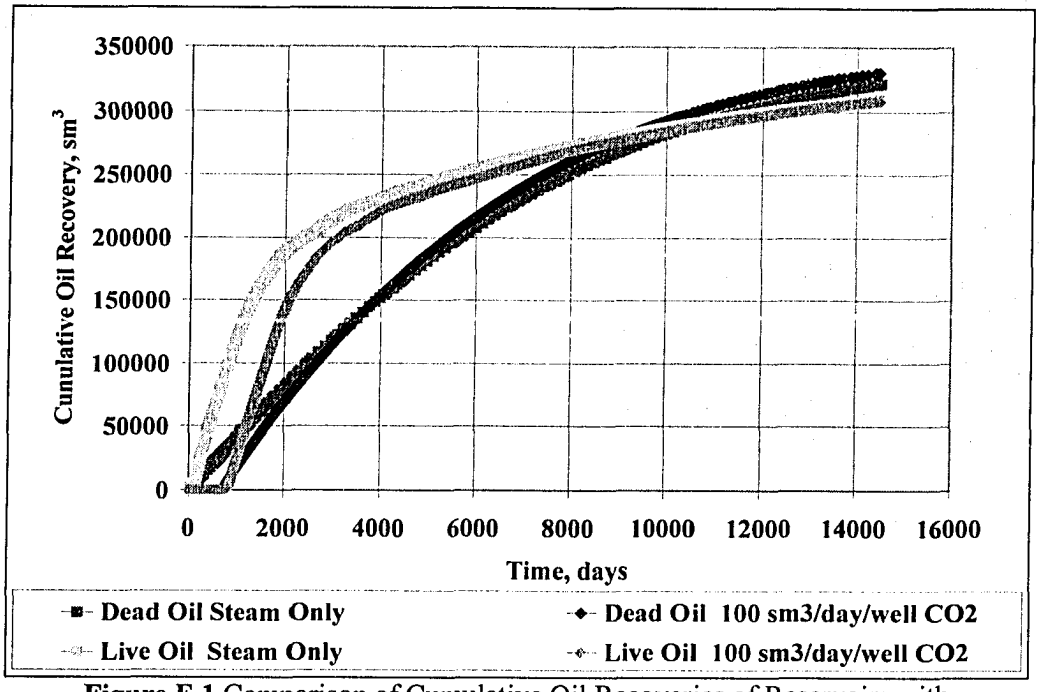

Figure E.1 Comparison of Cumulative Oil Recoveries of Reservoirs with Dead and Live Oil at 3000 kPa Pressure

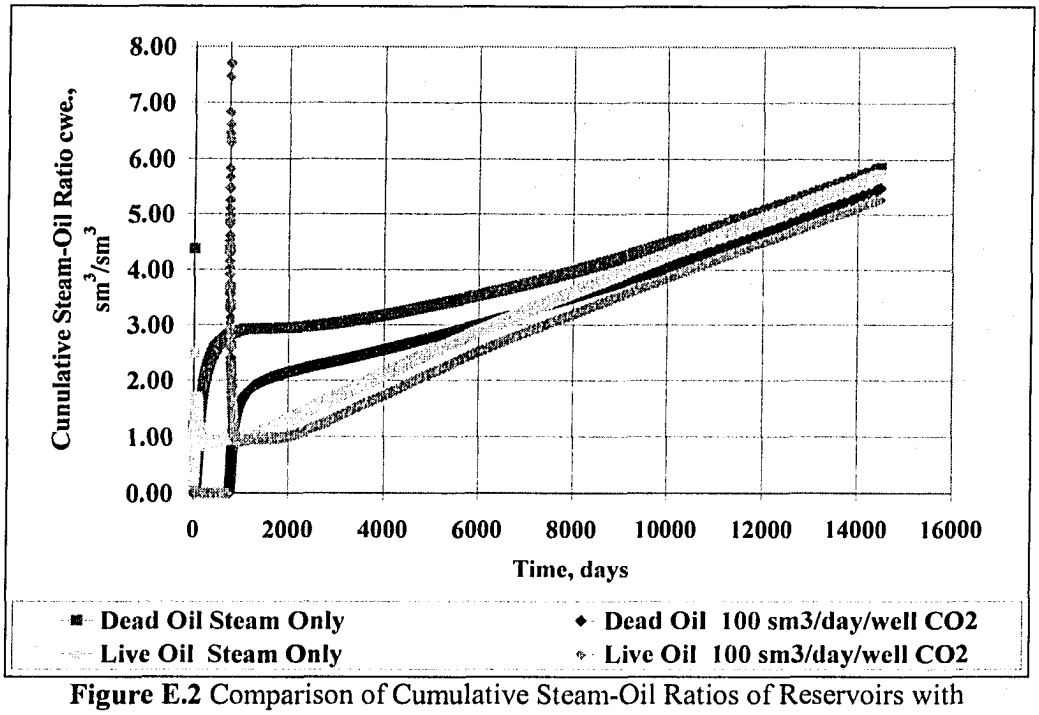

Figure E.2 Comparison of Cumulative Steam-Oil Ratios of Reservoirs with Dead and Live Oil at 3000 kPa Pressure

Reproduced with permission of the copyright owner. Further reproduction prohibited without permission.

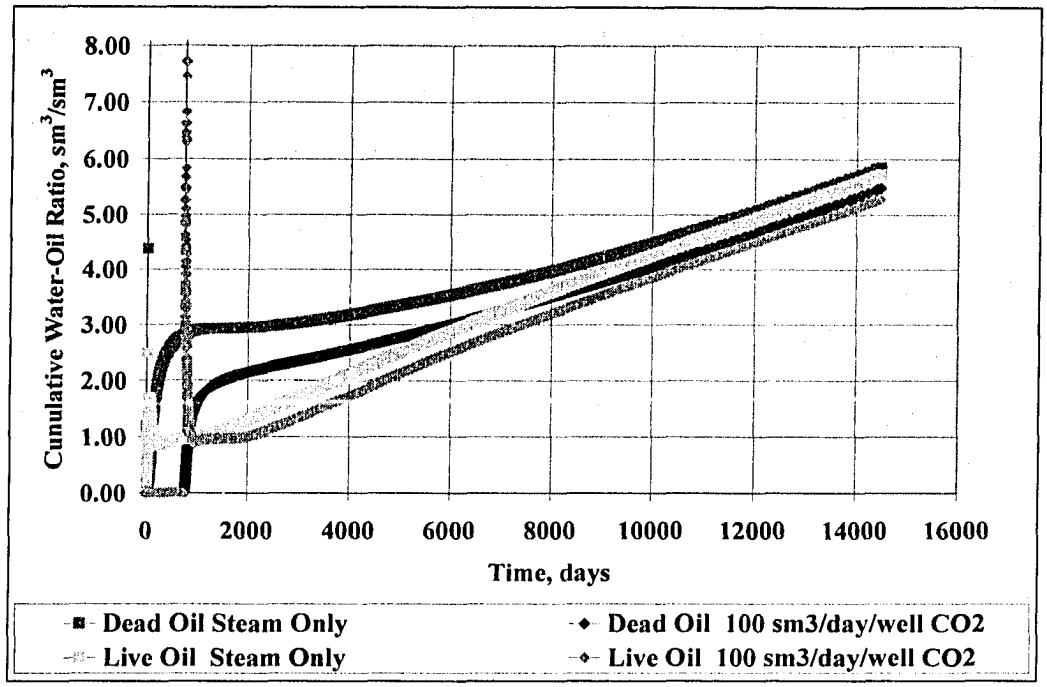

Figure E.3 Comparison of Cumulative Water-Oil Ratios of Reservoirs with Dead and Live Oil at 3000 kPa Pressure

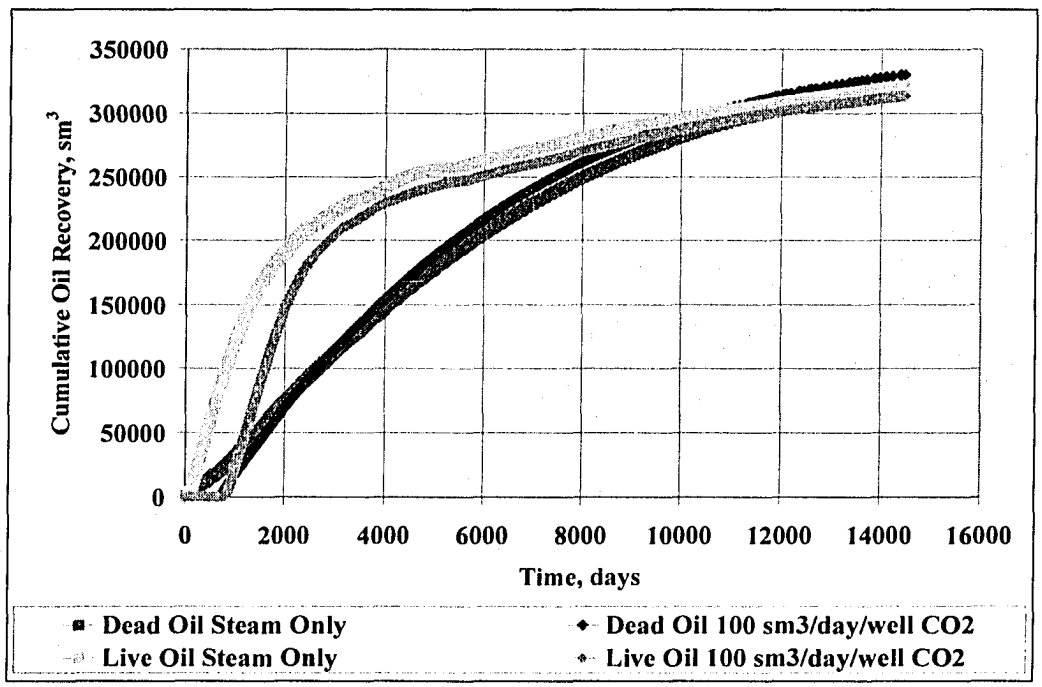

Figure E.4 Comparison of Cumulative Oil Recoveries of Reservoirs with Dead and Live Oil at 2500 kPa Pressure

Reproduced with permission of the copyright owner. Further reproduction prohibited without permission.

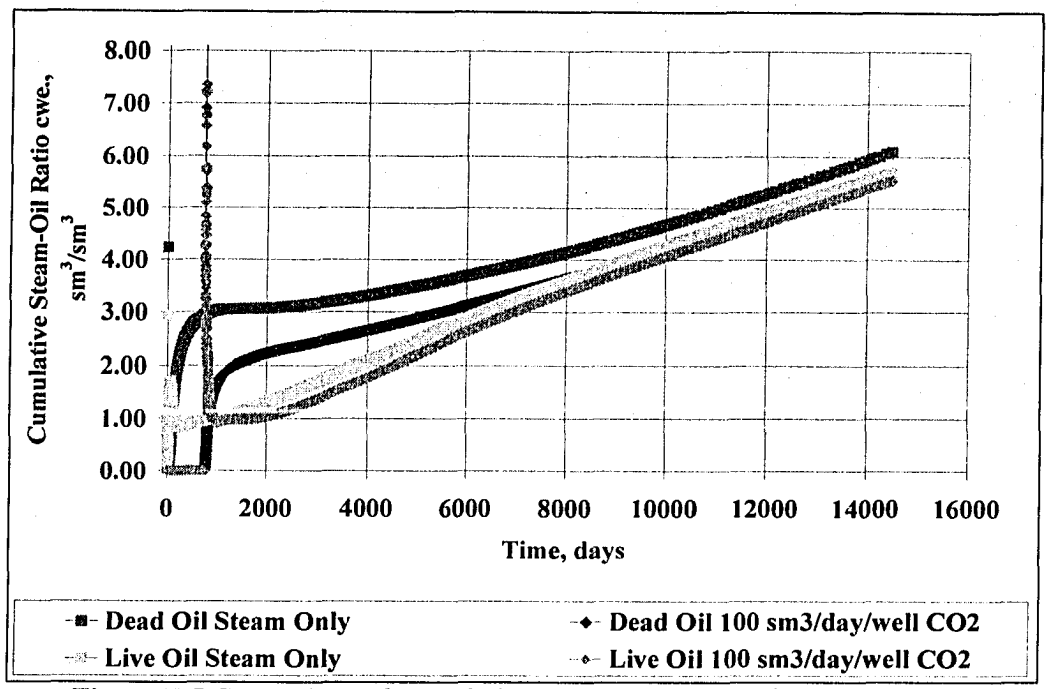

Figure E.5 Comparison of Cumulative Steam-Oil Ratios of Reservoirs with Dead and Live Oil at 2500 kPa Pressure

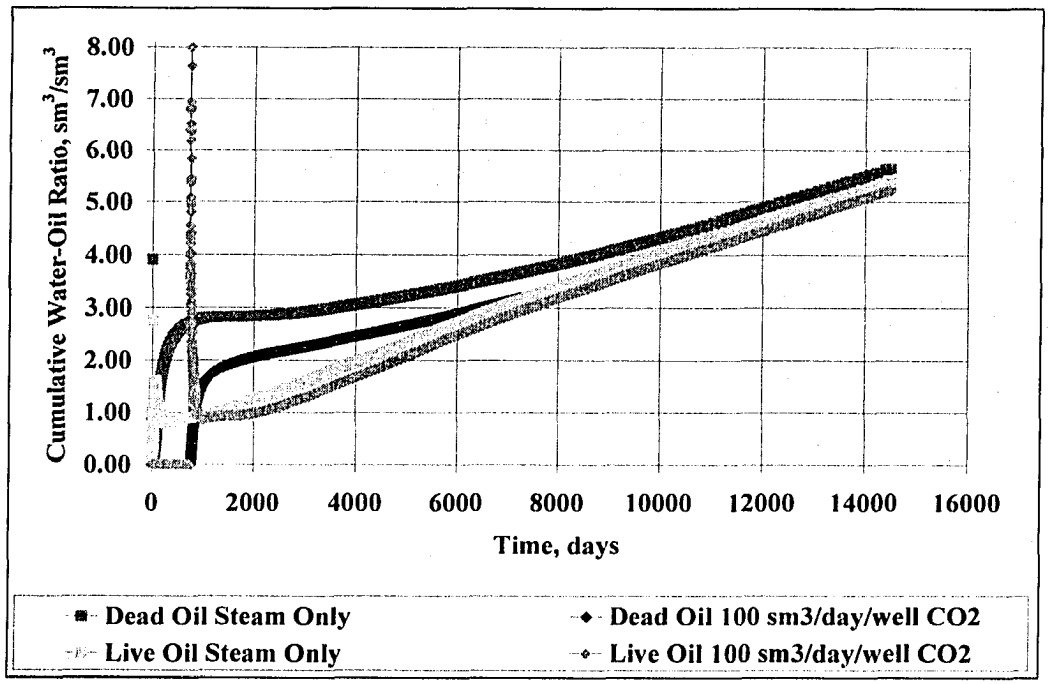

Figure E.6 Comparison of Cumulative Water-Oil Ratios of Reservoirs with Dead and Live Oil at 2500 kPa Pressure

Reproduced with permission of the copyright owner. Further reproduction prohibited without permission.

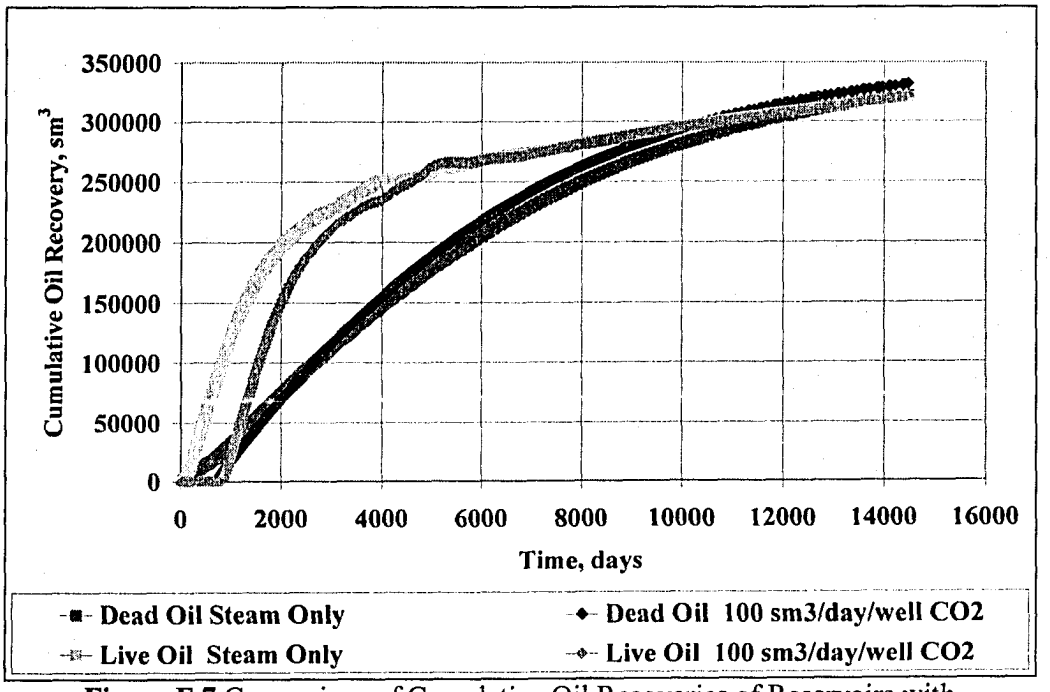

Figure E.7 Comparison of Cumulative Oil Recoveries of Reservoirs with Dead and Live Oil at 2000 kPa Pressure

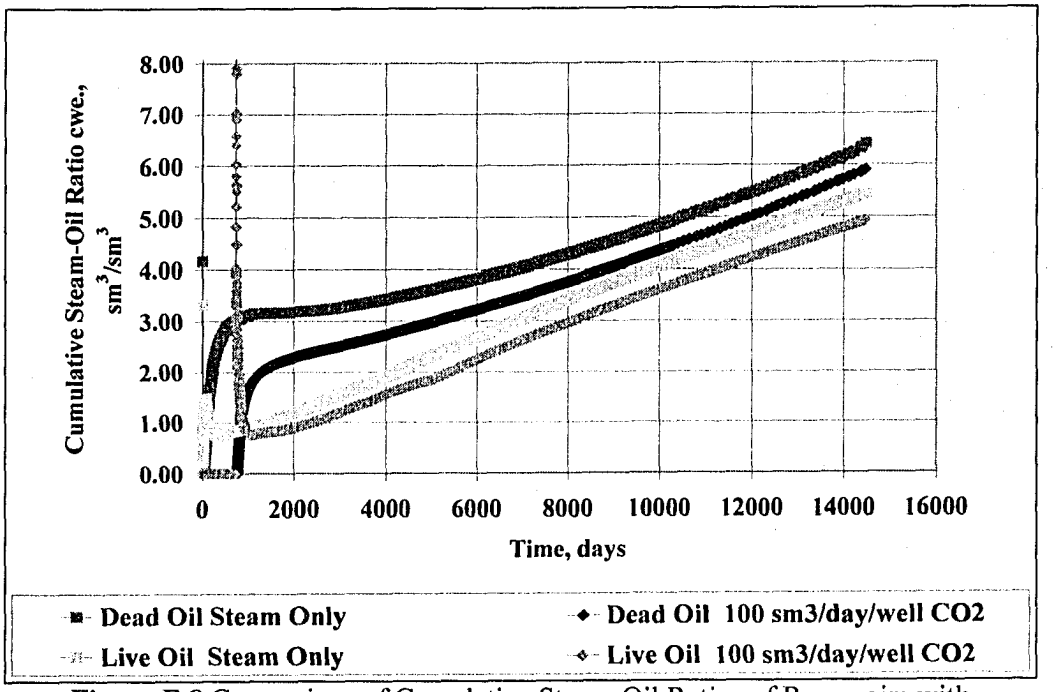

Figure E.8 Comparison of Cumulative Steam-Oil Ratios of Reservoirs with Dead and Live Oil at 2500 kPa Pressure

Reproduced with permission of the copyright owner. Further reproduction prohibited without permission.

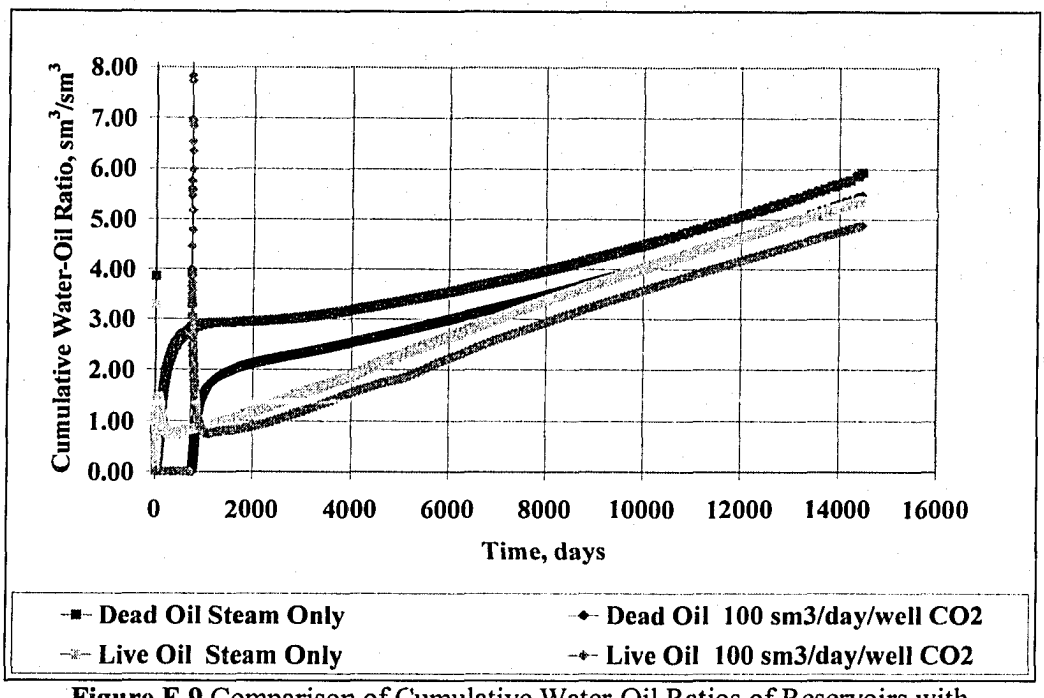

Figure E.9 Comparison of Cumulative Water-Oil Ratios of Reservoirs with Dead and Live Oil at 2000 kPa Pressure

Reproduced with permission of the copyright owner. Further reproduction prohibited without permission.